

URBAN FLOODING VULNERABILITY: A MULTIFACETED COMPARATIVE ASSESSMENT OF THE  
CHARLANTA MEGAREGION

by

NEIL ANDREW DEBBAGE

(Under the Direction of J. Marshall Shepherd)

ABSTRACT

Urban areas are particularly vulnerable to flood hazards due to impervious surfaces altering the runoff response and socio-economic pressures increasing the number of individuals residing in areas at risk for flooding. Despite the rich body of literature that has focused on urban flood hazards, the physical and social dimensions of this vulnerability are frequently analyzed independently of one another. This dissertation utilized a holistic and integrative human-environment interactions framework to simultaneously assess both the physical and social factors that enhanced urban flooding vulnerability throughout the Charlanta megaregion. Analyzing the entire megaregion enabled an assessment of how consistent these factors were across a variety of metropolitan areas. Developing a better understanding of the physio-social dimensions of urban flooding vulnerability is imperative to ensure the future sustainability of cities because urban population growth is projected to continue, and cities will be subjected to increased precipitation intensity due to climate change.

INDEX WORDS: Urban flooding, Climate modeling, Environmental justice, Urban climatology, Charlanta

URBAN FLOODING VULNERABILITY: A MULTIFACETED COMPARATIVE ASSESSMENT OF THE  
CHARLANTA MEGAREGION

By

NEIL ANDREW DEBBAGE

A.B., The University of Georgia, 2012

M.S., The University of Georgia, 2014

A Dissertation Submitted to the Graduate Faculty of The University of Georgia in Partial  
Fulfillment of the Requirements for the Degree

DOCTOR OF PHILOSOPHY

ATHENS, GEORGIA

2018

© 2018

Neil Andrew Debbage

All Rights Reserved

URBAN FLOODING VULNERABILITY: A MULTIFACETED COMPARATIVE ASSESSMENT OF THE  
CHARLANTA MEGAREGION

by

NEIL ANDREW DEBBAGE

Major Professor: J. Marshall Shepherd

Committee: Steven R. Holloway  
Lan Mu  
Todd C. Rasmussen

Electronic Version Approved:

Suzanne Barbour  
Dean of the Graduate School  
University of Georgia  
May 2018



## ACKNOWLEDGEMENTS

Firstly, I would like to thank my advisor, J. Marshall Shepherd, and committee members, Steven R. Holloway, Lan Mu, and Todd C. Rasmussen, for their invaluable guidance, insight, and support. I am deeply indebted to all four individuals, as they were instrumental in shaping and improving this work via their constructive feedback. I am also grateful for the funding provided by the Georgia Water Resources Institute that supported portions of this research. Additionally, I would like to thank my fellow graduate students and the faculty of the Department of Geography for providing a stimulating intellectual environment, which has been so influential in my academic development over the past decade. Finally, I am very grateful for my family and friends who provided support along this journey when it was needed most.

## TABLE OF CONTENTS

	Page
ACKNOWLEDGEMENTS .....	iv
LIST OF FIGURES .....	vii
LIST OF TABLES .....	xi
CHAPTER	
1 INTRODUCTION.....	1
1.1 Literature Review and Research Motivation.....	1
1.2 Research Study Area, Framework, and Objectives .....	4
1.3 References .....	9
2 THE INFLUENCE OF URBAN DEVELOPMENT PATTERNS ON STREAMFLOW CHARACTERISTICS .....	15
2.1 Introduction .....	17
2.2 Data and Methods .....	20
2.3 Results and Discussion .....	27
2.4 Conclusions and Urban Planning Implications .....	40
2.5 References .....	45
3 DETERMINING THE INFLUENCE OF URBANIZATION ON THE SPATIOTEMPORAL CHARACTERISTICS OF RUNOFF AND PRECIPITATION DURING THE 2009 ATLANTA FLOOD.....	68
3.1 Introduction .....	70
3.2 Data and Methods .....	73

3.3 Results and Discussion .....	77
3.4 Conclusions and Urban Planning Implications .....	86
3.5 References .....	90
4 MULTISCALAR ASSESSMENT OF FLOOD ZONE OCCUPATION AND ENVIRONMENTAL JUSTICE .....	112
4.1 Introduction .....	114
4.2 Background .....	116
4.3 Data and Methods .....	122
4.4 Results and Discussion .....	129
4.5 Conclusions and Policy Implications.....	138
4.6 References .....	142
5 SUMMARY AND CONCLUSIONS.....	155
5.1 Summary of Research Objectives.....	155
5.2 Conclusions .....	159
APPENDIX .....	162

## LIST OF FIGURES

	Page
Figure 1.1. Urban and rural population trends [ <i>United Nations</i> , 2014].....	13
Figure 1.2. Theoretical hydrograph highlighting the influence of urbanization [ <i>Harbor</i> , 1994]. .....	13
Figure 1.3. Human-Environment interactions research framework. ....	14
Figure 2.1. Location of the Charlanta Megaregion and study watersheds.....	51
Figure 2.2. Example of the peaks-over-threshold (POT) analysis from Peachtree Creek in Atlanta, Georgia for 2011. There were 25 low threshold exceedances and 35 high threshold exceedances during the year .....	52
Figure 2.3. Spatial distribution of a) high threshold exceedances per year, b) low threshold exceedances per year, and c) annual average peak unit discharge ( $\text{m}^3\text{s}^{-1}\text{km}^{-2}$ ) for the Atlanta MSA .....	53
Figure 2.4. Spatial distribution of a) high threshold exceedances per year, b) low threshold exceedances per year, and c) annual average peak unit discharge ( $\text{m}^3\text{s}^{-1}\text{km}^{-2}$ ) for the Charlotte MSA .....	54
Figure 2.5. Spatial distribution of a) high threshold exceedances per year, b) low threshold exceedances per year, and c) annual average peak unit discharge ( $\text{m}^3\text{s}^{-1}\text{km}^{-2}$ ) for the Greenville, Spartanburg, and Anderson MSAs.....	55
Figure 2.6. Relationships between a) high and b) low threshold exceedances and distance to the central business district (CBD) of each MSA in Charlanta. Pearson correlation coefficients ( $r$ ) and sample sizes ( $N$ ) are reported with p-values in parentheses. The grey shading around the lines represents the 95% confidence interval.....	56
Figure 2.7. Differences in a) threshold exceedances and b) annual peak unit discharge between the Charlanta MSAs. The F-values from the ANOVA tests are reported with the associated p-values in parentheses .....	57
Figure 2.8. Differences in a) the relative extent of urban development and b) the contiguity of urban development between the Charlanta MSAs. The F-values from the ANOVA tests are reported with the associated p-values in parentheses.....	58

Figure 2.9. Differences in the natural characteristics of the Charlanta watersheds by MSA. The F-values from the ANOVA tests are reported with the associated p-values in parentheses .....	59
Figure 2.10. Relationships between the percent of the watershed developed and the threshold exceedances. Pearson correlation coefficients (r) and sample sizes (N) are reported with p-values in parentheses. The grey shading around the lines represents the 95% confidence interval. In subplot d) the dashed lines represent loess curves fitted to the scatterplot .....	60
Figure 2.11. Relationships between the percent of the watershed developed and annual average peak unit discharge. Pearson correlation coefficients (r) and sample sizes (N) are reported with p-values in parentheses. The grey shading around the lines represents the 95% confidence interval.....	61
Figure 2.12. Relationships between the positioning metrics and the high threshold exceedances. Pearson correlation coefficients (r) and sample sizes (N) are reported with p-values in parentheses. The grey shading around the lines represents the 95% confidence interval .....	62
Figure 2.13. Example of headwater development in Downtown Atlanta. Each watershed exhibited a large number of high threshold exceedances as well as a notable mean imperviousness difference between their top and bottom halves.....	63
Figure 3.1. Location of the outer (outer black box) and inner (inner white box) modeling domains used to simulate the 2009 Atlanta Flood. The gray shading represents the extent of the Atlanta Metropolitan Statistical Area.....	95
Figure 3.2. Land use scenarios used in the a) urban run and b) non-urban run. Shades of red represent urban land use of various intensities and brown represents the cropland/vegetation mosaic used to replace the urban development. Major roadways are represented by thin black lines and state boundaries are indicated by thick black lines.....	96
Figure 3.3. Location of the downwind area of interest included in the areal averages (green box) and the north (orange line) and south (yellow line) vertical cross sections.....	97
Figure 3.4. Daily precipitation totals from the urban simulation (top row), MPE (middle row), and non-urban simulation (bottom row) for 20 September 1200 UTC (left column), 21 September 1200 UTC (middle column), and 22 September 1200 UTC (right column) .....	98
Figure 3.5. Comparison of the hourly precipitation from the urban WRF simulation averaged within the downwind area of interest with several proximate observations.....	99

Figure 3.6. Comparison of the hourly precipitation averaged within the downwind area of interest between the urban and non-urban WRF simulations .....	100
Figure 3.7. Difference in the surface runoff (Urban – Non-Urban) during the two heavy periods of precipitation at 9/20 0400 UTC (left) and 9/21 0500 UTC (right) .....	101
Figure 3.8. Surface flow patterns from the urban (left) and non-urban simulation (right) at 20 September 0000 UTC (top), 20 September 0100 UTC (middle top), 21 September 0200 UTC (middle bottom), and 21 September 0300 UTC (bottom) .....	102
Figure 3.9. Divergence/Convergence fields from the urban (left) and non-urban simulation (right) at 20 September 0200 UTC (top), 20 September 0400 UTC (middle top), 21 September 0200 UTC (middle bottom), and 21 September 0300 UTC (bottom). Negative values are indicative of convergence .....	104
Figure 3.10. Differences in the sensible heat flux between the urban simulation and non-urban simulation for 19 September 2300 UTC (left) and 21 September 0000 UTC (right). Positive values are indicative of greater sensible heat flux in the urban simulation .....	106
Figure 3.11. Vertical cross sections along the northern transect from the urban (left) and non-urban (right) simulation at 20 September 0000 UTC (top), 0100 UTC (middle top), 0200 UTC (middle bottom), and 0300 UTC (bottom) .....	107
Figure 3.12. Vertical cross sections along the southern transect from the urban (left) and non-urban (right) simulation at 21 September 0000 UTC (top), 0100 UTC (middle top), 0200 UTC (middle bottom), and 0300 UTC (bottom) .....	109
Figure 4.1. Location of the Charlanta Megaregion and individual MSAs included in the analysis .....	148
Figure 4.2. Example of the three different flood zone areas used during the dasymetric mapping techniques for a census block group adjacent to Peachtree Creek in Fulton County Georgia.....	149
Figure 4.3. Flood zone population characteristics for each MSA by dasymetric mapping technique .....	150
Figure 4.4. Risk Ratios at the county level for the a) areal weighting, b) urban filtered areal weighting, and c) low-high urban filtered areal weighting dasymetric mapping techniques. Panel d) maps the overall risk ratio difference (low-high filtered risk ratio – areal weighting risk ratio) .....	151
Figure 4.5. Census tract risk ratios for each dasymetric mapping technique summarized by Atlanta MSA counties (left panel), Charlotte MSA counties (middle panel), and Greenville-Spartanburg MSA counties (right panel) .....	152

Figure 4.6. Frequency of census tracts with significant (p-value < 0.05) risk ratios greater and less than one for each dasymetric mapping technique and MSA.....	152
Figure 4.7. Transformation of one Summerhill street between 2010 (top) and 2017 (bottom). The demolition, reconstruction, and/or modification of houses along the new street of permeable pavers is visible in the foreground while the topography that is partly responsible for the flooding issues can be seen in the background (Source: Google Street View) .....	153

## LIST OF TABLES

	Page
Table 2.1. Statistics describing the characteristics of the study watersheds. Median values are reported with standard deviations in parentheses. All the variables were obtained from the GAGES-II dataset [ <i>Falcone, 2011</i> ] except urbanized area, which was derived from the 2011 National Land Cover Database (NLCD).....	64
Table 2.2. Equations and technical descriptions of the spatial metrics used to quantify the extent and spatial configuration of the urban development within each watershed [ <i>McGarigal et al., 2012</i> ]. In this study, a patch is defined as a contiguous group of pixels that share a common land use/land cover type .....	65
Table 2.3. Correlations between the urban configuration metrics and high threshold exceedances, low threshold exceedances, annual average peak unit discharge, and PLAND averaged over the four NLCD urban intensity levels .....	66
Table 2.4. Correlations between the urban positioning metrics and high threshold exceedances, low threshold exceedances, and annual average peak unit discharge .....	66
Table 2.5. OLS regression results for the high and low threshold exceedances .....	66
Table 2.6. OLS and SEM regression results for annual average peak unit discharge. Lambda represents the spatial autoregressive coefficient. ....	67
Table 3.1. WRF-ARW physics options used in the simulations .....	111
Table 4.1. Flood zone population characteristics and risk ratios for the Charlanta megaregion according to the three dasymetric mapping techniques. Each risk ratio was significant with a p-value less than 0.01 .....	154
Table 4.2. Risk ratios for each MSA according to the three dasymetric mapping techniques. Each risk ratio was significant with a p-value less than 0.05 .....	154
Table 4.3. Detailed information for the census tracts with the ten largest and statistically significant risk ratios according to the low-high urban filtered areal weighting .....	154
Table A.1. List of abbreviations and descriptions .....	162



## CHAPTER 1

### INTRODUCTION

#### **1.1 Literature Review and Research Motivation**

Urban development is one of the most influential and readily apparent mechanisms responsible for anthropogenic alterations of the natural environment [*Grimm et al.*, 2008]. Increasing urban populations and expanding urban footprints have altered the energy balance, atmospheric composition, precipitation patterns, and hydrologic systems within cities [*Hollis*, 1975; *Oke*, 1982; *Jacobson*, 2010; *Shepherd et al.*, 2010]. With approximately 54% of the world's population already residing in urban areas as of 2014 and this proportion projected to approach 66% by 2050 [*United Nations*, 2014], the pressures placed on the natural environment by urban expansion will likely become magnified in the near future (Figure 1.1). Continued urbanization poses substantial environmental challenges, which highlights the importance of implementing more sustainable forms of urban development.

This dissertation focused specifically on the complex relationships between urbanization and the hydrologic system. Cities are particularly prone to flooding, as made evident by the recent, devastating floods that occurred in Ellicott City, Maryland; Columbia, South Carolina; and Houston, Texas. The heightened vulnerability of urban areas to flooding is partly due to the introduction of impervious surfaces, storm drainage systems, and enhanced soil compaction [*Burian and Pomeroy*, 2010]. It is widely recognized that urbanization typically increases peak discharge, runoff volume, and the flashiness of the runoff response [*Leopold*, 1968; *Sauer et al.*, 1984] (Figure 1.2). Additionally, urbanization can alter low flow regimes, which have notable

ecological implications, although these linkages are more complex and typically less generalizable across cities [Meyer, 2005; Bhaskar et al., 2016].

Researchers have traditionally documented the impacts of urban development on streamflow through temporal trend analysis [e.g. Ferguson and Suckling, 1990; Velpuri and Senay, 2013], but more recent studies have begun focusing on how the spatial arrangement and positioning of urban land use influences the hydrologic response within watersheds [e.g. Olivera and DeFee, 2007; Mejia and Moglen, 2009]. This dissertation aimed to improve the understanding of the effects of urban development configuration and positioning on high, peak, and low flow regimes by using robust multivariate statistical techniques. The findings could potentially help advance urban planning measures beyond overly simplistic estimates of land use change impacts [e.g. Harbor, 1994] and inform more nuanced policies aimed at minimizing hydrologic disturbances related to urbanization. Such progress appears imperative, given that cities will likely be exposed to both an increased frequency of extreme rainfall and drought in the future due to global climate change [Groisman et al., 2004; Sheffield and Wood, 2008; Pryor et al., 2009; Andersen and Shepherd, 2013; Fischer and Knutti, 2015].

Urban environments not only impact streamflow characteristics but can also influence precipitation patterns [Burian and Shepherd, 2005]. Urban-induced alterations of precipitation have generally been attributed to one or a combination of the following mechanisms [Shepherd, 2005]: 1) the increased surface roughness within urban environments enhancing surface convergence [Thielen et al., 2000], 2) the different thermal properties of the city producing unstable atmospheric conditions through the creation, enhancement, and/or displacement of mesoscale circulations [Shepherd and Burian, 2003], 3) elevated aerosol concentrations altering cloud microphysical processes by providing an abundant source of cloud condensation nuclei

(CCN) [*Molders and Olson*, 2004; *Schmid and Niyogi*, 2017], 4) urban irrigation and industrial activities increasing low-level atmospheric moisture availability [*Shepherd et al.*, 2002; *Diem and Brown*, 2003], and 5) the built environment acting as a barrier that bifurcates existing storm systems [*Bornstein and Lin*, 2000]. This dissertation sought to clarify the capability of these mechanisms to influence rainfall during synoptically driven events by analyzing potential urban precipitation effects during the major flood that occurred during 2009 in Atlanta.

Beyond altering the surface characteristics that largely govern the hydrometeorological response [*Schueler et al.*, 2009], the agglomeration of individuals in urban areas simultaneously increases the population exposed to urban flood hazards. The threat of urban flooding is unfortunately documented by fatality statistics. Unlike deaths related to other meteorological hazards, such as tornadoes and lightning, there has been no significant decrease in flood fatalities during the second half of the 21<sup>st</sup> century [*Ashley and Ashley*, 2008]. This implies that the advancements made in forecasting urban flood events, warning systems, and emergency recovery procedures have to some extent been overwhelmed by rapid urban population growth [*Terti et al.*, 2017]. Although urban residents are clearly susceptible to flood hazards, the social dimensions of this vulnerability and the potential for environmental injustices are infrequently acknowledged in flood risk assessments [*Tapsell et al.*, 2002; *Koks et al.*, 2015]. This dissertation was designed to provide a detailed assessment of urban flood hazard environmental injustices, which could potentially help direct resources to those communities that are most in need and enhance their adaptive capacity to flood threats. Additionally, a greater awareness of flood hazard inequities could inform emergency management plans and help ensure more equitable recovery efforts when flooding occurs.

## **1.2 Research Study Area, Framework, and Objectives**

The overarching goal of this dissertation was to comprehensively address both the physical and social aspects of urban flooding vulnerability throughout the Charlanta megaregion. A megaregion consists of numerous metropolitan areas across which labor and capital can be reallocated with minimal cost [Gottman, 1957; Florida *et al.*, 2008]. Megaregions share a common economic system and are linked by transportation infrastructure. Located in the Southeastern portion of the United States, the Charlanta megaregion includes the Atlanta, Charlotte, Greenville, and Spartanburg Metropolitan Statistical Areas (MSA) [Florida *et al.*, 2008]. Atlanta and Charlotte are the most populous MSAs within their respective states while Greenville ranks third in South Carolina. The individual MSAs that comprise Charlanta are economically integrated via the I-85 corridor. Charlanta contains over 20 million people and is responsible for an estimated economic output of \$730 billion [Florida *et al.*, 2008]. Due partly to the relatively low cost of living, the urban footprint of Charlanta is projected to continue expanding [Terando *et al.*, 2014], which will likely further exacerbate urban flooding issues.

A holistic human-environment interactions framework was used to address the multidimensionality of flood hazards in the Charlanta megaregion (Figure 1.3). The framework emphasized the reciprocal nature of the relationships connecting humans and the natural environment. Specifically, several portions of the dissertation addressed anthropogenic influences, primarily through urbanization and land use change, on components of the hydrologic system. Conversely, the research also focused on the differential impacts of hydrometeorological hazards, such as extreme precipitation and flooding, on certain communities. This specific part of the dissertation explored how urban flood hazards potentially effect certain vulnerable populations disproportionately and present environmental justice issues.

The individual research objectives, which collectively explored the two-way interactions between humans and the environment, were united by a shared emphasis on quantitative geospatial data analysis (Figure 1.3). The work relied largely upon GIS, landscape metrics, statistical modeling, numerical weather modeling, and dasymetric mapping. As suggested by *Bloschl et al. [2007]*, the dissertation incorporated both statistically and physically-based modeling techniques to provide a more comprehensive assessment of urban flooding vulnerability. Additionally, a standardized methodology was employed across the entire megaregion, which helped assess potential differences in urban flooding vulnerability between the individual metropolitan areas that comprise the megaregion. Each objective also sought to inform urban policy efforts designed to enhance the sustainability of urban environments by reducing the impacts of urbanization on the hydrologic system and increasing the resiliency of urban residents, particularly within communities that are disproportionality at risk to flood hazards.

Specifically, the dissertation explored the following three research objectives, which are described further below:

1. Quantify the influence of the composition, positioning, and configuration of urban development on various streamflow characteristics
2. Model the effects of urbanization on the hydrometeorological characteristics of the 2009 Atlanta flood
3. Analyze flood zone occupation at multiple scales to assess the degree of environmental injustice related to urban flood risk.

The first research objective aimed to elucidate the influence of urban development patterns on streamflow characteristics. Therefore, it was situated within the portion of the human-

environment interactions research framework that addressed anthropogenic effects on the hydrologic system (Figure 3.1). The urban development patterns were quantified using the public domain software FRAGSTATS [McGarigal *et al.*, 2012] and data obtained from the 2011 National Land Cover Database (NLCD) [Homer *et al.*, 2015] while the streamflow characteristics were evaluated using mean daily discharge and annual peak streamflow data gathered from the USGS National Water Information System (NWIS). The relationships between the urban development patterns and streamflow characteristics were evaluated through a case study of 119 watersheds within Charlanta using bivariate and multivariate statistical modeling. The specific research questions addressed in Chapter 2 were:

1. What is the relative influence of the extent, spatial configuration, and positioning of urban development on low, high, and annual peak flows?
2. How consistent are these relationships across the Charlanta megaregion and what factors explain any observed differences?

The second research objective also addressed anthropogenic influences on the hydrometeorological system. However, it focused explicitly on the effects of urbanization during the high impact flood that occurred in 2009 throughout Atlanta. The 2009 flood event was historic and resulted in catastrophic damage throughout the metropolitan area. The flood was the product of several hydrometeorological processes including moist antecedent conditions, ample atmospheric moisture, and mesoscale training. Previous studies also hypothesized that the urban environment of Atlanta altered the location and/or overall quantities of precipitation and runoff, which ultimately produced the flood [Shepherd *et al.*, 2011]. This hypothesis was quantitatively evaluated by conducting a series of numerical modeling experiments that utilized the Weather Research and Forecasting (WRF) model. WRF is a fully compressible, non-hydrostatic,

mesoscale model with advanced dynamics, physics, and numerical schemes that is supported by the National Center for Atmospheric Research (NCAR) [Skamarock *et al.*, 2008]. Two model runs were performed: 1) a base run designed to accurately depict the flood event, and 2) a non-urban simulation where the urban footprint of Atlanta was replaced with natural vegetation.

Chapter 3 specifically addressed the following research questions:

1. How did the urban environment of Atlanta influence the spatiotemporal characteristics of runoff and precipitation during the 2009 flood?
2. What physical mechanisms were potentially responsible for any urban influences?
3. Can urban environments influence precipitation during heavy rainfall events with prominent synoptic scale forcing?

Unlike Objectives 1 and 2, the final research objective addressed the impact of hydrologic hazards on urban communities. Therefore, Objective 3 considered the opposite directional pathway within the human-environment interactions framework (Figure 1.3). Although previous studies have utilized an environmental justice lens to address the socio-economic aspects of urban flooding vulnerability, they have produced contrasting results due to the different dasymetric mapping techniques used to estimate urban flood zone population characteristics, the various scales at which the estimates are calculated, and the specific geographical context of the individual study cities. Objective 3 evaluated the sensitivity of urban flood risk environmental injustices to these parameters by analyzing flood zone occupation with three different dasymetric mapping techniques at four scales for numerous metropolitan areas within the Charlanta megaregion. Specifically, 2010 US Census block group data, FEMA flood zones, and risk ratios were used to evaluate if African Americans were overrepresented in areas at risk for flooding. The specific research questions addressed in Chapter 4 included:

1. What is the degree of environmental injustice regarding urban flood risk within the Charlanta megaregion?
2. How sensitive are any observed environmental injustices to the dasymetric mapping technique, scale of analysis, and the specificities of individual metropolitan areas?

Overall, the three research objectives collectively provided a comprehensive assessment of urban flooding vulnerability by emphasizing the reciprocal nature of human-environment interactions within a more holistic research framework.



### **1.3 References**

- Andersen, T. K., and J. M. Shepherd (2013), Floods in a changing climate, *Geogr. Compass*, 7(2), 95–115, doi: 10.1111/gec3.12025.
- Ashley, S. T., and W. S. Ashley (2008), Flood fatalities in the United States, *J. Appl. Meteorol. Climatol.*, 47, 805–818, doi:10.1175/2007JAMC1611.1.
- Bhaskar, A. S., L. Beesley, M. J. Burns, T. D. Fletcher, P. Hamel, C. E. Oldham, and A. H. Roy (2016), Will it rise or will it fall? Managing the complex effects of urbanization on baseflow, *Freshw. Sci.*, 35(1), 293–310, doi:10.1086/685084.
- Bloschl, G., S. Ardoin-Bardin, M. Bonell, M. Dorninger, M. Goodrich, D. Gutknecht, D. Matamoros, B. Merz, P. Shand, and J. Szolgay (2007), At what scales do climate variability and land cover change impact flooding and low flows?, *Hydrol. Process.*, 21, 1241–1247, doi: 10.1002/hyp.6669.
- Bornstein, R., and Q. Lin (2000), Urban heat islands and summertime convective thunderstorms in Atlanta: three case studies, *Atmos. Environ.*, 34, 507–516, doi: 10.1016/S1352-2310(99)00374-X.
- Burian, S. J., and C. A. Pomeroy (2010), Urban impacts on the water cycle and potential green infrastructure implications, in *Urban Ecosystem Ecology*, edited by J. Aitkenhead-Peterson and A. Volder, pp. 277–296, American Society of Agronomy, Madison, WI.
- Burian, S. J., and J. M. Shepherd (2005), Effect of urbanization on the diurnal rainfall pattern in Houston, *Hydrol. Process.*, 19, 1089–1103, doi: 10.1002/hyp.5647.
- Diem, J. E., and D. P. Brown (2003), Anthropogenic impacts on summer precipitation in Central Arizona, U.S.A, *Prof. Geogr.*, 55, 343–355, doi: 10.1111/0033-0124.5503011.
- Ferguson, B. K., and P. W. Suckling (1990), Changing rainfall-runoff relationships in the urbanizing Peachtree Creek watershed, Atlanta, Georgia, *J. Am. Water Resour. Assoc.*, 26(2), 313–322, doi:10.1111/j.1752-1688.1990.tb01374.x.
- Fischer, E. M., and R. Knutti (2015), Anthropogenic contribution to global occurrence of heavy-precipitation and high-temperature extremes, *Nat. Clim. Chang.*, 5, 560–564, doi:10.1038/NCLIMATE2617.
- Florida, R., T. Gulden, and C. Mellander (2008), The rise of the mega-region, *Camb. J. Regions Econ. Soc.*, 1, 459–476, doi: 10.1093/cjres/rsn018.
- Gottmann, J. (1957), Megalopolis or the urbanization of the Northeastern seaboard, *Econ. Geogr.*, 33(3), 189–200, doi: 10.2307/142307.

- Grimm, N. B., S. H. Faeth, N. E. Golubiewski, C. L. Redman, J. Wu, X. Bai, and J. M. Briggs (2008), Global change and the ecology of cities, *Science*, 319, 756–760, doi: 10.1126/science.1150195.
- Groisman, P. Y., R. W. Knight, T. R. Karl, D. R. Easterling, B. Sun and J. H. Lawrimore (2004), Contemporary changes to the hydrological cycle over the contiguous United States: Trends derived from in situ observations, *J. Hydrometeorol.*, 5, 64–85, doi: 10.1175/1525-7541(2004)005<0064:CCOTHC>2.0.CO;2.
- Harbor, J. M. (1994), A practical method for estimating the impact of land-use change on surface runoff, groundwater recharge and wetland hydrology, *J. Am. Plann. Assoc.*, 60(1), 95–107, doi: 10.1080/01944369408975555.
- Hollis, G. E. (1975), The effect of urbanization on floods of different recurrence interval, *Water Resour. Res.*, 11(3), 431–435, doi:10.1029/WR011i003p0043.
- Homer, C. G., J. A. Dewitz, L. Yang, S. Jin, P. Danielson, G. Xian, J. Coulston, N. D. Herold, J. D. Wickham, and K. Megown (2015), Completion of the 2011 National Land Cover Database for the conterminous United States-Representing a decade of land cover change information, *Photogramm. Eng. Remote Sens.*, 81(5), 345–354, doi:10.14358/PERS.81.5.345.
- Koks, E. E., B. Jongman, T. G. Husby, and W. J. W. Botzen (2015), Combining hazard, exposure and social vulnerability to provide lessons for flood risk management, *Environ. Sci. Policy*, 47, 42–52, doi: 10.1016/j.envsci.2014.10.013.
- Leopold, L. B. (1968), Hydrology for urban planning – A guidebook on the hydrologic effects of urban land use, *U.S. Geol. Surv. Circ. 554*, U.S. Geol. Surv., Washington, D.C. [Available at <https://pubs.usgs.gov/circ/1968/0554/report.pdf>.]
- McGarigal, K., S. A. Cushman, and E. Ene (2012), FRAGSTATS v4: Spatial pattern analysis program for categorical and continuous maps, University of Massachusetts, Amherst, MA. [Available at <http://www.umass.edu/landeco/research/fragstats/fragstats.html>.]
- Mejia, A. I., and G. E. Moglen (2009), Spatial patterns of urban development from optimization of flood peaks and imperviousness-based measures, *J. Hydrol. Eng.*, 14(4), 416–424, doi:10.1061/(ASCE)1084-0699(2009)14:4(416).
- Meyer, S. C. (2005), Analysis of base flow trends in urban streams, northeastern Illinois, USA, *Hydrogeol. J.*, 13, 871–885, doi:10.1007/s10040-004-0383-8.
- Molders, N., and M. A. Olson (2004), Impact of urban effects on precipitation in high latitudes, *J. Hydrometeorol.*, 5, 409–429, doi: 10.1175/15257541(2004)005<0409:IOUEOP>2.0.CO;2.

- Oke, T. R (1982), The energetic basis of the urban heat island, *Q. J. Royal Meteorol. Soc.*, 108, 1–24, doi: 10.1002/qj.49710845502.
- Olivera, F., and B. B. DeFee (2007), Urbanization and its effect on runoff in the Whiteoak Bayou watershed, Texas, *J. Am. Water Resour. Assoc.*, 43(1), 170–182, doi:10.1111/j.1752-1688.2007.00014.x.
- Pryor, S. C., J. A. Howe, and K. E. Kunkel (2009), How spatially coherent and statistically robust are temporal changes in extreme precipitation in the contiguous USA?, *Int. J. Climatol.*, 29, 31–45, doi: doi.org/10.1002/joc.1696.
- Sauer, V. B., W. O. Thomas, V. A. Stricker, and K. V. Wilson (1984), Flood characteristics of urban watersheds in the United States. *U.S. Geol. Surv. Water Supply Paper 2207*, U.S. Gov. Print. Office, Washington, D.C. [Available at <https://pubs.usgs.gov/wsp/2207/report.pdf>.]
- Schmid, P. E., and D. Niyogi (2017), Modeling urban precipitation modification by spatially heterogeneous aerosols, *J. Appl. Meteor. Climatol.*, 56, 2141–2153, doi: 10.1029/2011JD017352.
- Schueler, T. R., L. Fraley-McNeal, K. Cappiella (2009), Is impervious cover still important? Review of recent research, *J. Hydrol. Eng.*, 14(4), 309–315, doi:10.1061/(ASCE)1084-0699(2009)14:4(309).
- Sheffield, J., and E. F. Wood (2007), Projected changes in drought occurrence under future global warming from multi-model, multi-scenario, IPCC AR4 simulations, *Clim. Dyn.*, 31, 79–105, doi:10.1007/s00382-007-0340-z.
- Shepherd, J. M., H. Pierce, and A. J. Negri (2002), Rainfall modification by major urban areas: Observations from spaceborne rain radar on the TRMM satellite, *J. Appl. Meteor.*, 41, 689–701, doi: 10.1175/1520-0450(2002)041<0689:RMBMUA>2.0.CO;2.
- Shepherd, J. M., M. Carter, M. Manyin, D. Messen, and S. Burian (2010), The impact of urbanization on current and future coastal precipitation: A case study for Houston, *Environ. Plan. B*, 37(2), 284–304, doi: 10.1068/b34102t.
- Shepherd, J. M., and S. J. Burian (2003), Detection of urban-induced rainfall anomalies in a major coastal city, *Earth Interact.*, 7, 1–17, doi: 10.1175/1087-3562(2003)007<0001:DOUIRA>2.0.CO;2.
- Shepherd, J. M., T. Mote, J. Dowd, M. Roden, P. Knox, S. C. McCutcheon, and S. E. Nelson (2011), An overview of synoptic and mesoscale factors contribution to the disastrous Atlanta flood of 2009, *Bull. Amer. Meteor. Soc.*, 92, 861–870, doi: 10.1175/2010BAMS3003.1.

- Skamarock, W. C., and Coauthors (2008), A description of the advanced research WRF version 3. NCAR Technical Note TN-475+STR, 125 pp. [Available at [http://www2.mmm.ucar.edu/wrf/users/docs/arw\\_v3.pdf](http://www2.mmm.ucar.edu/wrf/users/docs/arw_v3.pdf).]
- Tapsell, S. M., E. C. Penning–Rowse, S. M. Tunstall, and T. L. Wilson (2002), Vulnerability to flooding: Health and social dimensions, *Philos. Trans. Royal Soc. A*, *360*, 1511–1525, doi: 10.1098/rsta.2002.1013.
- Terando, A. J., J. Costanza, C. Belyea, R. R. Dunn, A. McKerrow, and J. A. Collazo (2014), The southern megalopolis: Using the past to predict the future of urban sprawl in the Southeast U.S., *PLoS ONE*, *9*(7), doi:10.1371/journal.pone.0102261.
- Terti, G., I. Ruin, S. Anquetin, and J. J. Gourley (2017), A situation-based analysis of flash flood fatalities in the United States, *Bull. Amer. Meteor. Soc.*, *98*, 333–345, doi: 10.1175/BAMS-D-15-00276.1.
- Thielen, J., W. Wobrock, A. Gadian, P. G. Mestayer, J. -D. Creutin (2000), The possible influence of urban surfaces on rainfall development: a sensitivity study in 2D in the meso- $\gamma$ -scale, *Atmos. Res.*, *54*, 15–39, doi: 10.1016/S0169-8095(00)00041-7.
- United Nations (2014), World urbanization prospectus: The 2014 revision highlights, United Nations, New York [Available at <https://esa.un.org/unpd/wup/Publications/Files/WUP2014-Highlights.pdf>.]
- Velpuri, N. M., & Senay, G. B. 2013. Analysis of long-term trends (1950–2009) in precipitation, runoff and runoff coefficient in major urban watersheds in the United States. *Environmental Research Letters*, *8* doi: 10.1088/1748-9326/8/2/023020.

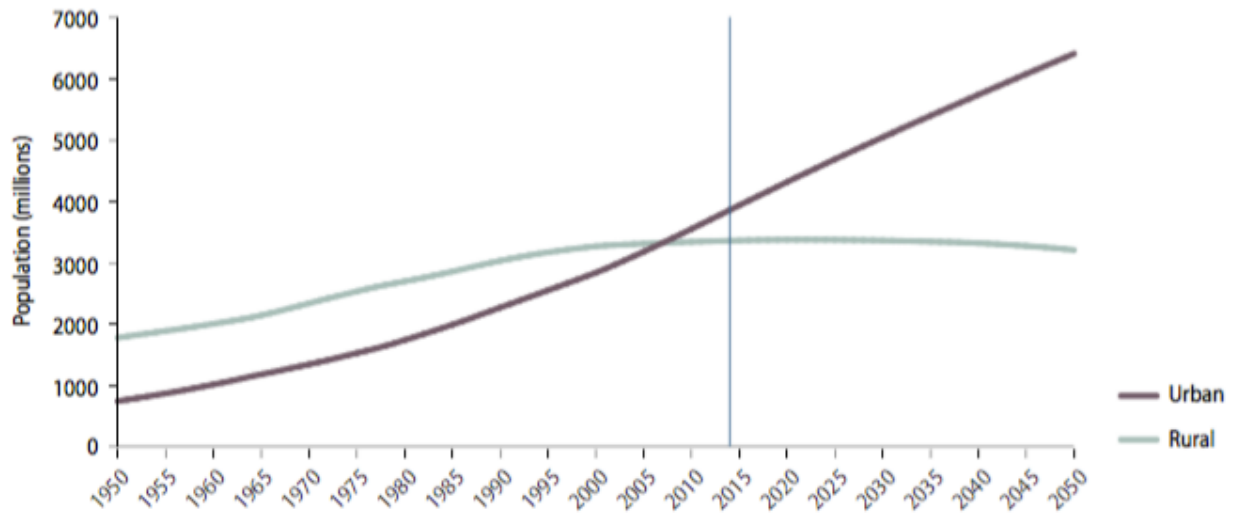


Figure 1.1. Urban and rural population trends [*United Nations*, 2014].

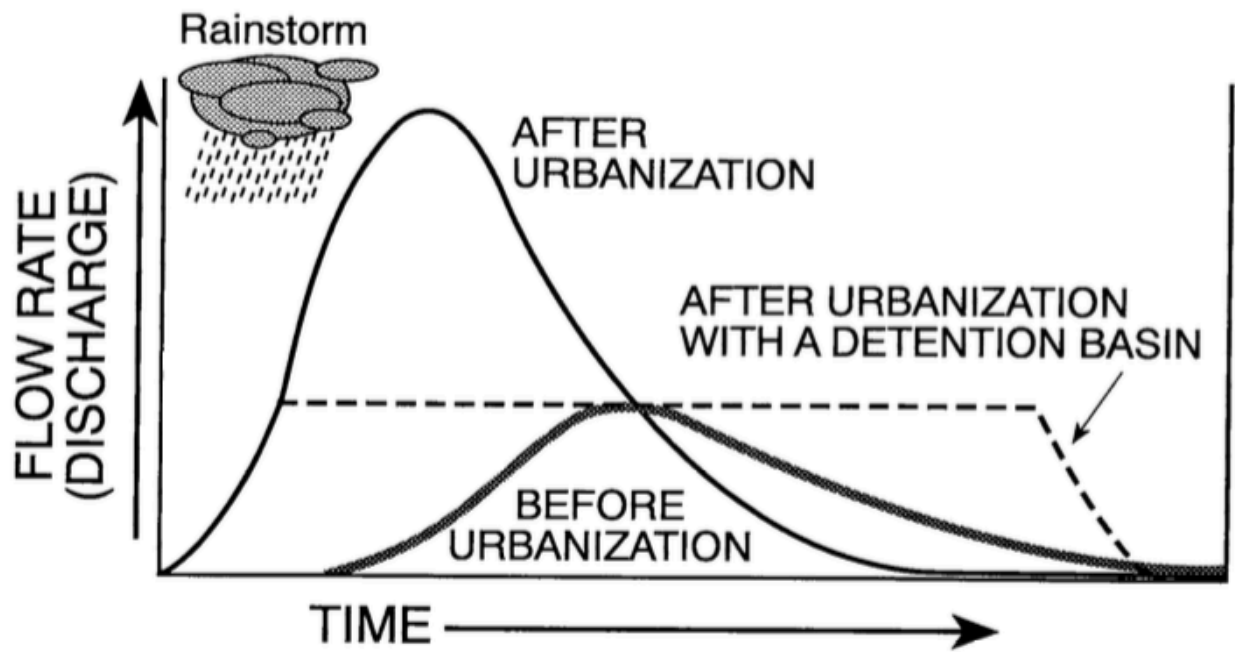


Figure 1.2. Theoretical hydrograph highlighting the influence of urbanization [*Harbor*, 1994].

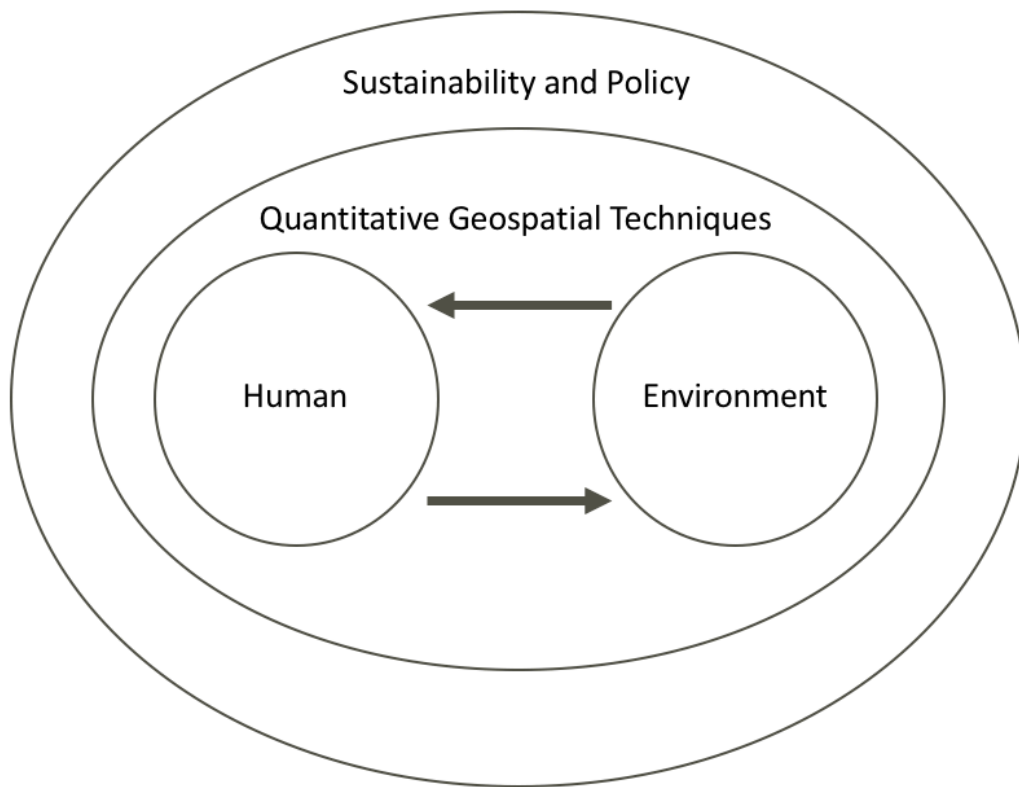


Figure 1.3. Human-Environment interactions research framework.

CHAPTER 2

THE INFLUENCE OF URBAN DEVELOPMENT PATTERNS ON STREAMFLOW  
CHARACTERISTICS<sup>1</sup>

---

<sup>1</sup> Debbage, N. and J. M. Shepherd. Submitted to *Water Resources Research*, 07/22/17.

## **Abstract**

Although it is widely recognized that urbanization has a notable impact on streamflow characteristics, the relative influence of the extent, spatial configuration, and positioning of urban development on low, high, and peak flow regimes is still not fully understood. The overarching research objective of this study was to clarify these relationships by analyzing 119 watersheds throughout the Charlanta megaregion, which stretches from Charlotte, NC to Atlanta, GA. Spatial metrics were derived from land use/land cover datasets to quantify the urban development patterns of each watershed while the streamflow characteristics were evaluated using mean daily discharge and annual peak streamflow data. Analysis of variance tests, bivariate correlations, and multivariate regression models were used to identify intra-regional variability and quantify the impact of urban development patterns on streamflow characteristics while controlling for the physical differences between watersheds. The statistical analysis revealed that increasing the extent of urban development enhanced high and low flow frequency as well as annual peak unit discharge. Therefore, urbanization within Charlanta generally produced a more extreme streamflow regime. In terms of the spatial configuration of urban development, the models indicated that more contiguous developed open space increased high and low flow frequency. Finally, the positional analysis suggested that clustering impervious surfaces in source areas distant from streams increased the frequency of high flows. The study highlights the overall importance of considering the extent, configuration, and positioning of urban development when devising land use policies aimed at minimizing streamflow alteration due to urbanization.

**Key Words:** Urban Hydrology, Urban Flooding, Low flows, Spatial Metrics, Urban Planning, Charlanta



## **2.1 Introduction**

With over half the world's population currently residing in urban areas and this proportion projected to approach 66% by 2050 [United Nations, 2014], the pressures placed on the natural environment by urban development are widely evident and likely to increase in the future. The hydrologic regimes of rivers are no exception, as continued urbanization has produced notable and widespread alterations of streamflow characteristics [DeWalle *et al.*, 2000; Poff *et al.*, 2006; Burian and Pomeroy, 2010]. The impervious surfaces, stormwater drainage systems, and compacted soils common throughout urban environments typically increase peak flows, runoff volumes, and flashiness [Leopold, 1968; Sauer *et al.*, 1984]. These alterations not only endanger urban infrastructure and human lives but also threaten the ecological sustainability of urban river systems [Ashley and Ashley, 2008; Brown *et al.*, 2009]. Consequently, moderating such impacts via effective land use planning appears imperative.

One of the original techniques utilized to encourage sustainable levels of development was the identification of total and/or effective impervious area thresholds above which urbanization noticeably degraded natural streamflow characteristics [Klein, 1979; Schueler, 1994; Booth and Jackson, 1997; Wang *et al.*, 2001; Shuster *et al.*, 2005; Schueler *et al.*, 2009]. Although such thresholds can inform best management practices, they often fail to explicitly address how the urban development is configured spatially and positioned within watersheds [Brabec, 2009]. Therefore, studies have begun exploring the influence of the spatial configuration of urban land use and the positioning of impervious surfaces, either near watershed outlets or in more distant headwaters, on streamflow characteristics to guide more precise land use planning measures.

Developing watershed headwaters is theorized to produce larger peak discharges because the time of concentration is reduced, which superposes the peaks observed in the distant portions of the watershed with those closer to the outlet [*Beighley and Moglen, 2002*]. However, studies based upon stream gage observations have largely been unable to establish clear statistical relationships between the positioning of urban development and streamflow responses [*Sauer et al., 1984; Beighley and Moglen, 2002; Beighley and Moglen, 2003; Wright et al., 2012; ten Veldhuis et al., 2017; Zhou et al., 2017*]. Modeling efforts evaluating hypothetical distributions of imperviousness have more successfully revealed that clustering urban development in headwater locations and source areas increases peak flows on an annual and individual storm basis [*Mejia and Moglen, 2009; Mejia and Moglen, 2010*]. The hydrologic influence of the spatial configuration of urban development, rather than its relative positioning within watersheds, has been analyzed less frequently, with more fragmented and less connected urban land use configurations generally found to minimize the impacts of urbanization on streamflow [*McMahon et al., 2003; Olivera and DeFee, 2007; Kim and Park, 2016*].

Although past studies have highlighted the importance of urbanization in governing streamflow characteristics, this paper aims to address several notable gaps present within the literature. Firstly, the inability of observational studies to identify consistent statistical relationships between the positioning of urban development and streamflow responses highlights the necessity of developing more nuanced methodologies for quantifying the relative positioning of impervious surfaces within watersheds. Relying upon simplistic measures, such as calculating the percentage of urban development within each quarter of a given watershed, may explain why modeling efforts have largely been more successful in elucidating these relationships. Secondly, the generalizability of the findings from previous studies may be limited because they often

analyze a small number of watersheds [e.g., *Beighley and Moglen*, 2003; *Olivera and DeFee*, 2007; *Roberts*, 2016]. The lack of substantial sample sizes has also prevented the widespread usage of rigorous multivariate statistical techniques, as the measures evaluating the positioning and spatial configuration of urban development are commonly used as qualitative aides when interpreting various streamflow responses [e.g., *Olivera and DeFee*, 2007; *Wright et al.*, 2012]. These concerns have led to numerous calls for studies with larger sample sizes to evaluate the generalizability of the relationships between urban development patterns and streamflow characteristics [*Olivera and DeFee*, 2007; *Roberts*, 2016].

Finally, apart from *McMahon et al.* [2003], previous research has focused primarily on how urban development patterns influence peak flows [*Ferguson and Suckling*, 1990; *Hamel et al.*, 2015]. Although peak flows are relevant to damaging flood events, baseflow alterations can have equally important ecological ramifications [*Poff et al.*, 2006]. Additionally, the relationships between urbanization and low flow patterns remain unclear [*Meyer*, 2005; *Brown et al.*, 2009; *Bhaskar et al.*, 2016]. Urban areas have traditionally been hypothesized to reduce baseflow due to the increased runoff from impervious surfaces limiting infiltration and groundwater recharge [*Leopold*, 1968; *Rose and Peters*, 2001; *Price*, 2011]. Conversely, leaky water infrastructure and irrigation can increase groundwater recharge and help sustain baseflow in certain urban settings [*Bhaskar et al.*, 2016]. Conflicting results have also emerged regarding the influence of urban development on annual peak streamflow. Urbanization is generally theorized to have less influence on annual peak discharges, relative to more frequent high flows, because the natural land cover is often saturated and effectively impervious during such events [*Hollis*, 1975; *Sauer et al.*, 1984; *Smith et al.*, 2002]. However, several studies have detected increasing trends in annual peak discharge due to urbanization [*Sheng and Wilson*, 2009; *Yang et*

*al.*, 2013] while others have reaffirmed that urbanization has no significant influence on annual peak streamflow [*Villarini et al.*, 2013].

The overarching goal of this study was to provide a comprehensive assessment of the relationships between urban development patterns and streamflow characteristics by addressing the shortcomings discussed above. Spatial metrics were utilized in conjunction with multivariate regression modeling to quantitatively describe the relative influence of the extent, spatial configuration, and positioning of urban development on low, high, and annual peak flows. The following section outlines the study watersheds in more detail as well as the data and methodologies used to quantify the streamflow characteristics and urban development patterns. The results are discussed in Section 2.3. Finally, Section 2.4 summarizes the main findings and explores the potential urban planning implications of the research.

## **2.2 Data and Methods**

### **2.2.1 Study Watersheds**

In total, 119 watersheds were analyzed throughout the Charlanta megaregion, which incorporates the Atlanta (ATL), Greenville, Spartanburg, Anderson (GSP), and Charlotte (CHA) Metropolitan Statistical Areas (MSAs) along the I-85 corridor [*Florida et al.*, 2008; *Shepherd et al.*, 2013; *Mitra and Shepherd*, 2016] (Figure 2.1). The study focused on Charlanta because its impervious footprint is projected to expand notably [*Terando et al.*, 2014] and heighten the pressures placed on river systems if additional land use guidelines are not implemented. Future urban expansion is particularly problematic given that Charlotte and Atlanta are already ranked as the 5<sup>th</sup> and 7<sup>th</sup> flashiest cities in the contiguous United States, respectively [*Smith and Smith*, 2015]. Finally, analyzing the entire Charlanta megaregion also helped assess the generalizability of the relationships between urban development patterns and streamflow characteristics.

The individual watersheds included in the analysis were selected primarily based upon continuous United States Geological Survey (USGS) stream gage data availability between 2009 and 2013 (Figure 2.1). The timeframe of the analysis was centered on 2011 because it was the vintage of the land use dataset used to quantify the patterns of urban development. Importantly, the five-year study period enabled a climatologically representative precipitation sample and was brief enough to reasonably assume that the 2011 land use was representative for the entire timeframe. Specifically, the average annual precipitation over the five-year period was 2.14 cm and 5.75 cm greater than the climatological normal value for Charlotte (105.74 cm) and Atlanta (126.26 cm), respectively [NWS, 2017a; NWS, 2017b]. The stream gages included in the study were also required to be in the Geospatial Attributes of Gages for Evaluating Streamflow (GAGES-II) dataset [Falcone, 2011], as it provided an extensive suite of variables describing the physical characteristics of the watersheds and delineated the watershed boundaries. Characteristics of the study watersheds are detailed in Table 2.1. The study watersheds had a median area of 77 km<sup>2</sup> because large rivers highly regulated by dam infrastructure, such as the Chattahoochee, Savannah, and Catawba, were avoided. Overall, the watersheds evaluated a gradient of urban intensities, with the GSP watersheds generally exhibiting lower levels of urban development.

### 2.2.2 Quantifying Streamflow Characteristics

Mean daily discharge and annual peak streamflow data were obtained from the USGS National Water Information System for each study watershed. A peaks-over-threshold (POT) technique was used to analyze the mean daily discharge because it allows for multiple high and low flow events within a given year [Villarini *et al.*, 2013]. This was particularly appropriate for analyzing the effects of urbanization since they are often most pronounced during more frequent,

lower magnitude high flow events [Hollis, 1975]. High and low flow frequency were evaluated by calculating the number of days during which the daily mean discharge remained above the 75<sup>th</sup> and below the 25<sup>th</sup> percentile for a given gage, respectively. The percentile values were based upon daily mean discharge data during the 2009–2013 study period. Threshold exceedances on consecutive days were considered only once to avoid double counting the same event. The number of exceedances was summarized from 2009 to 2013 and divided by five, producing a long-term annual average that minimized the influence of climatic variability. Although the POT analysis was likely sensitive to the specific thresholds selected, the 75<sup>th</sup> and 25<sup>th</sup> percentiles have been successfully used previously to identify high and low flow frequency [Hamel *et al.*, 2005; Hopkins *et al.*, 2015].

Figure 2.2 provides an example of the thresholding approach for one year of daily streamflow data at Peachtree Creek, which is a highly-urbanized watershed in Atlanta. Utilizing mean daily streamflow may potentially underestimate the influence of urban development in certain cases, but POT analysis of mean daily discharge is a widely adopted technique used to quantify the effects of urbanization on streamflow characteristics [e.g., Villarini *et al.*, 2013; Yang *et al.*, 2013; Hamel *et al.*, 2015; Hopkins *et al.*, 2015; Diem *et al.*, 2017]. The annual peak streamflow data required less processing, as it was converted to cubic meters per second, averaged over the five-year study period, and standardized by watershed area to produce annual average peak unit discharge [Choi *et al.*, 2016].

### 2.2.3 Quantifying Urban Development Patterns

The metrics used to quantify the extent, spatial configuration, and positioning of urban development within each watershed were derived from the 2011 National Land Cover Database (NLCD) [Homer *et al.*, 2015]. The 2011 NLCD was selected due to its relatively high spatial

resolution of 30 meters and detailed urban classification scheme. Specifically, the variables describing the positioning of urban development were derived from the 2011 NLCD percent developed raster, which specifies an imperviousness value ranging from 0 to 100 for each cell. Four positioning variables were calculated to explore the potential differences between traditional and more complex approaches. First, a partitioning technique similar to past studies was performed [*Beighley and Moglen, 2002*]. Each watershed was partitioned into a top and bottom half using one half of the longest drainage path length as the dividing threshold. The difference between the mean imperviousness of the top and bottom half was calculated, with positive values indicating that the headwaters were more heavily developed. The second positioning variable was the outlet imperviousness gradient. It was determined by measuring the distance of each pixel to the watershed outlet and calculating the relationship between those distances and the cell imperviousness values using ordinary least squares (OLS) regression. Larger positive values indicate that imperviousness increased more notably with distance from the watershed outlet. Thus, the outlet imperviousness gradient was conceptually analogous to the watershed partitioning technique although its calculation was more complex and less sensitive to arbitrary partitioning thresholds.

The third approach was a river imperviousness gradient designed specifically to evaluate the degree to which the positioning of urban development mirrored the hypothetical source clustering scenario of *Mejia and Moglen [2010]*, which according to their modeling experiments increased peak flows more substantially than clustering development near river channels. The river imperviousness gradient was calculated by measuring the distance of each pixel to the nearest river feature, as defined by the National Hydrography Dataset (NHD) flowlines, and determining the relationship between those distances and the cell imperviousness values using

OLS regression. Larger positive values suggest that imperviousness increased more notably with distance from the river features, which would be indicative of source clustering. The methodology of this approach was similar to the outlet imperviousness gradient, but it evaluated a fundamentally different positioning pattern. The final positioning variable evaluated the intensity of urban development within the riparian zone of each watershed by calculating the average imperviousness within 150 meters of the NHD flowlines. The 150-meter threshold was selected because it is the maximum recommended width of riparian buffers for flood attenuation purposes [Fischer and Fischenich, 2000].

To determine the extent and spatial configuration of urban development, spatial metrics were calculated using the FRAGSTATS software package [McGarigal *et al.*, 2012]. The spatial metrics were derived from the 2011 NLCD land cover dataset, which includes 20 land use/land cover (LULC) categories with four devoted to urban land uses of various intensities. Although a wide variety of spatial metrics exist, those most frequently utilized in studies focusing on urban development were selected [Debbage *et al.*, 2016]. Table 2.2 describes the six class-level metrics included in the analysis, which evaluated different aspects of urban morphology. Percentage of the landscape (PLAND) is a basic composition metric that quantifies the relative extent of urban development as a percentage of the total watershed area. The shape complexity of the urban land use was evaluated by the area-weighted mean shape index (AWMSI) and edge density (ED). AWMSI uses a modified perimeter-area ratio to evaluate shape complexity while ED compares the total urban edge length to the watershed area. In both cases, larger values are indicative of increasingly complex and irregular urban forms.

The degree of urban fragmentation in the watersheds was determined by the patch density (PD), largest patch index (LPI), and percentage of like adjacencies (PLADJ). PD counts the



number of urban patches within the watershed, which is subsequently standardized by watershed area. LPI evaluates the dominance of the largest urban patch by dividing its area by the watershed area. Finally, PLADJ provides a pixel-based measure of fragmentation by calculating the number of like adjacencies involving urban pixels relative to the total number of adjacencies involving urban pixels. Smaller LPI and PLADJ values as well as larger PD values are associated with less contiguous and more fragmented urban morphologies. Although this study focused primarily on the metrics calculated for the four NLCD urban land uses, the spatial metrics in Table 2.2 were derived for all the LULC categories present within each watershed.

#### 2.2.4 Statistical Analysis

Several statistical tests were used to analyze the variability of streamflow within the Charlanta megaregion and determine the influence of urban development patterns on streamflow characteristics. Firstly, analysis of variance (ANOVA) tests were conducted with MSA as the grouping variable to identify if the streamflow characteristics varied across the Charlanta megaregion. ANOVA tests were performed for the three streamflow metrics as well as the variables describing the patterns of urban development and physical characteristics of the watersheds to explain any observed dissimilarities in streamflow. Tukey's honest significant difference (HSD) tests were subsequently used to identify the specific MSAs that exhibited statistically significant differences [Tukey, 1949].

The variables that characterized the physical properties of the watersheds in the ANOVA tests and additional statistical analysis described below were obtained from the GAGES-II dataset [Falcone, 2011]. Although numerous variables were considered, several were central to the study including the: percentage of watershed surface area covered by lakes, ponds, and reservoirs (Lake Storage), ratio of baseflow to total streamflow (Baseflow Index), percentage of

soils in hydrologic soil groups A and B (Soil Groups A & B), mean annual precipitation within the watershed (Mean Ann. Precip.), and percentage of total streamflow produced by Horton overland flow.

To gain a further understanding of the relationships, bivariate Pearson correlation coefficients were calculated between the three streamflow variables and each of the measures evaluating the extent, spatial configuration, and positioning of urban development. Correlations were also calculated between the streamflow metrics and the potential control variables extracted from the GAGES-II dataset. More complex multivariate modeling was then explored to quantify the relative influence of urban development patterns on streamflow characteristics while controlling for potential confounding factors. The high threshold exceedances per year, low threshold exceedances per year, and annual average peak unit discharge were the dependent variables in the three OLS regression models estimated. The independent variables considered for inclusion in the models described the urban development patterns as well as the physical differences between the watersheds. The variables ultimately included in the models were selected manually based upon the bivariate analysis and regression diagnostics to avoid the potential issues associated with stepwise regression [Ssegane *et al.*, 2012]. The error terms of the models were assessed for heteroscedasticity, normalcy, and spatial autocorrelation using the Breusch-Pagan [Breusch and Pagan, 1979], Shapiro-Wilk [Shapiro and Wilk, 1965], and Moran's I tests [Moran, 1950], respectively. The degree of multicollinearity amongst the independent variables was evaluated through variable inflation factors (VIFs) [Marquardt, 1970]. Finally, potential outliers were detected using Cook's D [Cook and Weisberg, 1982] and DFBETAs [Belsley *et al.*, 1980].

The model diagnostics revealed that the assumptions of OLS regression were appropriate in most cases. Outliers were not a concern, as the Cook's D values of the three multivariate regression models were all less than 0.20 and the DFBETAs remained below 0.80. Multicollinearity amongst the independent variables was also not detected since the VIFs never exceeded 2. The p-values of the Breusch-Pagan and Shapiro-Wilk tests never fell below 0.05 so the null hypotheses of homoscedastic and normally distributed residuals were not rejected. However, the low threshold exceedances and annual average peak unit discharge models were estimated using a natural logarithm transformation of the dependent variables. The original statistical distribution of these dependent variables exhibited positive skewness, which resulted in the non-transformed models failing the diagnostic test for normally distributed residuals. Finally, Moran's I tests were performed to evaluate the degree of spatial autocorrelation amongst the residuals. A k-nearest neighbors approach was used to conceptualize the spatial relationships due to the varying density of stream gages across the megaregion. Specifically, the four gages nearest the gage of interest were considered its neighbors. This small neighborhood was utilized since spatial autocorrelation was most apparent at local rather than regional scales, which was likely attributable to the inclusion of nested watersheds in the sample. The Moran's I tests revealed that only the residuals of the annual average peak unit discharge model exhibited significant spatial autocorrelation. Therefore, a spatial error model (SEM) was also estimated for the annual peak unit discharge to enable comparisons with the OLS results [Anselin, 1988].

## **2.3 Results and Discussion**

### **2.3.1 Spatial Distribution of Streamflow Characteristics and Intra-Charlanta Variability**

The streamflow variables were initially mapped to gain a basic understanding of their spatial distributions throughout Charlanta. Figures 2.3-2.5 illustrate that the high and low

threshold exceedances were greatest proximate to the urban cores of each MSA. Therefore, urban development throughout Charlanta appeared to increase both high and low flow frequency, although the spatial distribution of low threshold exceedances did not align with urban land uses as consistently. The overall spatial patterns also suggest that the specific percentiles selected for the POT analysis were generally sensitive to the degree of urbanization. Unlike the threshold exceedances, annual average peak unit discharge generally exhibited a more ambiguous qualitative relationship with urbanization. This highlights the potential weaker influence of impervious surfaces on annual peak streamflow [e.g., *Hollis*, 1975; *Sauer et al.*, 1984]. In the case of Atlanta, the spatial mismatch between urbanized areas and large peak unit discharge values was partially attributable to the average peak streamflow being influenced by the extreme 2009 flood event [*Shepherd et al.*, 2011].

A quantitative examination of the spatial distributions was achieved by calculating correlation coefficients between the threshold exceedances and the distance to the central business district (CBD) of each MSA (Figure 2.6). The city halls of Atlanta, Charlotte, and Greenville served as proxies for the CBD locations [*U.S. Census Bureau*, 2012]. The high threshold exceedances exhibited a significant negative correlation with distance to the CBD for each MSA. Loess curves fitted to the scatterplot revealed a substantial upturn in high threshold exceedances between 15 and 30 km away from the CBDs, which corresponds roughly with the location of the perimeter highways of each city (i.e. I-285, I-485, and I-185). The increase in high threshold exceedances was most gradual for Atlanta, likely reflecting the expansive low-density urban development beyond the I-285 perimeter.

The low threshold exceedances displayed weaker negative correlations with distance from the CBD that were significant for Atlanta and Charlotte. The lack of a statistically

significant relationship in Greenville was largely due to the Reedy River stream gage near Waterloo, SC, which exhibited numerous low threshold exceedances despite its distance from the CBD. The enhanced low flow frequency near Waterloo likely occurred because the large areal extent of the watershed actually incorporated the urban core of Greenville. This highlights a shortcoming of using distance to the CBD as a proxy for urbanization, particularly for larger watersheds. When the Reedy River outlier was omitted, the correlation was significant ( $r = -0.57$ ;  $p = 0.03$ ) and similar to the coefficients calculated for the other MSAs. Finally, the low threshold exceedances demonstrated a less pronounced upturn within the 15-30 km window, as the relationships between distance to the CDB and low flow frequency appeared more linear.

The ANOVA and Tukey HSD tests revealed additional intra-regional variability. Charlotte exhibited a significantly higher number of low and high threshold exceedances compared to Atlanta and Greenville (Figure 2.7a). Furthermore, the number of high threshold exceedances observed in Atlanta was significantly greater than in Greenville. These findings suggest that urban development in Charlotte altered the natural streamflow regime more substantially than in Greenville or Atlanta. The differences in annual average peak unit discharge were less notable, as Charlotte and Atlanta displayed a similar range of values (Figure 2.7b). Greenville exhibited a significantly lower annual peak unit discharge than Charlotte and Atlanta. This was largely attributable to the greater areal extent of the Greenville watersheds, which resulted in smaller values when standardizing annual peak discharge by watershed area. The raw annual peak streamflow values were also analyzed and revealed no significant intra-regional differences.

The dissimilarities in the number of threshold exceedances between the Charlanta MSAs can be partly explained by differing urban development patterns. Specifically, the Greenville

watersheds appeared to be less urbanized than their counterparts in Atlanta and Charlotte across all urban intensity categories (Figure 2.8a), although these differences were only statistically significant ( $p\text{-value} < 0.05$ ) for low and medium intensity development. The lower levels of urbanization within Greenville watersheds likely contributed to the smaller number of threshold exceedances. Disparities in the extent of urban development did not explain the greater number of threshold exceedances observed in Charlotte relative to Atlanta, as the two MSAs exhibited no significant differences in the percentage of watershed area developed. Considering the contiguity of urban development helped further elucidate the variability of threshold exceedances between the MSAs (Figure 2.8b). The significantly less contiguous low and medium intensity development within Greenville watersheds likely further moderated high and low flow frequency. Differences in the contiguity of urban development were also observed between Atlanta and Charlotte. Specifically, Charlotte exhibited significantly higher levels of contiguity for developed open space, which likely contributed to the greater number of threshold exceedances observed in Charlotte relative to Atlanta. The important role of developed open space in governing the flood response of urbanized watersheds in Charlotte has also been identified by *Zhou et al.* [2017] and may potentially be related to the hydrologic properties of urban soils. These results highlight the importance of analyzing both the extent and configuration of urban development across a range of intensity levels to better understand the variable effects of urbanization on streamflow and potentially inform more detailed land use policies.

In addition to the disparate urban development patterns, differences in the natural properties of the watersheds also likely influenced the number of threshold exceedances observed in each MSA. Mean annual precipitation was significantly lower for Charlotte watersheds relative to Atlanta and Greenville (Figure 2.9a). Although less precipitation may have

contributed to the elevated number of low threshold exceedances in Charlotte, due to the increased likelihood for prolonged dry periods, it did not explain the greater number of high threshold exceedances. This apparent discrepancy was likely due to the mean annual precipitation not fully resolving the warm season thunderstorms that are primarily responsible for floods in Charlotte [Zhou *et al.*, 2017]. The percentage of Horton overland flow and baseflow provided more consistent explanations of the elevated threshold exceedances observed in Charlotte. The percentage of Horton overland flow was significantly higher in Charlotte relative to the other MSAs while baseflow contributions were significantly lower (Figure 2.9b-c). A greater propensity for Horton overland flow (i.e., infiltration excess flow) in Charlotte likely produced a more consistent rapid runoff response, resulting in more frequent high threshold exceedances. Additionally, the lower percentage of baseflow in Charlotte suggests that streamflow becomes stressed during prolonged dry periods, which would enhance low flow frequency. These hydrologic properties that potentially influenced the threshold exceedances are related to underlying geological differences between the watersheds. Charlotte watersheds contained a significantly lower percentage of hydrologic group A and B soils, which are characterized by moderate to high infiltration rates (Figure 2.9d). Overall, the natural factors likely worked in tandem with the differing urban development patterns to produce variable POT results within the megaregion.

### 2.3.2 Correlations between Streamflow Characteristics and Urban Development Patterns

To initially identify the aspects of urban development that were influential in governing streamflow, correlations were calculated between the streamflow characteristics and the variables describing the urban development patterns. The POT correlation analysis revealed that more urbanized watersheds exhibited a significantly greater number of high and low threshold

exceedances (Figure 2.10). This suggests that urbanization within Charlanta not only enhanced high flow frequency but also low flow frequency. Therefore, the reduction of groundwater recharge and baseflow throughout the megaregion due to impervious surfaces inhibiting infiltration appeared to outweigh urban contributions to baseflow (e.g., water infrastructure leakage, irrigation). The low threshold exceedances did exhibit weaker correlations than the high threshold exceedances with the percentage of the watershed developed, which was likely indicative of the more complex pathways through which urbanization influences low flow regimes [Bhaskar *et al.*, 2016].

The extent of the intermediate urban classes displayed the strongest correlations with both the low and high threshold exceedances (Figure 2.10b, 2.10c). The weaker relationships for developed open space were likely attributable to the larger quantities of natural vegetation allowed within the category obfuscating the connections between urbanization and enhanced low and high flow frequency. Additionally, developed open space often incorporates forms of low-density residential development that rely upon septic tanks, which further complicates the relationship between urbanization and low threshold exceedances [Burns *et al.*, 2005]. At the opposite end of the urban intensity spectrum, high intensity development displayed weaker correlations because many of the sampled watersheds contained small percentages of such development (Figure 2.10d). The dotted loess curves in the scatterplot suggest that the relationships were perhaps more exponential in nature, as the number of threshold exceedances increased notably with the percentage of high intensity development until roughly 5% after which the relationships weakened. Importantly, this implies that urban modifications of high and low flow regimes may even occur in watersheds with small quantities of high intensity



development (e.g., 5% of the watershed area), which highlights the potential tenuous nature of threshold-based land use policies [Mejia and Moglen, 2009].

The urban configuration metrics were also significantly ( $p < 0.05$ ) correlated with the threshold exceedances, but they were sensitive to the extent of urban development within the watersheds (PLAND). Table 2.3 provides the correlations, averaged over the four NLCD urban intensity classes, of each configuration metric with the high and low threshold exceedances as well as PLAND. ED exhibited the strongest correlations with the threshold exceedances, but it evaluated an aspect of urban configuration heavily influenced by PLAND ( $r = 0.97$ ). Although there is often some degree of redundancy between composition and configuration spatial metrics, the small areal extent of the watersheds potentially exacerbated this issue for ED. PD and PLADJ displayed stronger relationships with the threshold exceedances while being less influenced by PLAND. The positive correlations suggest that more contiguous urban development and a greater number of urban patches enhanced both high and low flow frequency. The large average correlation with the threshold exceedances exhibited by PD was driven by the patchiness of high intensity development whereas for PLADJ it was due to the contiguity of developed open space and low intensity development. This implies that the number of high intensity urban patches has a notable influence on low and high flow frequency because each patch substantially alters natural runoff processes regardless of its contiguousness. Conversely, the contiguity of less intense urban development was more relevant because a certain degree of contiguousness likely must be achieved before urbanization incorporating greater quantities of natural vegetation alters streamflow characteristics considerably.

The relationships between urban development patterns and annual average peak unit discharge were analyzed as well. The majority of the spatial metrics failed to exhibit significant

correlations with the raw peak streamflow values due to the differences in watershed area, but more urbanized watersheds displayed significantly higher annual average peak unit discharge (Figure 2.11). The correlations, however, were smaller than those calculated for the threshold exceedances, which highlights the weaker influence of urban development on the magnitude of larger, more infrequent floods [e.g., *Hollis*, 1975]. Additionally, this suggests that utilizing a higher threshold to quantify high flow frequency in the POT analysis would yield weaker correlations as well. The urban configuration metrics also generally exhibited smaller correlations with annual peak unit discharge that were occasionally not statistically significant across all four urban categories (Table 2.3). Nevertheless, these results indicate that urbanization within Charlanta increased the magnitude of annual peak streamflow in addition to enhancing low and high flow frequency. This supports the notion that positive temporal trends in annual peak streamflow may be due to watersheds undergoing urbanization [*Sheng and Wilson*, 2009; *Yang et al.*, 2013]. Collectively, the significant correlations imply that urban land use policies designed to manage the extent and configuration of urban development could potentially reduce urban alterations of low, high, and peak flows.

The final urban development pattern evaluated was the positioning of impervious surfaces throughout the watersheds. Correlations between the streamflow characteristics and the positioning variables were analyzed individually for each MSA because the results varied throughout the megaregion. Only Atlanta displayed a significant correlation between high threshold exceedances and the imperviousness difference between the top and bottom half of the watersheds (Figure 2.12a). The positive correlation suggests that in Atlanta clustering urban development in distant headwaters increased high flow frequency as hypothesized by previous studies [*Beighley and Moglen*, 2002]. However, the insignificant correlations for Greenville and

Charlotte highlight the inconsistent nature of this relationship, which may partly explain the inconclusive findings of past studies using similar positioning measures [e.g., *Beighley and Moglen*, 2003]. The relationship in Atlanta was likely significant because several of the watersheds exhibited simplistic distributions of imperviousness with distinct divisions between the top and bottom halves. Most notable were the Proctor Creek and Intrenchment Creek watersheds, which each contain a large portion of Atlanta's CBD in their headwaters (Figure 2.13). The urban development in the other MSAs appeared to be more complexly distributed throughout the watersheds and was thus less suitably described by mean imperviousness difference. Overall, this suggests that simplistic difference measures may be useful when the observed positioning of urban development closely mirrors idealistic scenarios, such as in Atlanta, but they may fail to capture the influence of more complex positioning patterns on high flow frequency.

The correlations between the outlet imperviousness gradient and high threshold exceedances (Figure 2.12b) largely mirrored the mean imperviousness difference results, which was anticipated given that it evaluated the same fundamental positioning pattern albeit via a more complex methodology. Conversely, mean imperviousness of the riparian zone was more consistently related to the high threshold exceedances and exhibited statistically significant positive correlations for each MSA (Figure 2.12c). The correlations were also stronger than those calculated between the extent of urban development and high flow frequency, illustrating the importance of the positioning of urban development within watersheds. Highly vegetated riparian zones likely provided a critical buffering mechanism by attenuating surface runoff, which emphasizes the need to preserve and expand existing riparian corridors throughout Charlanta.

The river imperviousness gradient, which evaluated how rapidly imperviousness within the watersheds increased with distance from the nearest river feature, was the final positioning metric considered. It exhibited significant positive correlations with the high threshold exceedances for each MSA (Figure 2.12d). This suggests that enhancing the imperviousness gradient by clustering urban development in source areas distant from river features would increase high flow frequency. Therefore, these findings support the hypothesis that developing source areas increases high flows because the time of concentration is reduced, superposing the peaks observed in the distant portions of the watershed with those closer to the outlet [Beighley and Moglen, 2002]. The river imperviousness gradient overall appeared to be a more robust and informative positioning metric from an urban land use planning perspective than the imperviousness difference calculation because it better acknowledged the complexity of urban land use distributions throughout the watersheds.

The relationships between the positioning variables and low threshold exceedances as well as annual peak unit discharge were also considered (Table 2.4). Generally, the results were similar to those observed for high flow frequency. The mean imperviousness difference and outlet imperviousness gradient only exhibited significant correlations for Atlanta, further demonstrating their inability to capture urban positioning patterns broadly relevant to streamflow characteristics. Conversely, mean imperviousness of the riparian zone and the river imperviousness gradient exhibited more consistent relationships with both the low threshold exceedances and annual peak unit discharge. The imperviousness of the riparian zone displayed significant positive correlations with the low threshold exceedances of each MSA and with annual peak unit discharge for each MSA except Greenville. This implies that the storage provided by highly vegetated riparian corridors can help sustain low flows during dry periods

and attenuate extreme flood events, which emphasizes the importance of land use policies protecting these corridors. Similarly, the river imperviousness gradient was significantly correlated with the low threshold exceedances and annual peak unit discharge for all the Charlanta MSAs except annual peak unit discharge in Greenville. The positive correlations indicate that clustering urban development in source areas and enhancing the river imperviousness gradient would increase annual peak streamflow and low flow frequency. While annual average peak unit discharge is potentially enhanced by a greater river imperviousness gradient due to mechanisms similar to those outlined for high threshold exceedances, the physical linkages for low flow frequency are less clear.

### 2.3.3 Multivariate Regression Models

Multivariate regression models were used to control for potential confounding factors, such as the physical differences between the watersheds, and better understand the relative influence of the extent, spatial configuration, and positioning of urban development on streamflow characteristics. Overall, the models performed well as they explained between 56 and 90 percent of the variability in streamflow characteristics (Tables 2.5-2.6). The explanatory power of the models largely mirrored the bivariate correlation results, as the R-squared was largest for the high threshold exceedances model and smallest for the annual average peak unit discharge model.

The partial slope coefficients of the high threshold exceedances model indicated that the extent, configuration, and positioning of urban development all had significant effects on high flow frequency even when controlling for physical differences between the watersheds (Table 2.5). A ten-percentage point increase in the extent of medium intensity development (PLAND Class 23) was predicted to enhance high threshold exceedances per year by 8.1 while a ten-

percentage point increase in the contiguity of developed open space (PLADJ Class 21) was estimated to enhance high threshold exceedances per year by 2.8. A greater river imperviousness gradient (River Imp. Gradient) was also predicted to significantly elevate high flow frequency although the coefficient magnitude was modest, as a 0.01 increase in the gradient was estimated to enhance high threshold exceedances per year by 0.59. The standardized regression coefficients also suggested that the positioning of urban development was of secondary importance relative to the extent and contiguity of urbanization. Finally, the control variables had a significant moderating influence on high flow frequency. A one-percentage point increase in the watershed area covered by lakes and/or reservoirs (Lake Storage) was predicted to reduce high threshold exceedances per year by 3.3, which was likely due to the increased storage capacity delaying runoff. Additionally, a ten-percentage point increase in the Baseflow Index was estimated to decrease high threshold exceedances per year by 1.9 because a larger baseflow proportion is associated with a greater propensity for runoff to reach streams via slower subsurface pathways.

For the low threshold exceedances model, the unstandardized coefficients were much smaller in magnitude and interpreted differently due to the natural logarithm transformation of the dependent variable (Table 2.5). Importantly, the river impervious gradient was not significantly related to low flow frequency in the multivariate analysis and was excluded from the final model. The extent of medium intensity development (PLAND Class 23) exhibited a significant partial slope coefficient, as a ten-percentage point increase was estimated to enhance low threshold exceedances by 24%. The contiguity of developed open space (PLADJ Class 21) also significantly influenced low flow frequency with a ten-percentage point increase predicted to enhance low threshold exceedances by 11%. The partial slope coefficients of the control variables were significant and moderated low flow frequency. A 10 cm increase in mean annual

precipitation (Mean Ann. Precip.) was estimated to decrease low threshold exceedances by 7%. Finally, an increase in the percentage of soils within hydrologic groups A and B (Soil Groups A & B) by ten-percentage points was predicted to decrease low threshold exceedances by 2%, which was expected since these soils are characterized by moderate to high infiltration rates and help sustain baseflow.

The annual average peak unit discharge results from both the OLS model and SEM are provided in Table 2.6. The SEM likely provided more robust estimates, as the spatial autoregressive coefficient  $\lambda$  was significant and the Akaike Information Criterion (AIC) was lower. However, since the coefficient values estimated using the OLS model and SEM were similar, particularly when considering their standard errors, only the results from the OLS model are discussed further to enable more direct comparisons with the POT models. The partial slope coefficient for the extent of low intensity development (PLAND Class 22) was significant, as a ten-percentage point increase was estimated to enhance annual peak unit discharge by 29%. However, the standardized regression coefficient for the extent of urban development in the annual peak unit discharge model (0.33) was smaller than its counterparts in the high (0.54) and low (0.44) threshold models. This suggests that the extent of urban development significantly influences peak streamflow, but the magnitude of this impact is modest relative to urban effects on more frequent high and low flow events. Additionally, the variables describing the spatial configuration and positioning of urban development were not significantly related to annual peak unit discharge within the multivariate context. This lack of significant relationships may be partly due to evaluating peak streamflow only at the watershed outlet, which likely emphasized the importance of the extent of urban development rather than its positioning or spatial configuration.

The remaining variables included in the model accounted for important natural differences between the watersheds that moderated annual peak unit discharge. Increasing the contiguity of woody wetlands (PLADJ Class 90) ten-percentage points was predicted to reduce peak unit discharge by approximately 46%, as more contiguous woody wetlands were often indicative of unfragmented and heavily vegetated riparian zones. Finally, a greater quantity of lake/reservoir storage (Lake Storage) and a larger proportion of baseflow (Baseflow Index) also significantly reduced annual average peak unit discharge.

## **2.4 Conclusions and Urban Planning Implications**

By analyzing the statistical relationships between urban development patterns and numerous streamflow characteristics across the Charlanta megaregion, this study aimed to further elucidate the role of urbanization in altering streamflow. The correlation analysis revealed that greater levels of urban development not only increased high threshold but also low threshold exceedances. Thus, urbanization within Charlanta appeared to produce a more extreme streamflow regime where both high and low flows were more frequent. This twofold impact of urban development has clear societal and ecological ramifications. Increased high flows enhance the potential for flood damage and stream bank erosion while more frequent low flows increase the likelihood of high water temperatures and contaminant concentrations that can ultimately alter in-stream species assemblages [Welty, 2009; O'Driscoll *et al.*, 2010; Bhaskar *et al.*, 2016]. The findings also indicated that more urbanized watersheds in Charlanta exhibited significantly greater annual average peak unit discharge, challenging the traditional notion that larger, more infrequent flooding events are not substantially influenced by urban development [Hollis, 1975]. However, the correlations between the relative extent of urban development and annual peak unit



discharge were weaker than the relationships with the threshold exceedances, which reaffirms that the impact of urbanization diminishes as flood recurrence interval increases.

The positioning of impervious surfaces within the watersheds emerged as an additional factor that governed streamflow characteristics. The river imperviousness gradient exhibited significant positive correlations with the threshold exceedances, highlighting its capability to describe hydrologically relevant positioning patterns. Conversely, the difference in imperviousness between the top and bottom half of a watershed, which has been commonly used to quantify the positioning of urban development, was not consistently related to the threshold exceedances. The simplistic partitioning technique largely failed to capture the complex positioning of urban land use within the watersheds, which potentially explains the inconclusive findings produced by studies utilizing similar measures [e.g., *Beighley and Moglen, 2002*]. Finally, the imperviousness of the riparian buffer was also a critical characteristic, as watersheds with highly developed riparian zones exhibited a larger number of high and low threshold exceedances.

The multivariate models indicated that the extent, configuration, and positioning of urban development significantly influenced certain streamflow characteristics even when controlling for potential confounding factors. Furthermore, the moderate to high explanatory power of the statistical models suggests that the results can be used to inform urban land use policies aimed at minimizing the impacts of urbanization on streamflow. In terms of the extent of urban development, the findings highlighted that increasing the urbanized percentage of a watershed enhances high and low flow frequency as well as annual average peak unit discharge. Although based upon these findings imperviousness thresholds appear to be a simple approach that could moderate streamflow alterations due to urbanization, studies have suggested that

threshold-based policies can have the unintended consequence of encouraging sprawl-like development that enhances the spatial extent of hydrological impacts [e.g., *Mejia and Moglen, 2009*]. These complexities emphasize the importance of also considering the configuration and positioning of urban development, in addition to its extent, when devising land use policies aimed at minimizing streamflow alteration due to urbanization.

The models revealed that the configuration of LULCs can likely be optimized to reduce impacts on streamflow. For high and low threshold exceedances, the models indicated that decreasing the contiguity of developed open space would reduce high and low flow frequency. Such a configuration could be achieved via policies that encourage a greater interspersion of natural vegetation in areas of low density residential development. The configuration of urban development was less influential for annual peak unit discharge, but the modeling results suggested that the annual peaks were moderated by the presence of highly contiguous woody wetlands. This finding emphasizes the critical importance of protecting contiguous wetlands from development due to their substantial storage capacity. Finally, the positioning of urban development was most important for high flow frequency. The results indicated that enhancing the river imperviousness gradient by developing source areas distant from rivers would increase high threshold exceedances. Given that urbanization proximate to rivers also increased high flow frequency, positioning urban land use outside the riparian zone while avoiding headwater regions distant from rivers may potentially provide an optimal arrangement.

Although achieving the ideal extent, configuration, and positioning of urban development within a watershed is unlikely in reality, the overarching importance of these findings from an urban planning perspective is that all three facets of urban development patterns did significantly influence streamflow characteristics. Each aspect therefore provides one potential avenue

through which land use policies can moderate the impacts of urbanization on streamflow. For example, although minimizing the total extent of urbanized land use is one technique for reducing streamflow alteration, the imposition of and adherence to an imperviousness threshold may be challenging in certain cases due to urban development pressures. In such scenarios where urbanization is deemed unavoidable, the results suggest that policies guiding the spatial configuration and/or positioning of impervious surfaces can effectively moderate streamflow alteration.

Of course, caution must be taken when extrapolating the urban planning implications of these findings to cities outside the Southeastern United States since hydrological processes are sensitive to different physiographical settings. This study also analyzed the hydrological impacts of urban development patterns largely in isolation without fully addressing the potential ramifications for other aspects of the urban system. Future research employing a broader perspective that considers the urban system in its entirety could identify potential synergies amongst land use management strategies. For example, decreasing the contiguity of urban development may not only reduce high and low flow frequency, as other studies have suggested it holds the potential to mitigate urban heat island intensities as well [*Debbage and Shepherd*, 2015; *Pearsall*, 2017].

Moving forward, the utilization of physically based models (e.g., Storm Water Management Model) that provide a more detailed evaluation of stormwater drainage systems will be necessary to fully assess the potential efficacy of mitigation strategies based upon idealized urban development patterns. Additional statistical analysis that considers highly urbanized and suburban watersheds separately as well as seasons independently may also reveal subtle differences in how urbanization influences streamflow that are relevant to land use

planning measures. Despite these avenues for future research, the current study provides an improved understanding of how urban development patterns influence high, low, and peak flows that can inform a broad suite of land use management strategies aimed at minimizing the impacts of urbanization on streamflow. Such progress appears imperative given that urban areas are projected to continue expanding and will likely be exposed to an increased frequency of extreme rainfall events as well as prolonged dry periods in the future due to climate change [*Sheffield and Wood, 2007; Fischer and Knutti, 2015; Chow, 2017*].

## **2.5 References**

- Anselin, L. (1988), *Spatial Econometrics: Methods and Models*, Kluwer Academic, Dordrecht.
- Ashley, S. T., and W. S. Ashley (2008), Flood fatalities in the United States, *J. Appl. Meteorol. Climatol.*, 47, 805–818, doi:10.1175/2007JAMC1611.1.
- Beighley, R. E., and G. E. Moglen (2002), Trend assessment in rainfall-runoff behavior in urbanizing watersheds, *J. Hydrol. Eng.*, 7(1), 27–34, doi:10.1061/(ASCE)10840699(2002)7:1(27).
- Beighley, R. E., and G. E. Moglen (2003), Adjusted measured peak discharges from an urbanizing watershed to reflect a stationary land use signal, *Water Resour. Res.*, 39(4), 1093, doi:10.1029/2002WR001846.
- Belsley, D. A., E. Kuh, and R. E. Welsch (1980), *Regression Diagnostics: Identifying Influential Data and Sources of Collinearity*, Wiley, New York.
- Bhaskar, A. S., L. Beesley, M. J. Burns, T. D. Fletcher, P. Hamel, C. E. Oldham, and A. H. Roy (2016), Will it rise or will it fall? Managing the complex effects of urbanization on baseflow, *Freshw. Sci.*, 35(1), 293–310, doi:10.1086/685084.
- Booth, D. B., and R. Jackson (1997), Urbanization of aquatic systems: Degradation thresholds, stormwater detection, and the limits of mitigation. *J. Am. Water Resour. Assoc.*, 33(5), 1077–1090, doi:10.1111/j.1752-1688.1997.tb04126.x.
- Brabec, E. A. (2009), Imperviousness and land-use policy: Toward an effective approach to watershed planning, *J. Hydrol. Eng.*, 14(4), 425–433, doi:10.1061/(ASCE)1084-0699(2009)14:4(425).
- Breusch, T. S., and A. R. Pagan (1979), A simple test for heteroscedasticity and random coefficient variation, *Econometrica*, 47, 1287–1294, doi:10.2307/1911963.
- Brown, L. R., T. F. Cuffney, J. F. Coles, F. Fitzpatrick, G. McMahon, J. Steuer, A. H. Bell, and J. T May (2009), Urban streams across the USA: Lessons learned from studies in 9 metropolitan areas, *J. North Am. Benthological Soc.*, 28(4), 1051–1069, doi:10.1899/08-153.1.
- Burian, S. J., and C. A. Pomeroy (2010), Urban impacts on the water cycle and potential green infrastructure implications, in *Urban Ecosystem Ecology*, edited by J. Aitkenhead-Peterson and A. Volder, pp. 277–296, American Society of Agronomy, Madison, WI.
- Burns, D., T. Vitvar, J. McDonnell, J. Hassett, J. Duncan, and C. Kendall (2005), Effects of suburban development on runoff generation in the Croton River basin, New York, USA, *J. Hydrol.*, 311, 266–281, doi:10.1016/j.jhydrol.2005.01.022.

- Choi, W., K. Nauth, J. Choi, and S. Becker (2016), Urbanization and rainfall-runoff relationships in the Milwaukee River Basin, *Prof. Geogr.*, 68(1), 14–25, doi:10.1080/00330124.2015.1007427.
- Chow, W. T. L (2017), The impact of weather extremes on urban resilience to hydro-climate hazards: A Singapore case study. *Int. J. Water Resour. D.*, doi:10.1080/07900627.2017.1335186.
- Cook, R. D., and S. Weisberg (1982), *Residuals and Influence in Regression*, Chapman and Hall, New York.
- Debbage, N., and J. M. Shepherd (2015), The urban heat island effect and city contiguity, *Comput. Environ. Urban Syst.*, 54, 181–194, doi:10.1016/j.compenvurbsys.2015.08.002.
- Debbage, N., B. Bereitschaft, and J.M. Shepherd (2016), Quantifying the spatiotemporal trends of urban sprawl among large U.S. metropolitan areas via spatial metrics, *Appl. Spat. Anal. Policy*, doi:10.1007/s12061-016-9190-6.
- DeWalle, D. R., B. R. Swistock, T. E. Johnson, and K. J. McGuire (2000), Potential effects of climate change and urbanization on mean annual streamflow in the United States, *Water Resour. Res.*, 36(9), 2655–2664, doi:10.1029/2000WR900134.
- Diem, J. E., T. C. Hill, and R. A. Milligan (2017), Diverse multi-decadal changes in streamflow within a rapidly urbanizing region, *J. Hydrol.*, doi: 10.1016/j.jhydrol.2017.10.026.
- Falcone, J. A. (2011), GAGES-II: Geospatial Attributes of Gages for Evaluating Streamflow, U.S. Geological Survey, Reston, VA. [Available at [https://water.usgs.gov/GIS/metadata/usgswrd/XML/gagesII\\_Sept2011.xml](https://water.usgs.gov/GIS/metadata/usgswrd/XML/gagesII_Sept2011.xml).]
- Ferguson, B. K., and P. W. Suckling (1990), Changing rainfall-runoff relationships in the urbanizing Peachtree Creek watershed, Atlanta, Georgia, *J. Am. Water Resour. Assoc.*, 26(2), 313–322, doi:10.1111/j.1752-1688.1990.tb01374.x.
- Fischer, E. M., and R. Knutti (2015), Anthropogenic contribution to global occurrence of heavy-precipitation and high-temperature extremes, *Nat. Clim. Chang.*, 5, 560–564, doi:10.1038/NCLIMATE2617.
- Fischer, R. A., and J. C. Fischenich (2000), Design recommendations for riparian corridors and vegetated buffer strips, U.S. Army Engineer Research and Development Center, Environmental Laboratory, Vicksburg, MS. [Available at <http://www.elkhornsloughctp.org/uploads/files/1381443282Fischer%20and%20Fischenich%202000%20buffer%20design.pdf>]
- Florida, R., T. Gulden, and C. Mellander (2008), The rise of the mega-region, *Camb. J. Regions Econ. Soc.*, 1, 459–476, doi: 10.1093/cjres/rsn018.

- Hamel, P., E. Daly, and T. D. Fletcher (2015), Which baseflow metrics should be used in assessing flow regimes of urban streams, *Hydrol. Process.*, 29, 4367–4378, doi:10.1002/hyp.10475.
- Hollis, G. E. (1975), The effect of urbanization on floods of different recurrence interval, *Water Resour. Res.*, 11(3), 431–435, doi:10.1029/WR011i003p0043.
- Homer, C. G., J. A. Dewitz, L. Yang, S. Jin, P. Danielson, G. Xian, J. Coulston, N. D. Herold, J. D. Wickham, and K. Megown (2015), Completion of the 2011 National Land Cover Database for the conterminous United States-Representing a decade of land cover change information, *Photogramm. Eng. Remote Sens.*, 81(5), 345–354, doi:10.14358/PERS.81.5.345.
- Hopkins, K. G., N. B. Morse, D. J. Bain, N. D. Bettez, N. B. Grimm, J. L. Morse, M. M. Palta, W. D. Shuster, A. R. Bratt, and A. Suchy (2015), Assessment of regional variation in streamflow responses to urbanization and the persistence of physiography. *Environ. Sci. Technol.*, 49, 2724–2732, doi:10.1021/es505389y.
- Kim, H. W., and Y. Park (2016), Urban green infrastructure and local flooding: The impact of landscape patterns on peak runoff in four Texas MSAs, *Appl. Geogr.*, 77, 72–81, doi: 10.1016/j.apgeog.2016.10.008.
- Klein, R. D. (1979), Urbanization and stream quality impairment, *J. Am. Water. Resour. Assoc.*, 15(4), 948–963, doi:10.1111/j.1752-1688.1979.tb01074.x.
- Leopold, L. B. (1968), Hydrology for urban planning – A guidebook on the hydrologic effects of urban land use, *U.S. Geol. Surv. Circ. 554*, U.S. Geol. Surv., Washington, D.C. [Available at <https://pubs.usgs.gov/circ/1968/0554/report.pdf>.]
- Marquardt, D. W. (1970), Generalized inverses, ridge regression, biased linear estimation, and nonlinear estimation, *Technometrics*, 12, 591–612, doi:10.2307/1267205.
- McGarigal, K., S. A. Cushman, and E. Ene (2012), FRAGSTATS v4: Spatial pattern analysis program for categorical and continuous maps, University of Massachusetts, Amherst, MA. [Available at <http://www.umass.edu/landeco/research/fragstats/fragstats.html>.]
- McMahon, G., J. D. Bales, J. F. Coles, E. M. P. Giddings, and H. Zappia (2003), Use of stage data to characterize hydrologic conditions in an urbanizing environment, *J. Am. Water Resour. Assoc.*, 39(6), 1529–1546, doi:10.1111/j.1752-1688.2003.tb04437.x.
- Mejia, A. I., and G. E. Moglen (2009), Spatial patterns of urban development from optimization of flood peaks and imperviousness-based measures, *J. Hydrol. Eng.*, 14(4), 416–424, doi:10.1061/(ASCE)1084-0699(2009)14:4(416).

- Mejia, A. I., and G. E. Moglen (2010), Impact of the spatial distribution of imperviousness on the hydrologic response of an urbanizing basin, *Hydrol. Process.*, 24, 3359–3373, doi:10.1002/hyp.7755.
- Meyer, S. C. (2005), Analysis of base flow trends in urban streams, northeastern Illinois, USA, *Hydrogeol. J.*, 13, 871–885, doi:10.1007/s10040-004-0383-8.
- Mitra, C., and J. M. Shepherd (2016), Urban precipitation: A global perspective, in *The Routledge Handbook of Urbanization and Global Change*, edited by K. C. Seto, W. D. Solecki, and C. A. Griffith, pp. 152–168, Routledge, London.
- Moran, P. A. P. (1950), Notes on continuous stochastic phenomena, *Biometrika*, 37, 17–23, doi:10.2307/2332142.
- NWS (2017a), Charlotte monthly precipitation. [Available at: <http://www.weather.gov/media/gsp/Climate/CLT/CLTmonthlyPobs.pdf>.]
- NWS (2017b), Atlanta rainfall scorecard. [Available at: [https://www.weather.gov/ffc/rainfall\\_scorecard](https://www.weather.gov/ffc/rainfall_scorecard)]
- O'Driscoll, M., S. Clinton, A. Jefferson, A. Manda, and S. McMillan (2010), Urbanization effects on watershed hydrology and in-stream processes in the Southern United States, *Water*, 2, 605–648, doi:10.3390/w2030605.
- Olivera, F., and B. B. DeFee (2007), Urbanization and its effect on runoff in the Whiteoak Bayou watershed, Texas, *J. Am. Water Resour. Assoc.*, 43(1), 170–182, doi:10.1111/j.1752-1688.2007.00014.x.
- Pearsall, H. (2017), Staying cool in the compact city: Vacant land and urban heating in Philadelphia, Pennsylvania, *Appl. Geogr.*, 79, 84–92, doi:10.1016/j.apgeog.2016.12.010.
- Poff, N. L., B. P. Bledsoe, and C. O. Cuhaciyan (2006), Hydrologic variation with land use across the contiguous United States: Geomorphic and ecological consequences for stream ecosystems, *Geomorphology*, 79, 264–285, doi:10.1016/j.geomorph.2006.06.032.
- Price, K. (2011), Effects of watershed topography, soils, land use, and climate on baseflow hydrology in humid regions: A review, *Prog. Phys. Geogr.*, 35(4), 465–442, doi:10.1177/0309133311402714.
- Roberts, A. D. (2016), The effects of current landscape configuration on streamflow within selected small watersheds of the Atlanta metropolitan region, *J. Hydrol. Reg. Stud.*, 5, 276–292, doi:10.1016/j.ejrh.2015.11.002.
- Rose, S., and N. E. Peters (2001), Effect of urbanization on streamflow in the Atlanta area (Georgia, USA): A comparative hydrological approach, *Hydrol. Process.*, 15, 1441–1457, doi:10.1002/hyp.218.



- Sauer, V. B., W. O. Thomas, V. A. Stricker, and K. V. Wilson (1984), Flood characteristics of urban watersheds in the United States. *U.S. Geol. Surv. Water Supply Paper 2207*, U.S. Gov. Print. Office, Washington, D.C. [Available at <https://pubs.usgs.gov/wsp/2207/report.pdf>.]
- Schueler, T. R. (1994), The importance of imperviousness, *Watershed Prot. Techniq.*, 1(3), 100–111.
- Schueler, T. R., L. Fraley-McNeal, K. Cappiella (2009), Is impervious cover still important? Review of recent research, *J. Hydrol. Eng.*, 14(4), 309–315, doi:10.1061/(ASCE)1084-0699(2009)14:4(309).
- Shapiro, S. S., and M. B. Wilk (1965), An analysis of variance test for normality (complete samples), *Biometrika*, 52, 591–611, doi:10.2307/2333709.
- Sheffield, J., and E. F. Wood (2007), Projected changes in drought occurrence under future global warming from multi-model, multi-scenario, IPCC AR4 simulations, *Clim. Dyn.*, 31, 79–105, doi:10.1007/s00382-007-0340-z.
- Sheng, J., and J. P. Wilson (2009), Watershed urbanization and changing flood behavior across the Los Angeles metropolitan region, *Nat. Hazards*, 48, 41–57, doi:10.1007/s11069-008-9241-7.
- Shepherd, J. M., T. Mote, J. Dowd, M. Roden, P. Knox, S. C. McCutcheon, and S. E. Nelson (2011), An overview of synoptic and mesoscale factors contributing to the disastrous Atlanta flood of 2009, *Bull. Amer. Meteor. Soc.*, 92, 861–870, doi:10.1175/2010BAMS3003.1.
- Shepherd, J. M., T. Andersen, C. Strother, A. Horst, L. Bounoua, and C. Mitra (2013), Urban climate archipelagoes: A new framework for urban impacts on climate, *IEEE Earthzine*, [Available at <https://earthzine.org/2013/11/29/urban-climate-archipelagos-a-new-framework-for-urban-impacts-on-climate/>.]
- Shuster, W. D., J. Bonta, H. Thurston, E. Warnemuende, and D. R. Smith (2005), Impacts of impervious surface on watershed hydrology: A review, *Urban Water J.*, 2, 263–275, doi:10.1080/15730620500386529.
- Smith, B. K., and J. A. Smith (2015), The flashiest watersheds in the contiguous United States, *J. Hydrometeorol.*, 16, 2365–2381, doi:10.1175/JHM-D-14-0217.1.
- Smith, J. A., M. L. Baeck, J. E. Morrison, P. Sturdevant-Rees, D. F. Turner-Gillespie, and P. D. Bates (2002), The regional hydrology of extreme floods in an urbanizing drainage basin, *J. Hydrometeorol.*, 3, 267–282, doi: 10.1175/1525-7541(2002)003<0267:TRHOEF>2.0.CO;2.

- Ssegane, H., E. W. Tollner, Y. M. Mohamoud, T. C. Rasmussen, and J. F. Dowd (2012), Advances in variable selection methods I: Causal selection methods versus stepwise regression and principal component analysis on data of known and unknown functional relationships, *J. Hydrol.*, 438–439, 16–25, doi: 10.1016/j.jhydrol.2012.01.008.
- ten Veldhuis, M. C., Z. Zhou, L. Yang, S. Liu, and J. Smith (2017), The role of storm dynamics and scale in controlling urban flood response, *Hydrol. Earth Syst. Sci.*, doi:10.5194/hess-2017-197.
- Terando, A. J., J. Costanza, C. Belyea, R. R. Dunn, A. McKerrow, and J. A. Collazo (2014), The southern megalopolis: Using the past to predict the future of urban sprawl in the Southeast U.S., *PLoS ONE*, 9(7), doi:10.1371/journal.pone.0102261.
- Tukey, J. W. (1949), Comparing individual means in the analysis of variance, *Biometrics*, 5, 99–114, doi:10.2307/3001913.
- United Nations (2014), World urbanization prospectus: The 2014 revision highlights, United Nations, New York [Available at <https://esa.un.org/unpd/wup/Publications/Files/WUP2014-Highlights.pdf>.]
- U.S. Census Bureau (2012), Patterns of metropolitan and micropolitan change: 2000 to 2010, U.S. Gov. Print. Office, Washington, D.C. [Available at: <https://www.census.gov/prod/cen2010/reports/c2010sr-01.pdf>.]
- Villarini, G., J. A. Smith, M. L. Baeck, B. K. Smith, and P. Sturdevant-Rees (2013), Hydrologic analyses of the July 17–18, 1996, flood in Chicago and the role of urbanization, *J. Hydrol. Eng.*, 18(2), 250–259, doi:10.1061/(ASCE)HE.1943-5584.0000462.
- Wang, L., J. Lyons, P. Kanehl, and R. Bannerman (2001), Impacts of urbanization on stream habitat and fish across multiple scales, *Environ. Manage.*, 28(2), 255–266, doi:10.1007/s002670010222.
- Welty, C. (2009), The urban water budget, in *The Water Environment of Cities*, edited by L. A. Baker, pp. 17–28, Springer, New York.
- Wright, D. B., J. A. Smith, G. Villarini, and M. L. Baeck (2012), Hydroclimatology of flash flooding in Atlanta, *Water Resour. Res.*, 48, W045, doi: 10.1029/2011WR011371.
- Yang, L., J. A. Smith, D. B. Wright, M. L. Baeck, G. Villarini, F. Tian, and H. Hu (2013), Urbanization and climate change: An examination of nonstationarities in urban flooding, *J. Hydrometeorol.*, 14, 1791–1809, doi:10.1175/JHM-D-12-095.1.
- Zhou, Z., J. A. Smith, L. Yang, M. L. Baeck, M. Chaney, M.-C. Ten Veldhuis, H. Deng, and S. Liu (2017), The complexities of urban flood response: Flood frequency analyses for the Charlotte metropolitan region, *Water Resour. Res.*, 53, doi:10.1002/2016WR019997.

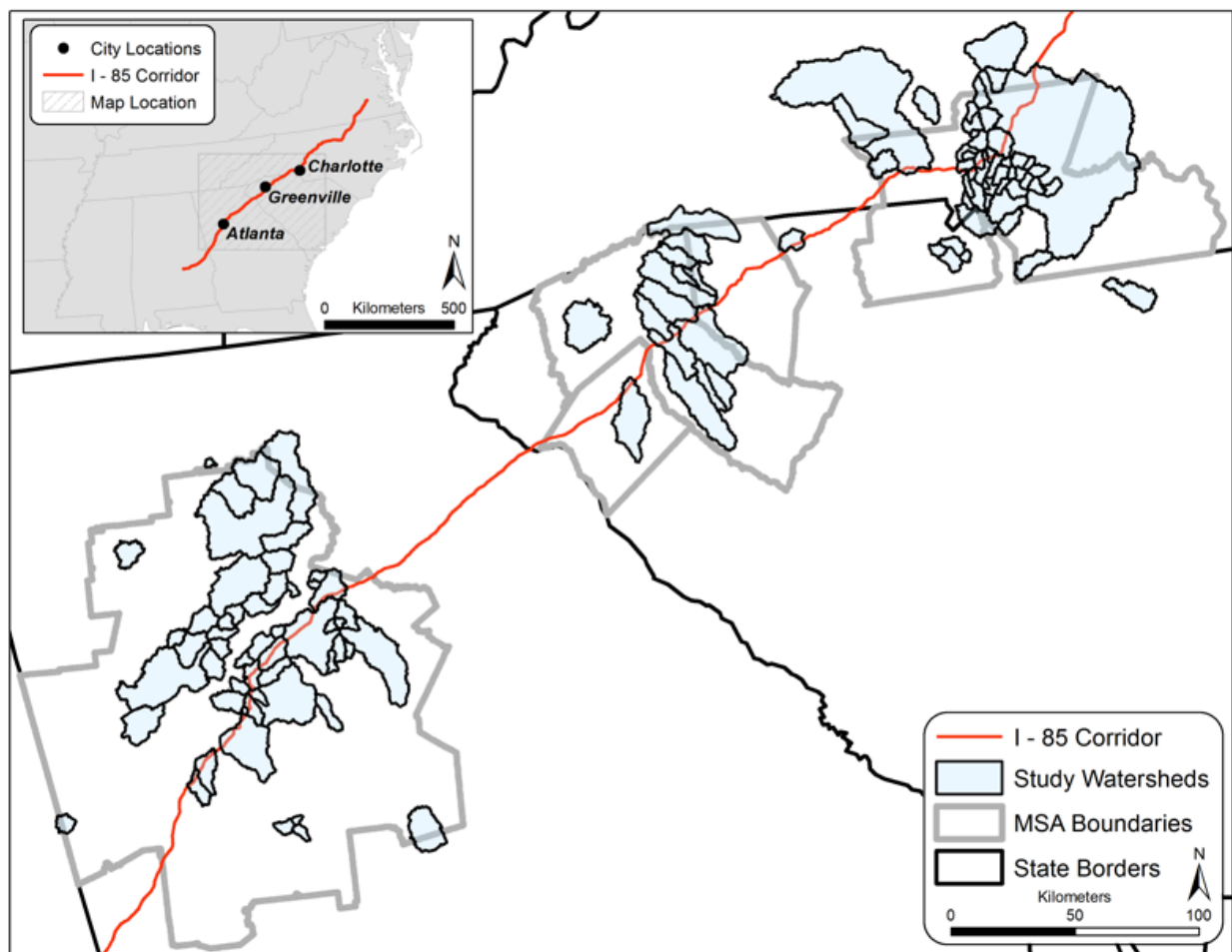


Figure 2.1. Location of the Charlanta Megaregion and study watersheds.

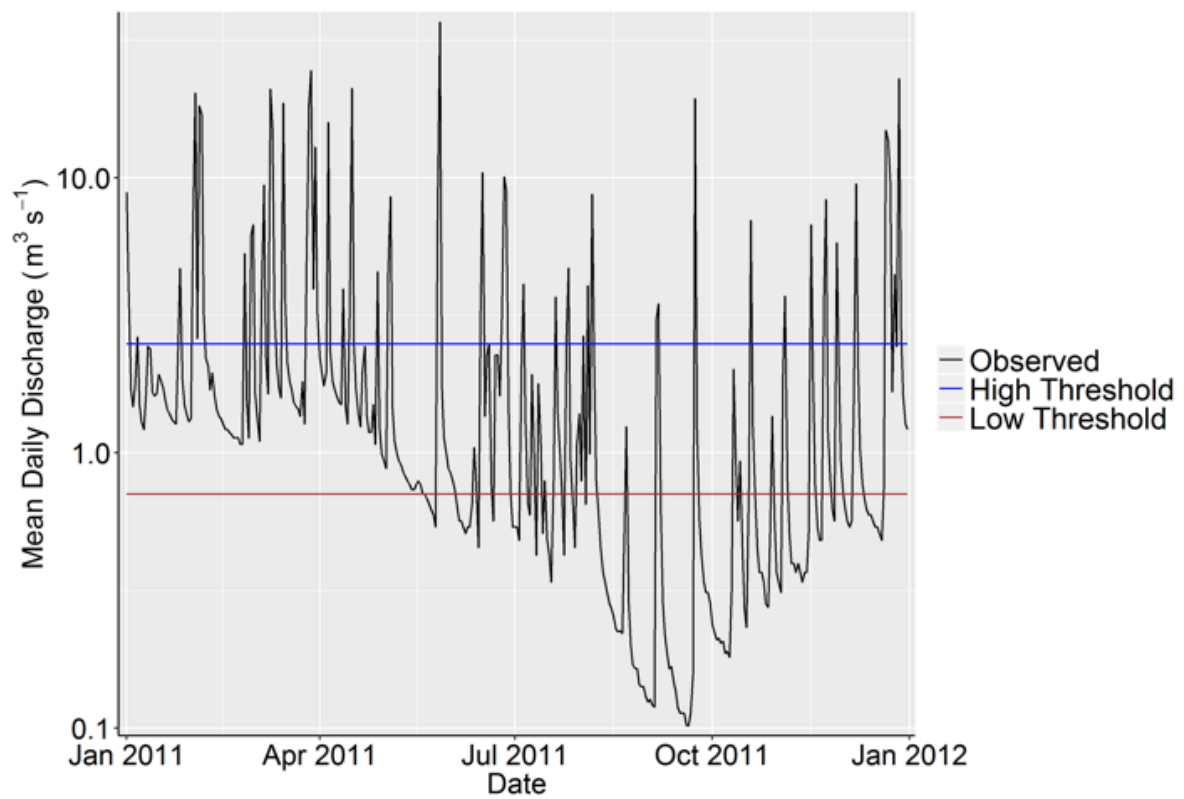


Figure 2.2. Example of the peaks-over-threshold (POT) analysis from Peachtree Creek in Atlanta, Georgia for 2011. There were 25 low threshold exceedances and 35 high threshold exceedances during the year.

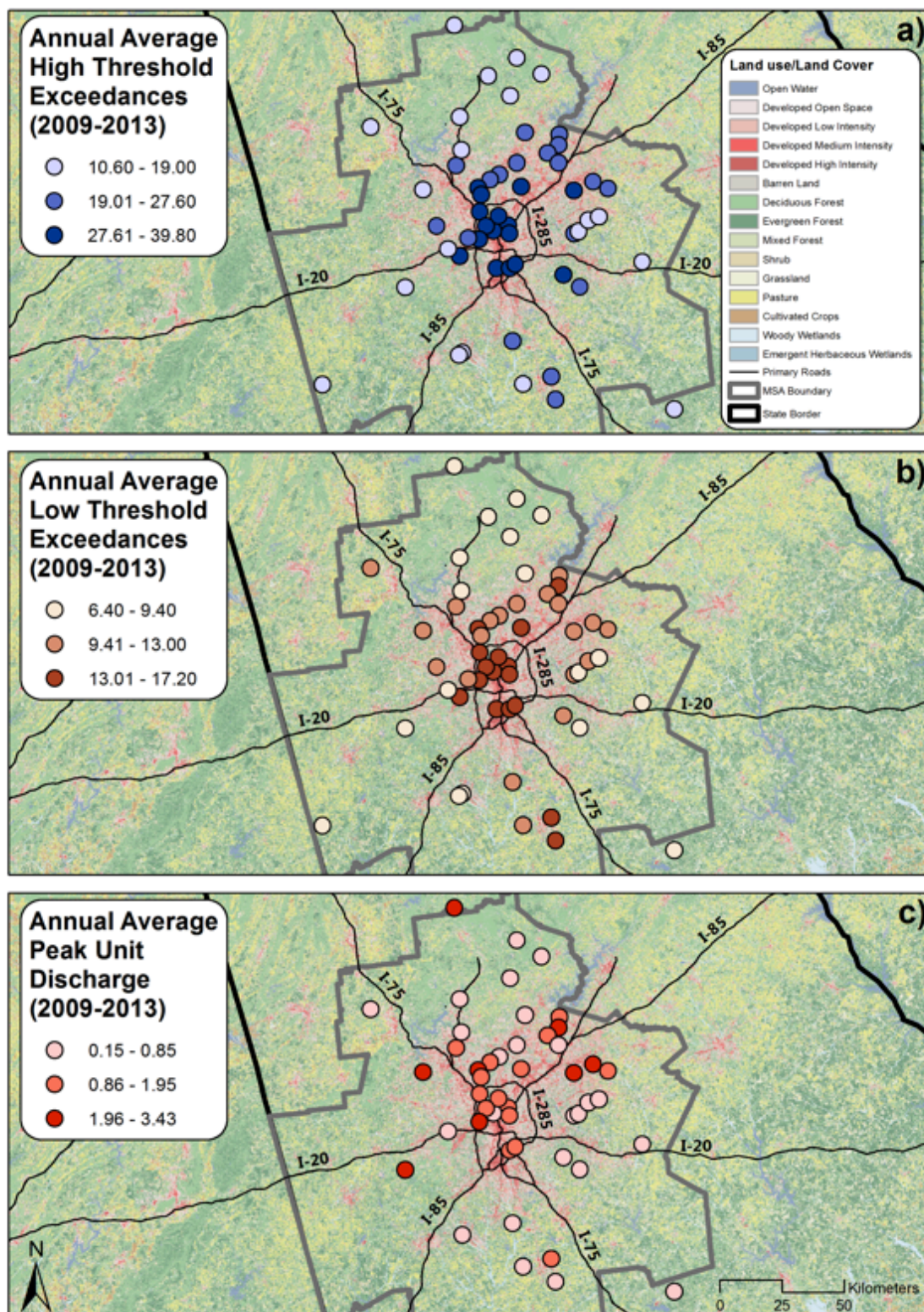
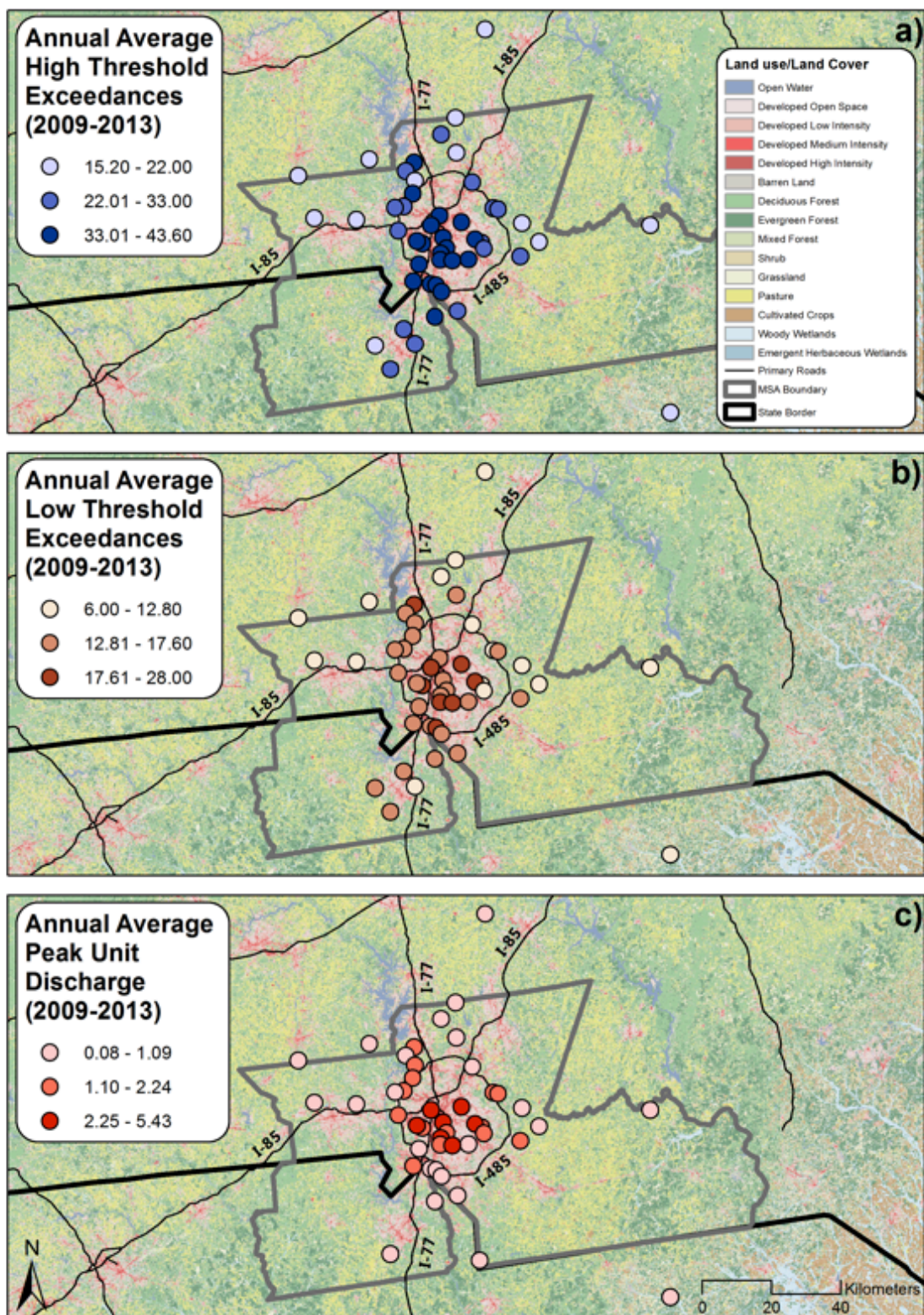
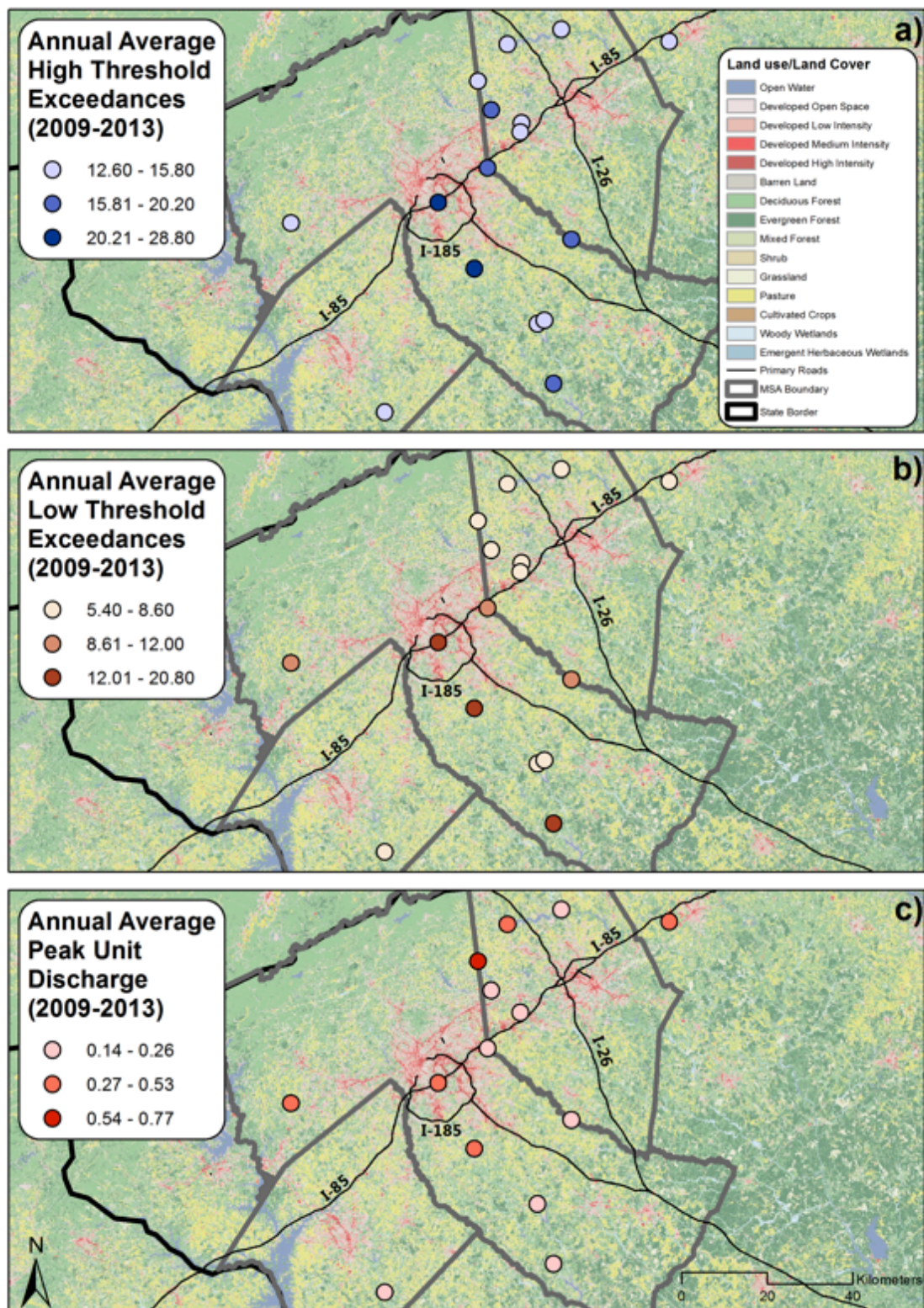


Figure 2.3. Spatial distribution of a) high threshold exceedances per year, b) low threshold exceedances per year, and c) annual average peak unit discharge ( $\text{m}^3\text{s}^{-1}\text{km}^{-2}$ ) for the Atlanta MSA.









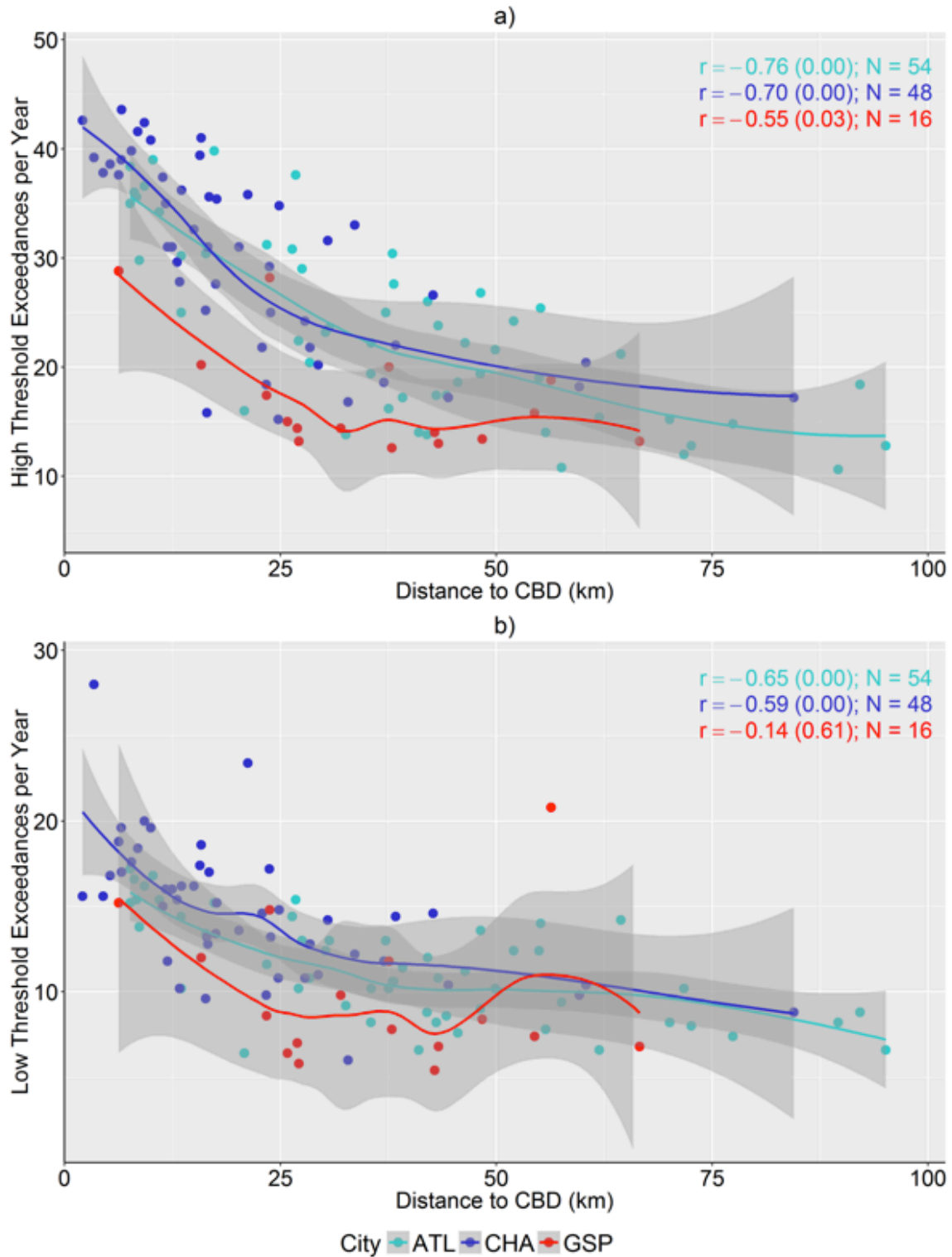


Figure 2.6. Relationships between a) high and b) low threshold exceedances and distance to the central business district (CBD) of each MSA in Charlanta. Pearson correlation coefficients ( $r$ ) and sample sizes ( $N$ ) are reported with  $p$ -values in parentheses. The grey shading around the lines represents the 95% confidence interval.



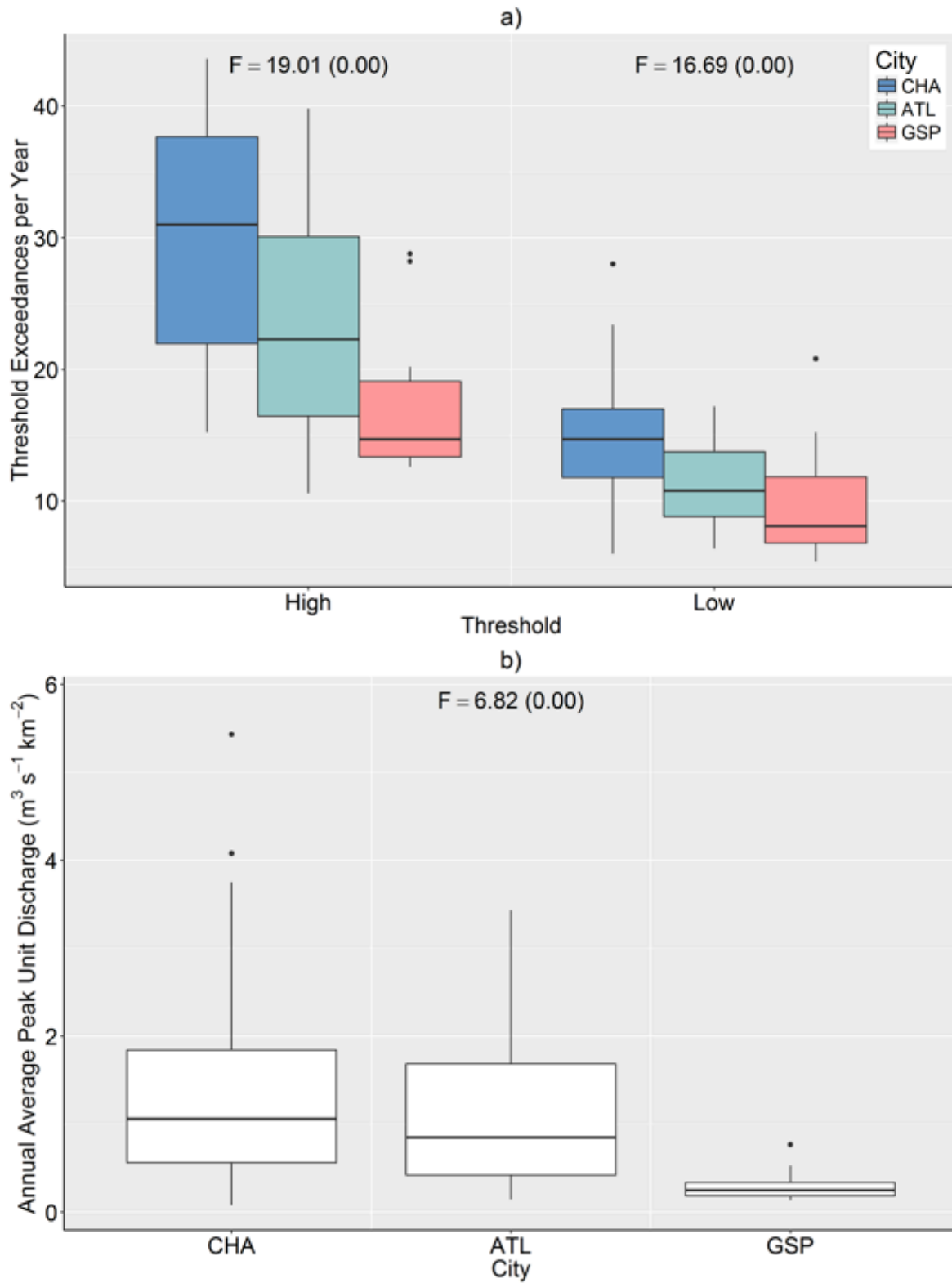


Figure 2.7. Differences in a) threshold exceedances and b) annual peak unit discharge between the Charlanta MSAs. The F-values from the ANOVA tests are reported with the associated p-values in parentheses.

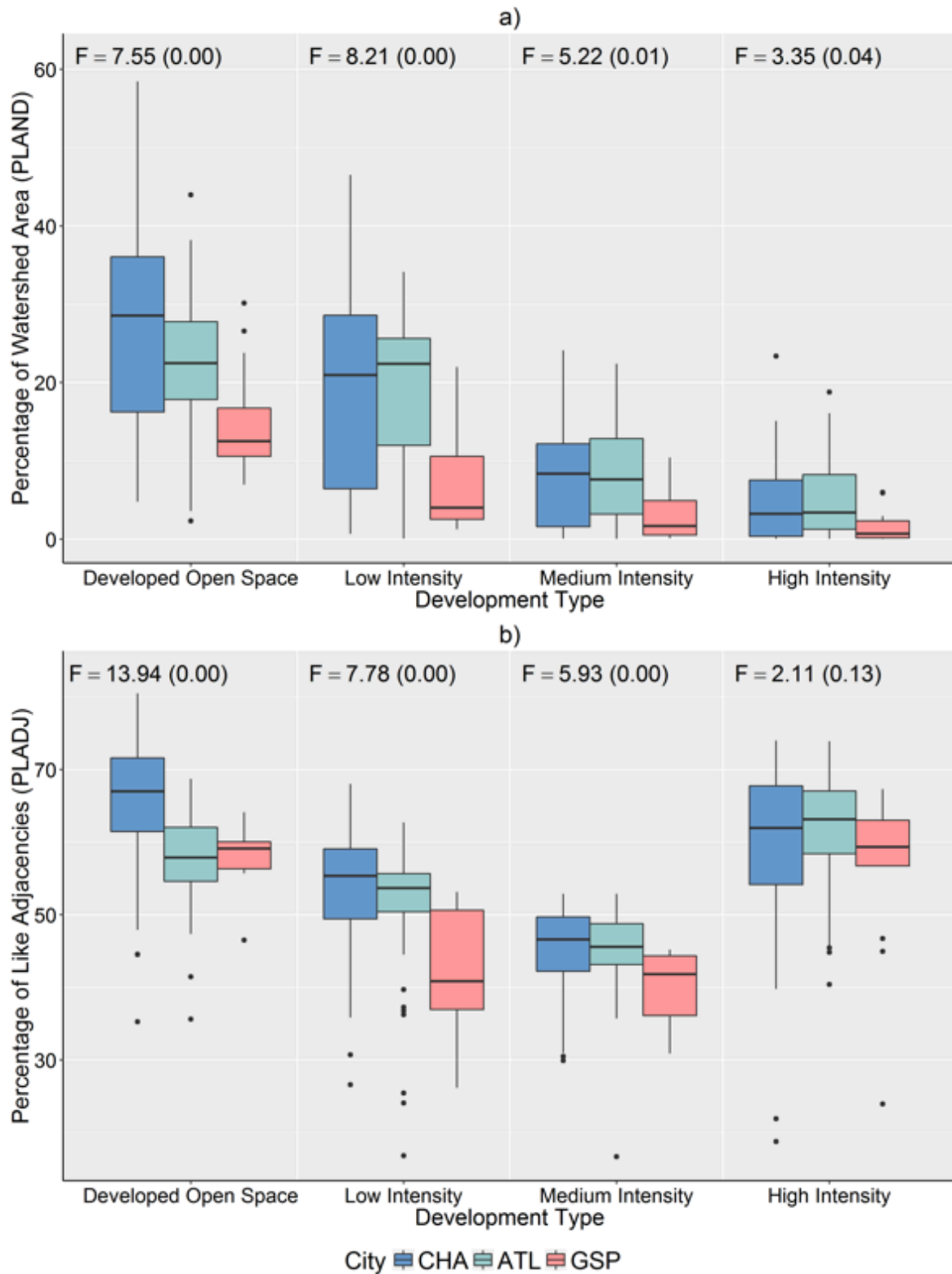


Figure 2.8. Differences in a) the relative extent of urban development and b) the contiguity of urban development between the Charlanta MSAs. The F-values from the ANOVA tests are reported with the associated p-values in parentheses.

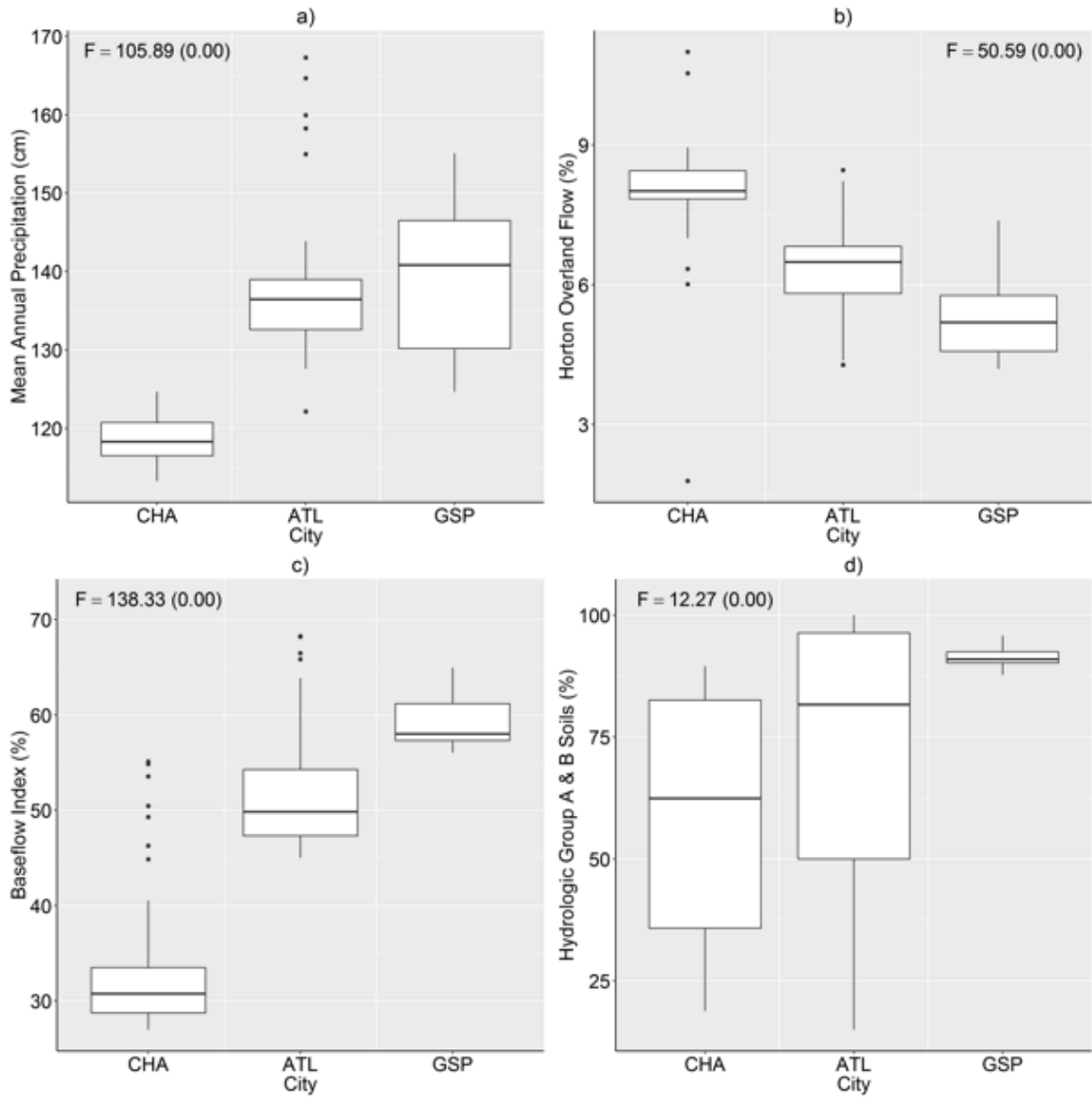


Figure 2.9. Differences in the natural characteristics of the Charlanta watersheds by MSA. The F-values from the ANOVA tests are reported with the associated p-values in parentheses.

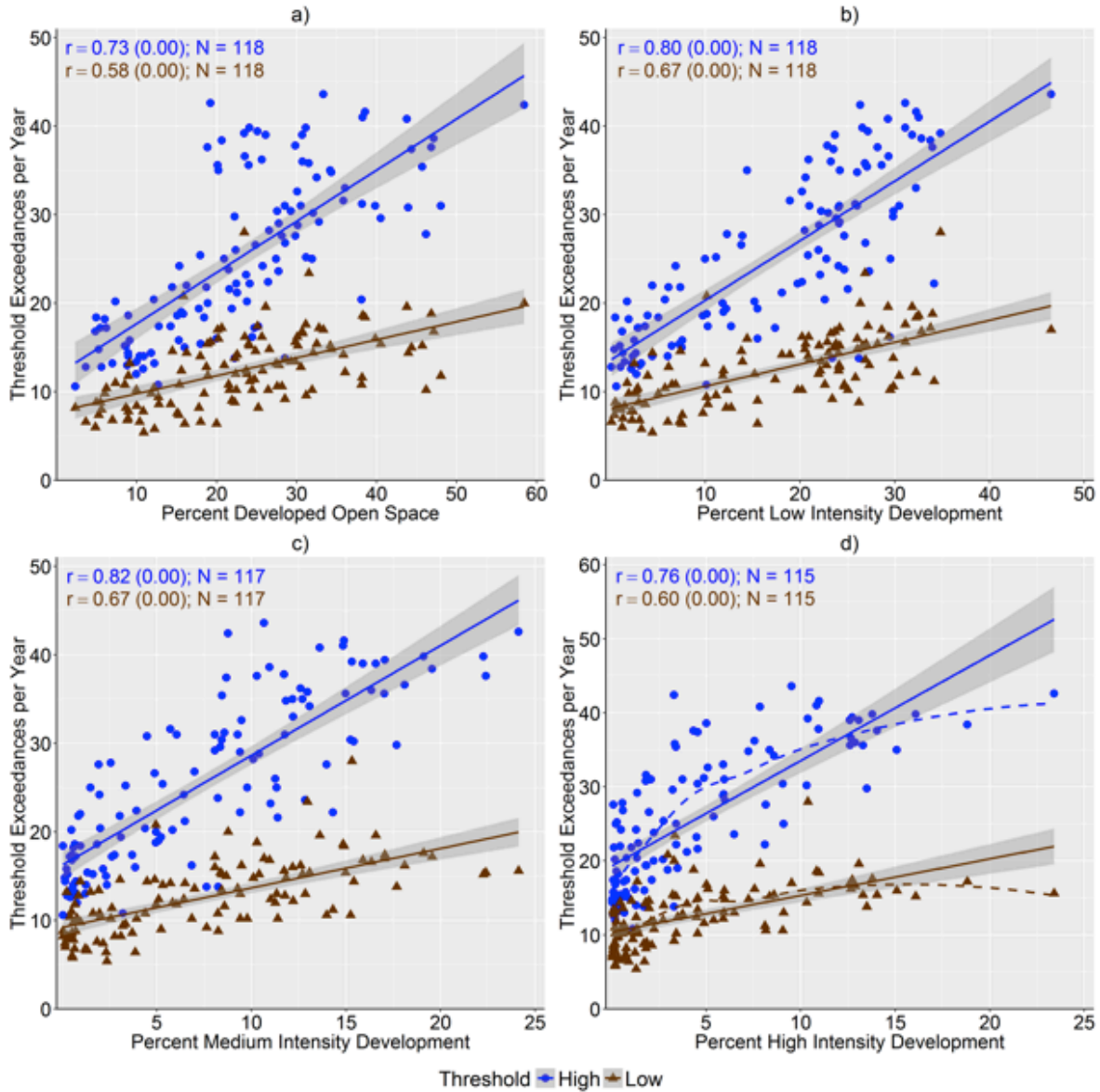


Figure 2.10. Relationships between the percent of the watershed developed and the threshold exceedances. Pearson correlation coefficients ( $r$ ) and sample sizes ( $N$ ) are reported with  $p$ -values in parentheses. The grey shading around the lines represents the 95% confidence interval. In subplot d) the dashed lines represent loess curves fitted to the scatterplot.

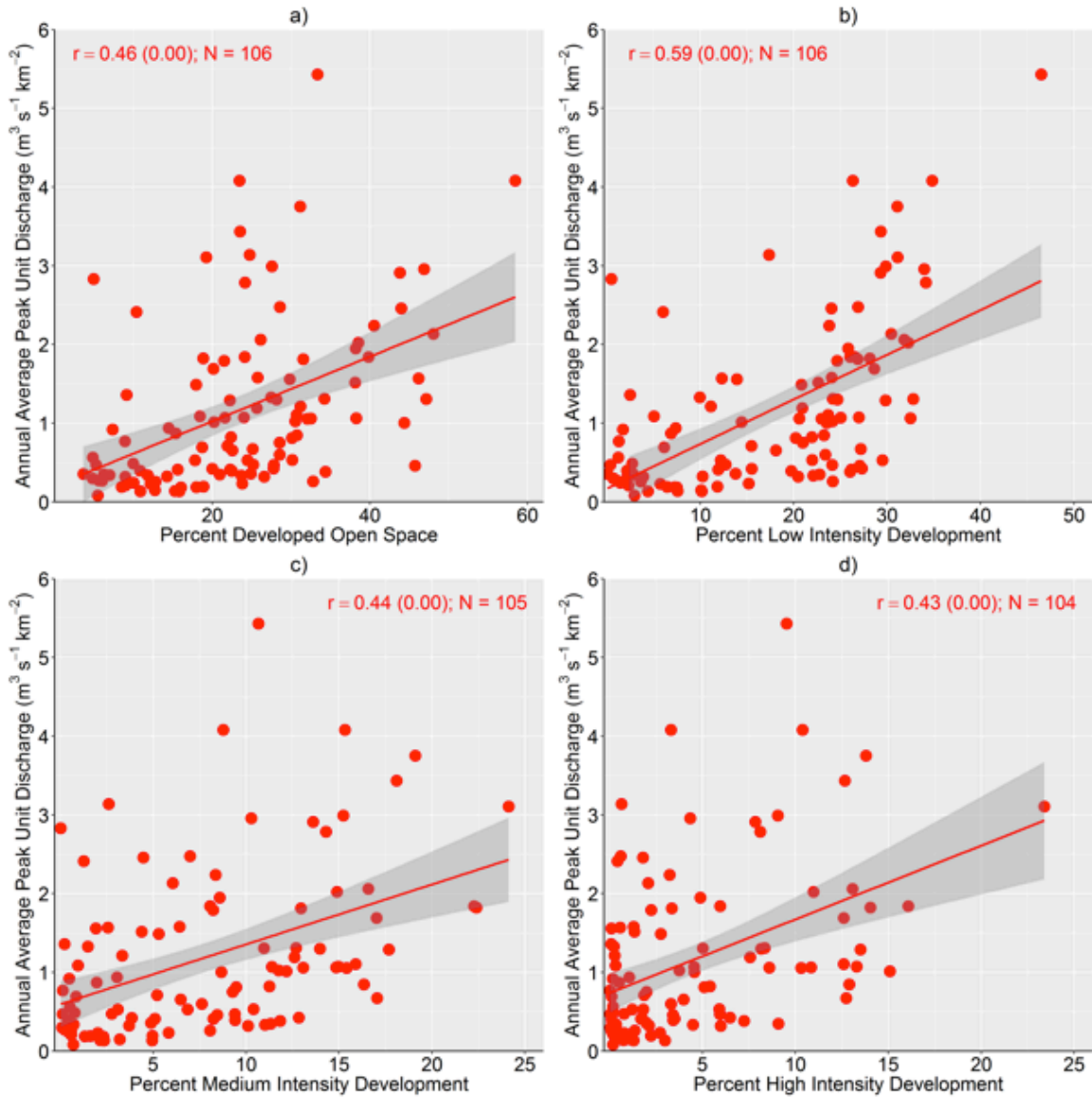


Figure 2.11. Relationships between the percent of the watershed developed and annual average peak unit discharge. Pearson correlation coefficients ( $r$ ) and sample sizes ( $N$ ) are reported with  $p$ -values in parentheses. The grey shading around the lines represents the 95% confidence interval.

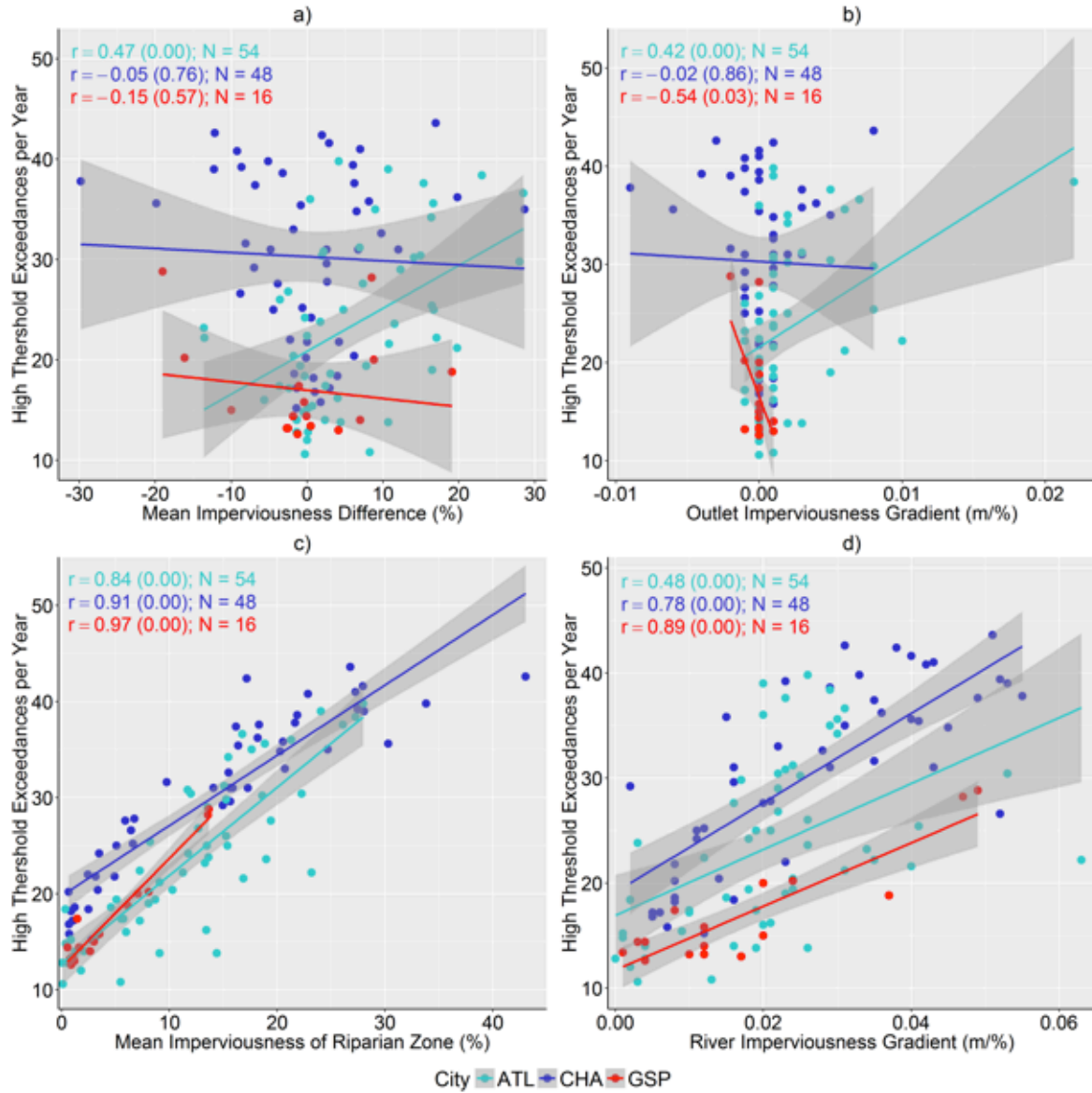


Figure 2.12. Relationships between the positioning metrics and the high threshold exceedances. Pearson correlation coefficients ( $r$ ) and sample sizes ( $N$ ) are reported with  $p$ -values in parentheses. The grey shading around the lines represents the 95% confidence interval.

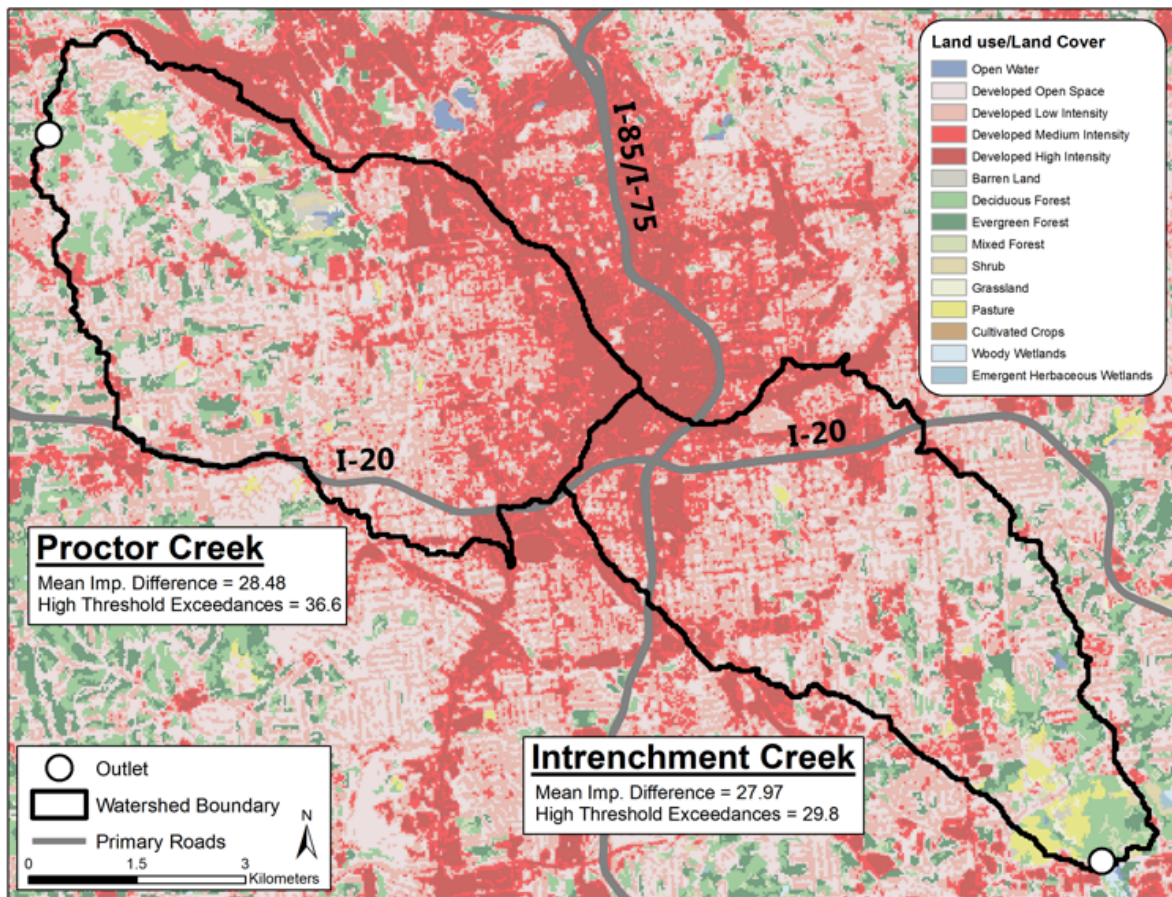


Figure 2.13. Example of headwater development in Downtown Atlanta. Each watershed exhibited a large number of high threshold exceedances as well as a notable mean imperviousness difference between their top and bottom halves.



Table 2.1. Statistics describing the characteristics of the study watersheds. Median values are reported with standard deviations in parentheses. All the variables were obtained from the GAGES-II dataset [*Falcone, 2011*] except urbanized area, which was derived from the 2011 National Land Cover Database (NLCD).

Metropolitan Area	Number	Area (km <sup>2</sup> )	Population Density (persons/km <sup>2</sup> )	Urbanized Area (%)	Mean Annual Precipitation (cm)	Mean Annual Temperature (°C)
Atlanta (ATL)	54	79.5 (242.7)	465.0 (420.1)	61.1 (26.3)	136.4 (8.7)	15.3 (0.7)
Charlotte (CHA)	49	48.5 (506.4)	354.7 (410.6)	66.4 (32.1)	118.3 (2.9)	15.5 (0.4)
Greenville-Spartanburg-Anderson (GSP)	16	198.8 (183.7)	73.8 (170.8)	18.0 (18.6)	140.8 (10.0)	15.6 (0.2)
All Watersheds	119	76.8 (368.4)	340.3 (408.0)	60.8 (29.6)	130.4 (11.9)	15.5 (0.6)



Table 2.2. Equations and technical descriptions of the spatial metrics used to quantify the extent and spatial configuration of the urban development within each watershed (McGarigal et al. 2012). A patch is defined as a contiguous group of pixels that share a common land use/land cover type.

Spatial Metric	Equation	Technical Description
Area-Weighted Mean Shape Index (AWMSI)	$AWMSI = \sum_{j=1}^n \left[ \left( \frac{0.25p_{ij}}{\sqrt{a_{ij}}} \right) \left( \frac{a_{ij}}{\sum_{j=1}^n a_{ij}} \right) \right]$	Where $p_{ij}$ is the perimeter of patch $ij$ and $a_{ij}$ is the area of patch $ij$ ( $i$ = number of patch types, $j$ = number of patches) Units: None
Edge Density (ED)	$ED = \frac{\sum_{k=1}^m e_{ik}}{A} * 10,000$	Where $e_{ik}$ is the total edge length (m) of class $i$ in the landscape and $A$ is the total landscape area; the result is multiplied by 10,000 to convert to hectares Units: Meters per hectare
Largest Patch Index (LPI)	$LPI = \frac{\max_{j=1}^n (a_{ij})}{A} * 100$	Where $\max(a_{ij})$ is the area ( $m^2$ ) of the largest patch of the corresponding class and $A$ is the total landscape area ( $m^2$ ); the result is multiplied by 100 to convert to a percentage Units: Percent
Patch Density (PD)	$PD = \frac{n_i}{A} * 10,000 * 100$	Where $n_i$ is the number of patches in the landscape of patch type $i$ and $A$ is the total landscape area ( $m^2$ ) Units: Number per 100 hectare
Percentage of Like Adjacencies (PLADJ)	$PLADJ = \left( \frac{g_{ii}}{\sum_{k=1}^m g_{ik}} \right) * 100$	Where $g_{ii}$ is the number of like adjacencies between pixels of patch type $i$ and $g_{ik}$ is the number of adjacencies between pixels of patch types $i$ and $k$ Units: Percent
Percentage of Landscape (PLAND)	$PLAND = \frac{\sum_{j=1}^n a_{ij}}{A} * 100$	Where $a_{ij}$ is the area ( $m^2$ ) of patch $ij$ and $A$ is the total landscape area ( $m^2$ ); the result is multiplied by 100 to convert to a percentage Units: Percent

Table 2.3. Correlations between the urban configuration metrics and high threshold exceedances, low threshold exceedances, annual average peak unit discharge, and PLAND averaged over the four NLCD urban intensity levels.

Configuration Metric	High Threshold	Low Threshold	Annual Peak Unit Discharge	PLAND
PD	0.67*	0.54*	0.39*	0.72*
PLADJ	0.58*	0.51*	0.25	0.73*
LPI	0.52*	0.41*	0.53*	0.73*
AWMSI	0.52*	0.43*	0.19	0.75*
ED	0.76*	0.61*	0.45*	0.97*

\* = all four correlation coefficients used to calculate the average had a p-value < 0.05

Table 2.4. Correlations between the urban positioning metrics and high threshold exceedances, low threshold exceedances, and annual average peak unit discharge.

	ATL			CHA			GSP		
Positioning Metric	High Threshold	Low Threshold	Annual Peak Unit Discharge	High Threshold	Low Threshold	Annual Peak Unit Discharge	High Threshold	Low Threshold	Annual Peak Unit Discharge
Mean Imp. Difference	0.47*	0.54*	0.24	-0.05	-0.07	-0.05	-0.15	0.24	-0.33
Outlet Imp. Gradient	0.42*	0.48*	0.33*	-0.02	-0.07	0.14	-0.54*	-0.39	-0.37
Riparian Imp.	0.84*	0.77*	0.32*	0.91*	0.71*	0.61*	0.97*	0.73*	0.00
River Imp. Gradient	0.48*	0.46*	0.30*	0.78*	0.53*	0.45*	0.89*	0.76*	-0.06

\* = p-value of correlation < 0.05

Table 2.5. OLS regression results for the high and low threshold exceedances.

Independent Variable	High Threshold Exceedances			Low Threshold Exceedances*		
	Coefficient	P-Value	Std. Coef.	Coefficient	P-value	Std. Coef.
Intercept	12.04	~0.00	---	2.746	~0.00	---
PLAND Class 23	0.81	~0.00	0.54	0.024	~0.00	0.44
PLADJ Class 21	0.28	~0.00	0.24	0.011	~0.00	0.25
River Imp. Gradient	59.06	0.02	0.09	---	---	---
Lake Storage	-3.30	~0.00	-0.18	---	---	---
Baseflow Index	-0.19	~0.00	-0.25	---	---	---
Soil Groups A & B	---	---	---	-0.002	0.02	-0.15
Mean Ann. Precip.	---	---	---	-0.007	~0.00	-0.27
R-Squared	0.90	---	---	0.67	---	---
Adj. R-Squared	0.90	---	---	0.66	---	---
N	117	---	---	117	---	---

\*Note: Dependent variable was transformed by the natural logarithm

Table 2.6. OLS and SEM regression results for annual average peak unit discharge. Lambda represents the spatial autoregressive coefficient.

Independent Variable	Annual Peak Unit Discharge* (OLS)				Annual Peak Unit Discharge* (SEM)		
	Coefficient	Std. Error	P-Value	Std. Coef	Coefficient	Std. Error	P-value
Intercept	3.310	0.674	~0.00	---	3.651	0.714	~0.00
PLAND Class 22	0.029	0.007	~0.00	0.33	0.023	0.007	~0.00
PLADJ Class 90	-0.046	0.008	~0.00	-0.42	-0.039	0.006	~0.00
Lake Storage	-0.267	0.126	0.04	-0.14	-0.301	0.117	0.01
Baseflow Index	-0.023	0.006	~0.00	-0.31	-0.039	0.010	~0.00
Lambda	---	---	---	---	0.634	---	~0.00
R-Squared	0.56	---	---	---	---	---	---
AIC	202.21	---	---	---	181.09	---	---
N	103	---	---	---	103	---	---

\*Note: Dependent variable was transformed by the natural logarithm

## CHAPTER 3

# DETERMINING THE INFLUENCE OF URBANIZATION ON THE SPATIOTEMPORAL CHARACTERISTICS OF RUNOFF AND PRECIPITATION DURING THE 2009 ATLANTA FLOOD<sup>2</sup>

---

<sup>2</sup> Debbage, N. and J. M. Shepherd. Submitted to *Journal of Hydrometeorology*, 01/18/18.

## **Abstract**

The 2009 Atlanta flood was a historic event that resulted in catastrophic damage throughout the metropolitan area. The flood was the product of several hydrometeorological processes including moist antecedent conditions, ample atmospheric moisture, and mesoscale training. Additionally, previous studies hypothesized that the urban environment of Atlanta altered the location and/or overall quantities of precipitation and runoff that ultimately produced the flood. This hypothesis was quantitatively evaluated by conducting a series of numerical modeling experiments that utilized the Weather Research and Forecasting model. Two model runs were performed: 1) a base run designed to accurately depict the flood event, and 2) a non-urban simulation where the urban footprint of Atlanta was replaced with natural vegetation. Comparing the output from the two simulations revealed that interactions with the urban environment likely enhanced the precipitation and runoff associated with the flood. Specifically, the non-urban model underestimated the cumulative precipitation by approximately 100 mm in the area downwind of Atlanta where urban rainfall enhancement was hypothesized. This notable difference was due to the increased surface convergence observed in the urban simulation, which was likely attributable to the enhanced surface roughness and thermal properties of the urban environment. Overall, the findings suggest that interactions with the urban environment can influence mesoscale hydrometeorological characteristics even during events with prominent synoptic scale forcing. Additionally, from an urban planning perspective, the results highlight a potential two-pronged vulnerability of urban environments to extreme rainfall, as they may enhance both the initial precipitation and subsequent runoff.

**Key Words:** Urbanization, Precipitation, Flood, Weather Research and Forecasting Model, Atlanta

### **3.1 Introduction**

Due to a complex combination of both social and physical factors, urban areas are particularly vulnerable to flooding. The pressures of urbanization have likely increased flood zone occupancy, particularly amongst vulnerable individuals [*Houston et al.*, 2011], while simultaneously altering the physical surface properties that largely govern rainfall-runoff processes [*Leopold*, 1968; *Debbage and Shepherd*, Submitted]. A striking example of this urban vulnerability to extreme rainfall occurred in Atlanta, Georgia during late September 2009, as the city suffered from a historic flooding event [*McCallum and Gotvald*, 2010]. The flood was created by a prolonged period of rainfall from 16 September to 22 September. The most intense precipitation occurred on 21 September, with a maximum 24-hour rainfall total of 534.16 mm observed west of downtown Atlanta in Douglas County [*NWS Atlanta*, 2014]. Throughout metropolitan Atlanta, the prolonged and intense rainfall overwhelmed the urbanized watersheds and the streamflow at numerous gages across the region approached or exceeded the discharge associated with a 100-year flood [*McCallum and Gotvald*, 2010]. In terms of societal impacts, the flood was categorized as “catastrophic” according to the damage-based flash flood severity index of *Schroeder et al.* [2016]. Additionally, almost a dozen fatalities were unfortunately attributed to the flood and damage claims approached \$500 million [*McCallum and Gotvald*, 2010; *NWS Atlanta*, 2014].

The extreme flooding was the product of several different meteorological processes that were consistent with the broader flood climatology of the region [*Gamble and Meentemeyer*, 1997; *Shepherd et al.*, 2011]. At the synoptic scale, a weak cut-off low stalled over the lower Mississippi Valley on 17 September and resulted in substantial precipitation prior to the heaviest rainfall. The high antecedent moisture conditions produced by the cut-off low likely exacerbated

the flood peaks observed several days later. Throughout the flood event, there was also persistent southerly and easterly flow in the region associated with a surface low-pressure system over the lower Mississippi Valley and a surface high-pressure system over the Great Lakes, respectively. This circulation pattern advected atmospheric moisture from the Gulf of Mexico and Atlantic Ocean into the greater Atlanta region for several days, which provided ample water vapor for the most intense precipitation events. At the mesoscale, training occurred, possibly due to interactions with the local topography, and contributed to the localized pockets of anomalously high precipitation. Finally, *Shepherd et al.* [2011] hypothesized that boundary layer interactions with the urban land cover of Atlanta may have enhanced the overall quantity of precipitation and/or influenced its location. This hypothesis appeared plausible because the largest precipitation totals were located downwind of Atlanta, primarily in Douglas and Cobb counties, which is where urban rainfall enhancement would likely occur based upon the framework established by *Shepherd et al.* [2002].

The hypothesis that the urban environment of Atlanta influenced the precipitation which ultimately led to the 2009 flood was informed by previous research focusing on urban modifications of precipitation and convective activity. These studies date back to at least *Horton* [1921], who provided anecdotal evidence that urban environments may be preferential areas for convective activity. Subsequent observational and climatological analyses produced by the Metropolitan Meteorological Experiment (METROMEX) [*Huff and Changnon*, 1973; *Changnon et al.*, 1977] largely supported Horton's hypothesis. Specifically, the METROMEX identified a 9–17% increase in warm-season precipitation over background values due to urban effects within and 15–55 km downwind of the city [*Huff and Changnon*, 1973]. Over the past four decades, studies have largely validated and extended the original findings of the METROMEX by more

conclusively identifying the casual mechanism responsible for the urban rainfall effect [Burian and Shepherd, 2005]. Urban-induced alterations of precipitation have generally been attributed to one or a combination of the following mechanisms [Shepherd, 2005]: 1) the increased surface roughness within urban environments enhancing surface convergence [Thielen *et al.*, 2000], 2) the different thermal properties of the city producing unstable atmospheric conditions through the creation, enhancement, and/or displacement of mesoscale circulations [Shepherd and Burian, 2003], 3) elevated aerosol concentrations altering cloud microphysical processes by providing an abundant source of cloud condensation nuclei (CCN) [Molders and Olson, 2004; Schmid and Niyogi, 2017], 4) urban irrigation and industrial activities increasing low-level atmospheric moisture availability [Shepherd *et al.*, 2002; Diem and Brown, 2003], and 5) the built environment acting as a barrier that bifurcates existing storm systems [Bornstein and Lin, 2000]. Both observational and modeling studies have identified the capability of these mechanisms to alter convection, precipitation, and lightning activity specifically within and downwind of Atlanta [Bronstein and Lin, 2000; Dixon and Mote, 2003; Diem and Mote, 2005; Rose *et al.*, 2008; Shem and Shepherd, 2009; Ashley *et al.*, 2012; Haberlie *et al.*, 2015; Debbage *et al.*, 2015; McLeod *et al.*, 2017].

The overarching goal of this study was to quantitatively evaluate the hypothesis of Shepherd *et al.* [2011] that interactions with the urban environment influenced the location and/or quantity of precipitation during the 2009 Atlanta flood. A better understanding of the degree to which urbanization influenced the flood will help inform policies aimed at making the city more resilient to extreme rainfall. Additionally, this paper provides an extension of past research, which has primarily addressed urban precipitation effects under synoptically benign conditions (i.e. warm season convection), by analyzing possible urban-induced alterations of



precipitation during an event with prominent synoptic-scale forcing. Although several modeling studies have indicated that the urban environment can influence the spatial distribution and quantity of precipitation even under strong large-scale forcing [Ntelekos *et al.*, 2008; Yang *et al.*, 2014; Yu and Liu, 2015], these case studies generally focused on shorter-lived extreme rainfall events during the warm season. Therefore, the complexities of urban rainfall modification during sustained synoptic-scale forcing merit further investigation. It is important to note that urbanization is certainly not the primary contributor to large-scale precipitation systems, such as those responsible for the 2009 Atlanta flood. However, the urban environment may play an important secondary role through localized enhancements of convection and precipitation within the synoptically driven event.

By conducting a numerical weather modeling experiment, this study aimed to answer the following research questions: 1) how did the urban environment of Atlanta influence the spatiotemporal characteristics of runoff and precipitation during the 2009 flood, and 2) what physical mechanisms were potentially responsible for any urban modifications? The subsequent section describes the data and methods used to identify potential urban modifications of the hydrometeorological characteristics of the flood. Section 3.3 presents the results of the numerical modeling experiments. Finally, section 3.4 summarizes the major findings and explores the potential urban planning implications of the study.

## **3.2 Data and Methods**

### **3.2.1 Weather Research and Forecasting Model Configuration**

Due to the overall complexity of the 2009 Atlanta flood, it is difficult to conclusively discern the second-order influences of the urban environment from observational records alone. Therefore, this study relied upon the Weather Research and Forecasting (WRF) model to conduct

a controlled modeling experiment. WRF is a fully compressible, non-hydrostatic, mesoscale model with advanced dynamics, physics, and numerical schemes that is supported by the National Center for Atmospheric Research (NCAR) [Skamarock *et al.*, 2008]. Specifically, version 3.8.1 of Advanced Research WRF (ARW) was used. The WRF-ARW model was selected because it has been utilized previously to successfully identify urban modifications of precipitation and convective activity in North American cities [e.g. Shem and Shepherd, 2009; Ntelekos *et al.*, 2008].

To simulate the 2009 Atlanta Flood, a two-way nested modeling domain was employed. The outer domain covered a majority of the Southeastern United States at a 10 km resolution while the inner domain was centered over Georgia and had a resolution of 2 km (Figure 3.1). North American Regional Reanalysis (NARR) was used to initialize the model and provided the boundary conditions throughout the simulations. NARR was selected primarily due to its higher temporal resolution of 3 hours and moderate spatial resolution of 32 km [Mesinger *et al.*, 2006]. The simulations were initialized on 1200 UTC 13 September to provide ample spin-up time prior to the heaviest precipitation events and concluded on 1200 UTC 23 September. A 30 second time step was used in both the inner and outer domains. The WRF-ARW physics options selected in all the simulations are summarized in Table 3.1. The physics options, except the cumulus parametrization, were kept the same for both the outer and inner domain to minimize inconsistencies at the boundary. For the cumulus parametrization, the Kain-Fritsch scheme was used in the outer domain, but parameterization was not necessary within the inner domain since the resolution was sufficient to explicitly resolve convection.

### 3.2.2 Modeling Experiments: Urban and Non-Urban Simulations

Two different model runs, an urban and non-urban simulation, were performed to evaluate the influence of the urban environment on the 2009 Atlanta flood. In both the urban and non-urban simulations, the configurations described in the previous section remained the same, but the treatment of land use varied. For the urban run, the default MODIS land use incorporated within WRF, which contains a single urban category, was augmented within the inner domain by including urban land use data obtained from the National Land Cover Database (NLCD) 2011 [Homer *et al.*, 2015] (Figure 3.2a). The four NLCD urban classes were reclassified into three categories (i.e. low intensity residential, high intensity residential, and commercial/industrial/transportation) to provide the necessary urban parameter information for the single layer urban canopy model (SLUCM) used to depict urban-related meteorological processes [Kusaka *et al.*, 2001; Chen *et al.*, 2011]. The SLUCM was coupled to the Noah land surface model (LSM) [Chen and Dudhia, 2001] and provided a more realistic representation of heat, momentum, and water vapor exchanges within urban environments by incorporating a simplified urban canyon geometry and considering the shadowing, reflection, and trapping of radiation. Finally, to provide a more spatially heterogeneous depiction of the urban land use, the urban fraction parameter (FRC\_URB2D) was specified using percent developed imperviousness data from the NLCD 2011 rather than relying upon the default WRF look-up tables.

For the non-urban simulation, the urban footprint of Atlanta was removed from the model. Specifically, the NLCD urban land use within the inner domain was replaced with a cropland/natural vegetation mosaic, which is one of the dominant land cover types within the vicinity of the Atlanta metropolitan area (Figure 3.2b). Since the urban environment was

excluded from the non-urban run, the SLUCM was no longer coupled to the Noah LSM and FRC\_URB2D was not specified.

### 3.2.3 Analysis of WRF Simulation Output

Several different techniques were used to analyze the output from the two simulations and identify any urban influences on the hydrometeorological characteristics of the flood. The analysis focused primarily on 19–22 September since this was the period of the most intense precipitation. Firstly, the precipitation from the urban simulation was compared with three different sets of observations to ensure that the model adequately captured the dominant features of the storm event. The spatial distribution of the modeled rainfall was evaluated using the Multi-Sensor Precipitation Estimates (MPE). MPE is a gridded precipitation product with a spatial resolution of approximately 4 km that combines Doppler radar estimates and observations from station gages [Seo, 1998; Seo *et al.*, 2010]. The overall mean RMSE of the MPE throughout the eastern United States is 8.13 mm, although this can vary for individual storm events [Wootten and Boyles, 2014]. Both the 6-hour and daily MPE datasets were utilized in the model validation. To gain an understanding of how the model resolved the temporal evolution of the storm, comparisons were drawn between the simulated precipitation and hourly observations obtained from the Fulton County Airport (KFTY) ASOS station. Lastly, the modeled output was compared to the average daily precipitation totals from the Community Collaborative Rain, Hail and Snow Network (CoCoRaHS) [Cifelli *et al.*, 2005] stations located in Douglas County and southern Fulton County.

After evaluating the model performance, potential urban modifications were detected by comparing areal averages of precipitation between the urban and non-urban simulations. The region included in the areal averages incorporated a majority of Douglas County and the

southern portions of Cobb and Fulton counties (Figure 3.3). This specific location was selected not only because it contained the heaviest rainfall, but it also represented the area downwind of Atlanta where *Shepherd et al.* [2011] hypothesized urban rainfall enhancement occurred. Although this region west of Atlanta is not commonly downwind of the city in terms of the broader climatology, the area is consistent with the “flow regime dependent” downwind area concept introduced by *McLeod et al.* [2017] because the predominant surface flow during the flood event was southeasterly. To further highlight any discrepancies between the urban and non-urban model runs, difference maps were created for variables such as surface runoff and sensible heat fluxes. Finally, the evolution of the circulations associated with the precipitation event were examined by creating cross sections of vertical velocity along two transects that spanned the city of Atlanta (Figure 3.3).

### **3.3 Results and Discussion**

#### **3.3.1 Model Validation**

The model performance was evaluated by comparing the daily precipitation accumulation from the urban simulation with the 24-hour MPE totals for 20–22 September 2009. The model appeared to capture the major elements of the rainfall distribution each day (Figure 3.4). The areas with the greatest precipitation totals on 20 September in northwest Georgia, northeast Georgia, and west of Atlanta were accurately depicted in the model. More detailed features were also resolved including the narrow band of heavy precipitation west of Atlanta that stretched north of I-20 roughly along the border of Paulding and Cobb county. Additionally, the model captured the pocket of intense precipitation over the southwestern quadrant of Atlanta. On 21 September, the urban simulation again adequately captured the regions of intense precipitation in northwest and northeast Georgia. The model also resolved the heavy rainfall directly over the

northern and western portions of Atlanta as well as the region of intense precipitation west of the city in Douglas and Cobb counties. Finally, the heavy precipitation within the vicinity of I-575 was accurately depicted by the urban simulation on 22 September.

Although the spatial patterning of precipitation and overall rainfall totals associated with the 2009 flood event were well represented in the urban model run, a few minor discrepancies emerged. Firstly, the simulation underestimated precipitation around the boundary of the inner domain, which was likely due to the cumulus parametrization being utilized in the outer domain but not the inner domain. Since the predominant surface flow was southeasterly, care was taken to position Atlanta further away from the southeastern domain boundary to prevent these possible edge effects from influencing the area of potential urban rainfall enhancement downwind of the city. Secondly, the precipitation totals appeared to be slightly higher in the urban simulation on 20 September relative to the MPE but lower on 22 September. This disparity could be due to the inherent limitations of the MPE dataset, which include the errors associated with radar beam geometry, assumptions of Z-R relationships, and gage undercatch [Smith *et al.*, 1996; Sieck *et al.*, 2007; Kitzmiller *et al.*, 2013; Wootten and Boyles, 2014]. Conversely, these differences might be indicative of a minor timing discrepancy, as the WRF simulation may have initiated the heaviest rainfall earlier. Despite these slight inconsistencies, the general spatial distribution and quantity of precipitation predicted by the urban model run was in reasonable agreement with the MPE daily totals.

Additional model validation was performed, which focused explicitly on the region downwind of Atlanta where urban rainfall enhancement potentially occurred. The hourly simulated precipitation was averaged within the downwind area of interest (Figure 3.3) and compared to hourly observations from the KFTY ASOS station to gain an understanding of how

the model resolved the temporal evolution of the storm. This comparison revealed that the urban simulation initiated rainfall earlier, however, the model did accurately depict two distinct periods of heavy precipitation (Figure 3.5). Although the KFTY observations appeared to indicate that there were three periods of intense rainfall, this was largely an artifact since the abrupt lull in precipitation on 21 September between 0900 and 1500 UTC was likely due to a gage malfunction. The values for most of the ASOS variables were reported as missing during these six hours and the METAR indicated that maintenance was needed on the system. Due to this missing data during the second period of intense rainfall, the cumulative precipitation total of approximately 200 mm reported at KFTY was likely a gross underestimate.

The precipitation within the downwind area of interest was also compared to CoCoRaHS and MPE precipitation values averaged over approximately the same region. Although these datasets were less suitable for examining the temporal accuracy of the model, due to their daily and 6-hour temporal resolutions, they were used to examine how well the model resolved the overall precipitation accumulation in the region of potential urban rainfall enhancement. The urban simulation performed satisfactorily, as the cumulative precipitation closely aligned with the areal averaged MPE and CoCoRaHS data (Figure 3.5). Specifically, the model predicted a total accumulation of 267 mm, which was only 9 and 16 mm less than the cumulative precipitation of the CoCoRaHS and MPE, respectively. Overall, the realistic depiction of the major elements associated with the 2009 Atlanta flood by the urban simulation suggests that the modeling experiment (i.e. removing the urban footprint of Atlanta) provided a substantive assessment of how urbanization influenced the hydrometeorological characteristics of the flood event.

### 3.3.2 Comparison of Precipitation and Runoff between the Urban and Non-Urban Simulations

The predicted daily precipitation accumulation from the non-urban simulation was also mapped to provide a qualitative comparison between urban and non-urban model runs (Figure 3.4). Several notable differences were immediately observable. On 20 September, the non-urban simulation failed to capture the intense precipitation in Douglas County south of I-20. Instead, the model appeared to incorrectly shift this pocket of heavy rainfall northward. The non-urban simulation also erroneously predicted a broad swath of intense precipitation northwest of Atlanta parallel to I-75, which was not observed in the MPE. Perhaps most importantly, the non-urban simulation failed to resolve the narrow band of heavy precipitation that stretched north of I-20 roughly along the border of Paulding and Cobb County.

Similar discrepancies were observed on 21 September. The non-urban simulation again underestimated the quantity of precipitation in Douglas County and southern Fulton County. Additionally, the model failed to capture the intense precipitation directly over the northern and western quadrants of Atlanta. The non-urban simulation also overestimated precipitation south of Atlanta between LaGrange and Macon during this period. Although overestimates in this region were also observed in the urban model, they were even more pronounced in the non-urban model. Finally, the differences between the two simulations were less notable on 21 September, as both models underestimated the daily total precipitation likely due to the earlier initiation of the extreme rainfall in WRF. The non-urban simulation, however, still produced less precipitation in the area of potential urban enhancement, particularly within I-285 over northwest Atlanta. Overall, the notable visual differences between the two models suggest that the urban environment played a notable role in governing both the location and the overall quantity of precipitation.



Averaging the precipitation from each simulation within the area of interest downwind of Atlanta (Figure 3.3) provided a more quantitative assessment of the potential urban rainfall enhancement (Figure 3.6). The non-urban simulation severely underestimated the precipitation during both periods of intense rainfall. Overall, the non-urban model predicted a precipitation total of 172 mm during the five-day period analyzed, which was approximately 100 mm less than the cumulative precipitation from the urban model. The underestimation by the non-urban simulation was so severe that the total cumulative precipitation was less than that reported by KFTY, which malfunctioned during the second phase of intense rainfall. The substantial magnitude of the differences revealed by this quantitative assessment further indicated that interactions with the urban environment of Atlanta likely amplified precipitation in Douglas county and southern Fulton and Cobb counties.

The notable disparities in precipitation had clear implications in terms of the surface runoff and flooding that was ultimately observed. To visualize these discrepancies, difference maps were created for surface runoff by subtracting the runoff values produced by the non-urban model from the urban model (Figure 3.7). On 20 September, a well-defined positive surface runoff anomaly of 80 mm was observed north of I-20 roughly along the border of Paulding and Cobb county. This was likely due to the non-urban simulation failing to resolve the narrow band on intense precipitation that developed downwind of Atlanta. Anomalies of a greater magnitude occurred on the following day, as the urban simulation produced 120 mm of additional surface runoff directly over Southwest Atlanta. The magnitudes of the anomalies perhaps suggest that they were not attributable to urban precipitation enhancement alone but were a combined effect of additional rainfall and increased surface runoff due to impervious surfaces. Overall, this highlights a potential two-pronged vulnerability of cities to extreme rainfall, as interactions with

the urban environment may enhance both the quantity of precipitation and the subsequent surface runoff [Yang *et al.*, 2013; McLeod *et al.*, 2017].

### 3.3.3 Potential Mechanisms Responsible for Urban Modification

To identify the potential mechanisms responsible for the observed urban rainfall enhancement downwind of Atlanta, the surface flow, convergence, sensible heat fluxes, and vertical circulations from both simulations were examined. The surface flow regime appeared to be altered substantially by the urban environment (Figure 3.8). Prior to the first period of intense precipitation, a clear boundary developed downwind of Atlanta at 20 September 0000 UTC along the urban-rural interface in the urban simulation. Importantly, this boundary was not observed when the urban footprint of Atlanta was removed from the model. One hour later, the boundary was still well pronounced, particularly along the border of Paulding and Cobb county north of I-20, in the urban simulation while it was largely nonexistent in the non-urban simulation. The failure of the non-urban model to resolve the surface flow boundary at the urban-rural interface likely contributed to its underestimation of precipitation in this area. Similar discrepancies were observed the following day during the second phase of intense precipitation. At 0200 UTC on 21 September, a boundary developed in the urban model over the southwest portion of Atlanta that stretched southwestward along I-85. In the non-urban simulation, this boundary was less pronounced, shifted towards the northwest, and no longer located directly over the city. Additionally, the boundary largely dissipated by 0300 UTC in the non-urban model while in the urban simulation it was still present over the city and roughly parallel to I-85. The less persistent boundary observed in the non-urban simulation was likely instrumental in the lower rainfall totals predicted by the model within the I-285 perimeter highway. Overall, interactions with the urban environment appeared to alter the surface flow regime substantially

and support the formation of persistent and well distinguished boundaries, which were conducive for extreme precipitation.

Divergence/convergence fields were also computed using the u and v wind components to visualize how the urban environment potentially enhanced near-surface convergence. Prior to the first period of extreme rainfall on 20 September 0200 UTC, a strong, linear band of convergence developed downwind of Atlanta north of I-20 along the borders of Paulding and Cobb county in the urban simulation (Figure 3.9). Although a localized pocket of convergence was observed in the non-urban model in this region, the linear extent and strength of the convergence zone was not fully captured. This suggests that interactions with the urban environment helped establish a linear convergence zone downwind of Atlanta that contributed to the prodigious rainfall totals observed in Cobb, Paulding, and Douglas counties. Several hours later at 0400 UTC, two distinct linear ribbons of convergence were still present in the urban simulation downwind of Atlanta along the urban-rural interface. This tight linear banding was absent in the non-urban simulation, which demonstrated the potential importance of the urban environment in sustaining the convergence zone along the urban-rural interface during the first period of intense precipitation. Previous studies have similarly indicated that urban land use can enhance convergence along the urban-rural interface rather than directly over the urban core [Shem and Shepherd, 2009].

Differences in convergence during the second phase of extreme precipitation were also observed (Figure 3.9). On 21 September 0200 UTC, both models initially resolved pockets of convergence over Atlanta. However, the non-urban simulation predicted that the areas of convergence would progress eastward beyond I-285 by 0300 UTC while in the urban model a band of convergence was still present directly over the city roughly parallel to I-85. This

suggests that interactions with the urban environment helped sustain the convergence zone directly over Atlanta. Overall, the less persistent convergence over Atlanta in the non-urban model likely contributed to its underestimation of precipitation within the city during the second period of intense rainfall.

Several different physical mechanisms may explain how interactions with the urban environment of Atlanta altered the surface flow and subsequent convergence fields. Firstly, it is widely documented that the increased surface roughness associated with urbanized land cover can enhance surface convergence [e.g. *Thielen et al.*, 2000]. Prior to the first period of intense rainfall, the surface flow appeared to be bifurcated slightly by the city due to the elevated surface roughness [e.g. *Bornstein and Lin*, 2000]. This bifurcation of the surface flow around the city potentially contributed to the linear convergence zone observed downwind of Atlanta in the urban simulation. Secondly, the convergence may have been enhanced by mesoscale circulations that were the product of thermal and/or flux gradients created by the different surface properties of the urban land use. When comparing the sensible heat fluxes of the urban and non-urban simulations, positive anomalies were observed within Atlanta in the urban model prior to each rainfall event due to the differing surface properties (Figure 3.10). The higher sensible heat fluxes within Atlanta in the urban simulation may have helped create, invigorate, and/or sustain mesoscale circulations that further enhanced the near-surface convergence. The second period of intense rainfall was perhaps more likely influenced by urban induced thermal circulations since the area of elevated convergence occurred directly over the urban core of Atlanta where the sensible heat flux was greater in the urban simulation (Figure 3.10). Although the differences in the sensible heat flux between the urban and non-urban simulations within Atlanta were relatively modest ( $\sim 40\text{-}60\text{ W/m}^2$ ) compared to similar modeling studies [*Shepherd et al.*, 2010],

they were perhaps great enough to invigorate or sustain mesoscale circulations. In all likelihood, a combination of both mechanisms as well as other factors not explicitly considered in the simulations, such as aerosol effects, contributed to the differences observed between the urban and non-urban model runs. It is challenging to conclusively determine the relative importance of each mechanism without more detailed sensitivity analyses that control for each factor individually.

Finally, vertical velocity cross sections were created for both the urban and non-urban simulations to visualize how the urban environment of Atlanta potentially altered the circulation patterns during the flood event. For the first period of rainfall, the vertical circulations associated with the narrow band of intense precipitation north of I-20 along the border of Cobb and Paulding county were examined using the northern cross-section (Figure 3.3). On 20 September 0000 UTC, the urban simulation predicted notable vertical velocities exceeding 4 m/s at the downwind urban-rural interface while the maximum vertical velocity predicted by the non-urban simulation at the same location was less than 1 m/s (Figure 3.11). The following hour substantial vertical velocities were still observed at the downwind urban-rural interface in the urban simulation. Although an updraft was also present in the non-urban model at 0100 UTC in a similar location, it exhibited less vertical development and displayed weaker vertical velocities. A comparable scenario occurred at 0200 UTC, as updrafts were present in both models but the urban simulation produced stronger vertical velocities. The discrepancies between the simulations were more pronounced by 0300 UTC. In the urban model run, strong updrafts exceeding 7 m/s were still present at the urban-rural interface, which were likely supported by a well-defined circulation that emerged over the city. Contrastingly, the vertical velocities in the non-urban simulation were less than 4 m/s and the strongest updraft had progressed further east.

Overall, the differences in the circulation patterns suggest that the urban environment supported an earlier formation of updrafts that exhibited greater vertical velocities and were ultimately more persistent along the urban-rural interface. These differences at least partially explain the greater rainfall totals observed along the border of Cobb and Paulding county in the urban simulation relative to the non-urban simulation.

A cross-section analysis was also performed for the second period of intense rainfall, which focused on the convergence zone located directly over the city using the southern cross-section (Figure 3.3). Similar differences were observed, as the vertical velocities were greater in the urban simulation relative to the non-urban simulation between 0000 and 0200 UTC (Figure 3.12). This capability of urban environments to enhance vertical velocities and the resulting convection is also documented by previous modeling studies that have performed similar urban versus non-urban comparisons [Niyogi *et al.*, 2011]. Surprisingly, the updraft was marginally stronger in the non-urban simulation by 0300 UTC, but it had shifted eastward and was no longer located over the urban core of Atlanta. Conversely, in the urban model, two updrafts were still present with one located closer to the downwind urban-rural interface and one positioned more directly over the city. The streamlines highlighted that low-level convergence potentially contributed to the stronger updraft observed over the city in the urban simulation at 0300 UTC. Overall, the cross-section results suggest that the urban environment played an important role in sustaining the quasi-stationary convective events, which *Shepherd et al.* [2011] identified as an important contributor to the prodigious precipitation totals.

### **3.4 Conclusions and Urban Planning Implications**

By constructing one of the first WRF representations of the 2009 Atlanta flood, this study explored the potential influence of urbanization on the storm's hydrometeorological

characteristics. A base run urban simulation was first conducted, which appeared to accurately capture the general spatial patterning and overall quantity of precipitation when compared with ASOS, MPE, and CoCoRaHS measurements. A non-urban simulation was then performed by replacing the urbanized land use with natural vegetation. To quantitatively assess the influence of the urban environment, comparisons were made between the urban and non-urban models.

The comparative analysis revealed noticeable discrepancies between the two simulations in the area downwind of Atlanta where *Shepherd et al.* [2011] hypothesized urban rainfall enhancement occurred. Specifically, the non-urban model underestimated the cumulative precipitation in this region by approximately 100 mm. The substantial differences in precipitation combined with the impervious land cover of the urban environment produced notable disparities in the surface runoff between the urban and non-urban simulations as well. In some regions of Atlanta, the urban simulation predicted 120 mm of additional surface runoff. Overall, the findings indicated that the urban environment of Atlanta played a notable role in governing the location and quantity of the precipitation and runoff that ultimately produced the record breaking 2009 flood.

Several different physical mechanisms were potentially responsible for the stark contrasts between the urban and non-urban simulations. Interactions with the urban environment appeared to alter the surface flow regime, which created, invigorated, and/or sustained areas of convergence particularly along the urban-rural interface. The observed surface flow alterations were partially due to the enhanced surface roughness within the urban environment. Additionally, the greater sensible heat fluxes in the urban simulation relative to the non-urban simulation likely altered the surface flow as well as the evolution of vertical circulation patterns. These two mechanisms potentially acted in tandem to produce the stronger and more persistent

updrafts observed in the urban model, which amplified the precipitation directly over and downwind of Atlanta. By quantitatively evaluating the urban rainfall effect during the 2009 Atlanta flood and identifying potential explanatory mechanisms, this study largely confirms the hypothesis of *Shepherd et al.* [2011] that urbanization substantially increased not only the surface runoff but also the quantity of precipitation that produced the flood. Furthermore, the findings suggest that interactions with the urban environment can alter the mesoscale hydrometeorological characteristics of a storm event even if it is synoptically driven.

From an urban planning perspective, these findings highlight a potential two-pronged vulnerability of urban environments to extreme rainfall. While it is widely understood that impervious surfaces can increase surface runoff during extreme rainfall events [e.g. *Yang et al.*, 2013; *Debbage and Shepherd*, Submitted], the capability of urban environments to also amplify the actual precipitation is not as broadly acknowledged. Fortunately, this two-pronged vulnerability may indicate that mitigation strategies aimed at reducing the influence of urbanization on runoff have previously unrecognized synergistic benefits. For example, while incorporating green infrastructure within a city can enhance infiltration and mitigate increases in surface runoff due to urbanization [*Kim and Park*, 2016], it could also potentially reduce the surface roughness as well as the thermal and flux gradients within the urban environment that are often responsible for urban rainfall enhancement. This highlights the critical importance of green infrastructure as a possible synergistic policy solution due to its well-recognized runoff benefits and its potential to reduce urban rainfall enhancement as well. Importantly, the National Research Council has examined many facets of this topic and provided specific recommendations on how to transition such knowledge into urban planning and flood management [*National Research Council*, 2012].



Of course, the results are certainly sensitive to the model specifications as well as the unique characteristics of the storm itself. Due to the lack of detailed urban land use for Atlanta, this study relied upon the NLCD dataset and a single layer urban canopy model. Future modeling efforts that utilize more complex urban land use based on urban climate zones and incorporate a multilayer urban canopy model may provide further insights into the physical mechanisms responsible for the differences observed between the urban and non-urban simulations. Furthermore, considering additional case studies is imperative to more conclusively determine the commonality of urban rainfall enhancement during large-scale flooding events. Despite these avenues for future research, this study provides an important contribution to the emerging body of literature [e.g. *Ntelekos et al., 2008*; *Yang et al. 2014*; *Yu and Liu, 2015*] that suggests urban environments can influence the magnitude and location of precipitation even during events with prominent synoptic scale forcing.

### **3.5 References**

- Ashley, W. S., M. L. Bentley, and J. A. Stallins (2012), Urban-induced thunderstorm modification in the Southeast United States, *Clim. Change*, *113*, 481–498, doi: 10.1007/s10584-011-0324-1.
- Bornstein, R., and Q. Lin (2000), Urban heat islands and summertime convective thunderstorms in Atlanta: three case studies, *Atmos. Environ.*, *34*, 507–516, doi: [https://doi.org/10.1016/S1352-2310\(99\)00374-X](https://doi.org/10.1016/S1352-2310(99)00374-X).
- Burian, S. J., and J. M. Shepherd (2005), Effect of urbanization on the diurnal rainfall pattern in Houston, *Hydrol. Process.*, *19*, 1089–1103, doi: 10.1002/hyp.5647.
- Changnon, S. A., F. A. Huff, P. T. Schickedanz, and J. L. Vogel (1977), Summary of METROMEX, Volume 1: Weather anomalies and impacts, *Illinois State Water Survey, Bulletin 62*, 260 pp. [Available at <https://www.isws.illinois.edu/pubdoc/B/ISWSB-62.pdf>.]
- Chen, F., and Coauthors (2011), The integrated WRF/urban modelling system: development, evaluation, and applications to urban environmental problems, *Int. J. Climatol.*, *31*, 273–288, doi: 10.1002/joc.2158.
- Chen, F., and J. Dudhia (2001), Coupling an advanced land surface-hydrology model with the Penn State-NCAR MM5 modeling system: Part I: Model implementation and sensitivity, *Mon. Wea. Rev.*, *129*, 569–585, doi: 10.1175/1520-0493(2001)129<0569:CAALSH>2.0.CO;2.
- Cifelli, R., N. Doesken, P. Kennedy, L. D. Carey, S. A. Rutledge, C. Gimmestad, and T. Depue (2005), The community collaborative rain, hail, and snow network: Informal education for scientists and citizens, *Bull. Amer. Meteor. Soc.*, *86*, 1069–1077, doi: 10.1175/BAMS-86-8-1069.
- Debbage, N., J. McLeod, J. Rackley, L. Zhu, T. Mote, and A. J. Grundstein (2015), The influence of point source aerosol emissions on atmospheric convective activity in the vicinity of power plants in Georgia, USA, *Pap. Appl. Geogr.*, *1*, 134–142, doi: 10.1080/23754931.2015.1012430.
- Debbage, N., and J. M. Shepherd (Submitted), The influence of urban development patterns on streamflow characteristics in the Charlanta Megaregion, *Water Resour. Res.*
- Diem, J. E., and D. P. Brown (2003), Anthropogenic impacts on summer precipitation in Central Arizona, U.S.A, *Prof. Geogr.*, *55*, 343–355, doi: 10.1111/0033-0124.5503011.
- Diem, J. E., and T. L. Mote (2005), Interepothal changes in summer precipitation in the Southeastern United States: Evidence of possible urban effects near Atlanta, Georgia, *J. Appl. Meteor.*, *44*, 717–730, doi: 10.1175/JAM2221.1.

- Dixon, P. G., and T. L. Mote (2003), Patterns and causes of Atlanta's urban heat island-initiated precipitation, *J. Appl. Meteor.*, *42*, 1273–1284, doi: 10.1175/1520-0450(2003)042<1273:PACOAU>2.0.CO;2.
- Gamble, D. W., and V. G. Meentemeyer (1997), A synoptic climatology of extreme unseasonable floods in the Southeastern United States, 1950–1990, *Phys. Geogr.*, *18*(6), 496–524, doi: 10.1080/02723646.1997.10642632.
- Haberlie, A. M., W. S. Ashley, and T. J. Pingel (2015), The effect of urbanisation on the climatology of thunderstorm initiation, *Q. J. R. Meteorol. Soc.*, *141*, 663–675, doi: 10.1002/qj.2499.
- Homer, C. G., J. A. Dewitz, L. Yang, S. Jin, P. Danielson, G. Xian, J. Coulston, N. D. Herold, J. D. Wickham, and K. Megown (2015), Completion of the 2011 National Land Cover Database for the conterminous United States-Representing a decade of land cover change information, *Photogramm. Eng. Remote Sens.*, *81*(5), 345–354, doi:10.14358/PERS.81.5.345.
- Horton, R. E. (1921), Thunderstorm–breeding spots, *Mon. Wea. Rev.*, *49*, 193, doi: 10.1175/1520-0493(1921)49<193a:TS>2.0.CO;2.
- Houston, D., A. Werritty, D. Bassett, A. Geddes, A. Hoolachan, and M. McMillan (2011), Pluvial (rain-related) flooding in urban areas: The invisible hazard. Joseph Rowntree Foundation, 96 pp. [Available at <https://www.jrf.org.uk/report/pluvial-rain-related-flooding-urban-areas-invisible-hazard>.]
- Huff, F. A., and S. A. Changnon (1973), Precipitation modification by major urban areas, *Bull. Amer. Meteor. Soc.*, *54*, 1220–1232, doi: 10.1175/1520-0477(1973)054<1220:PMBMUA>2.0.CO;2.
- Kitzmillier, D., D. Miller, R. Fulton, and F. Ding (2013), Radar and multisensor precipitation techniques in National Weather Service hydrologic operations, *J. Hydrol. Eng.*, *18*, 133–142, doi: 10.1061/(ASCE)HE.1943-5584.0000523.
- Kim, H. W., and Y. Park (2016), Urban green infrastructure and local flooding: The impact of landscape patterns on peak runoff in four Texas MSAs, *Appl. Geogr.*, *77*, 72–81, doi: 10.1016/j.apgeog.2016.10.008.
- Kusaka, H., H. Kondo, Y. Kikegawa, and F. Kimura (2001), A simple single-layer urban canopy model for atmospheric models: Comparison with multi-layer and slab models, *Bound.-Layer Meteorol.*, *101*, 329–358, doi: 10.1023/A:101920792.
- Leopold, L. B. (1968), Hydrology for urban planning – A guidebook on the hydrologic effects of urban land use, *U.S. Geol. Surv. Circ. 554*, U.S. Geol. Surv., Washington, D.C. [Available at <https://pubs.usgs.gov/circ/1968/0554/report.pdf>.]

- McCallum, B. E., and A. J. Gotvald (2010), Historic flooding in northern Georgia, September 16–22, 2009. *USGS Fact Sheet 2010-3061*, 3 pp. [Available at <http://pubs.usgs.gov/fs/2010/3061/pdf/fs2010-3061.pdf>.]
- McLeod, J., J. M. Shepherd, and C. E. Konrad (2017), Spatio-temporal rainfall patterns around Atlanta, Georgia and possible relationships to urban land cover, *Urban Clim.*, *21*, 27–42, doi: 10.1016/j.uclim.2017.03.004.
- Mesinger, F., and Coauthors (2006), North American regional reanalysis, *Bull. Amer. Meteor. Soc.*, *87*, 343–360, doi: 10.1175/BAMS-87-3-343.
- Molders, N., and M. A. Olson (2004), Impact of urban effects on precipitation in high latitudes, *J. Hydrometeor.*, *5*, 409–429, doi: 10.1175/1525-7541(2004)005<0409:IOUEOP>2.0.CO;2.
- National Research Council (2012), *Urban Meteorology: Forecasting, Monitoring, and Meeting Users' Needs*, The National Academies Press, 190 pp.
- Niyogi, D., P. Pyle, M. Lei, S. P. Arya, C. M. Kishtawal, M. Shepherd, F. Chen, and B. Wolfe (2011), Urban modification of thunderstorms: An observational storm climatology and model case study for the Indianapolis urban region, *J. Appl. Meteor. Climatol.*, *50*, 1129–1144, doi: 10.1175/2010JAMC1836.1.
- Ntelekos, A. A., J. A. Smith, M. L. Baeck, W. F. Krajewski, A. J. Miller, and R. Goska (2008), Extreme hydrometeorological events and the urban environment: Dissecting the 7 July 2004 thunderstorm over the Baltimore MD metropolitan regions, *Water Resour. Res.*, *44*, doi: 10.1029/2007WR006346.
- NWS Atlanta (2014), 5th Anniversary Atlanta Flood. NOAA, 1 pp. [Available at [http://www.weather.gov/images/ffc/events/SeptFlood2009/September2009\\_infographic.png](http://www.weather.gov/images/ffc/events/SeptFlood2009/September2009_infographic.png).]
- Rose, L. S., J. A. Stallins, and M. L. Bentley (2008), Concurrent cloud-to-ground lightning and precipitation enhancement in the Atlanta, Georgia (United States), urban region, *Earth Interact.*, *12*, 1–30, doi: 10.1175/2008EI265.1.
- Schmid, P. E., and D. Niyogi (2017), Modeling urban precipitation modification by spatially heterogeneous aerosols, *J. Appl. Meteor. Climatol.*, *56*, 2141–2153, doi: 10.1029/2011JD017352.
- Schroeder, A. J., and Coauthors (2016), The development of a flash flood severity index, *J. Hydrol.*, *541*, 523–532, doi: 10.1016/j.jhydrol.2016.04.005.
- Seo, D. J. (1998), Real-time estimation of rainfall fields using radar rainfall and rain gage data, *J. Hydrol.*, *208*, 37–52, doi: 10.1016/S0022-1694(98)00141-3.

- Seo, D. J., A. Seed, and G. Delrieu (2010), Radar and multisensory rainfall estimation for hydrologic applications, in *Rainfall: State of the Science*, edited by F. Y. Testik and M. Gebremichael, pp. 79–104, American Geophysical Union.
- Shem, W., and J. M. Shepherd (2009), On the impact of urbanization on summertime thunderstorms in Atlanta: Two numerical model case studies, *Atmos. Res.*, *92*, 172–189, doi: 10.1016/j.atmosres.2008.09.013.
- Shepherd, J. M. (2005), A review of current investigations of urban-induced rainfall and recommendations for the future, *Earth Interact.*, *9*, 1–27, doi: 10.1175/EI156.1.
- Shepherd, J. M., H. Pierce, and A. J. Negri (2002), Rainfall modification by major urban areas: Observations from spaceborne rain radar on the TRMM satellite, *J. Appl. Meteor.*, *41*, 689–701, doi: 10.1175/1520-0450(2002)041<0689:RMBMUA>2.0.CO;2.
- Shepherd, J. M., and S. J. Burian (2003), Detection of urban-induced rainfall anomalies in a major coastal city, *Earth Interact.*, *7*, 1–17, doi: 10.1175/1087-3562(2003)007<0001:DOUIRA>2.0.CO;2.
- Shepherd, J. M., T. Mote, J. Dowd, M. Roden, P. Knox, S. C. McCutcheon, and S. E. Nelson (2011), An overview of synoptic and mesoscale factors contribution to the disastrous Atlanta flood of 2009, *Bull. Amer. Meteor. Soc.*, *92*, 861–870, doi: 10.1175/2010BAMS3003.1.
- Sieck, L. C., S. J. Burges, M. Steiner (2007), Challenges in obtaining reliable measurements of point rainfall, *Water Resour. Res.*, *43*, W01420, doi: 10.1029/2005WR004519.
- Skamarock, W. C., and Coauthors (2008), A description of the advanced research WRF version 3, *NCAR Technical Note TN-475+STR*, 125 pp. [Available at [http://www2.mmm.ucar.edu/wrf/users/docs/arw\\_v3.pdf](http://www2.mmm.ucar.edu/wrf/users/docs/arw_v3.pdf).]
- Smith, J. A., D. J. Seo, M. L. Baeck, and M. D. Hudlow (1996), An intercomparison study of NEXRAD precipitation estimates, *Water Resour. Res.*, *32*, 2035–2045, doi: 10.1029/96WR00270.
- Thielen, J., W. Wobrock, A. Gadian, P. G. Mestayer, J. -D. Creutin (2000), The possible influence of urban surfaces on rainfall development: a sensitivity study in 2D in the meso- $\gamma$ -scale, *Atmos. Res.*, *54*, 15–39, doi: 10.1016/S0169-8095(00)00041-7.
- Wootten, A., and R. P. Boyles (2014), Comparison of NCEP multisensor precipitation estimates with independent gauge data over the Eastern United States, *J. Appl. Meteor. Climatol.*, *53*, 2848–2862, doi: 10.1175/JAMC-D-14-0034.1.

- Yang, L., J. A. Smith, D. B. Wright, M. L. Baeck, G. Villarini, F. Tian, and H. Hu (2013), Urbanization and climate change: An examination of nonstationarities in urban flooding, *J. Hydrometeorol.*, *14*, 1791–1809, doi:10.1175/JHM-D-12-095.1.
- Yang, L., J. A. Smith, M. L. Baeck, E. Bou-Zeid, and S. M. Jessup (2014), Impact of urbanization on heavy convective precipitation under strong large-scale forcing: A case study over the Milwaukee-Lake Michigan region, *J. Hydrometeor.*, *15*, 261–278, doi: 10.1175/JHM-D-13-020.1.
- Yu, M., and Y. Liu (2015), The possible impact of urbanization on a heavy rainfall event in Beijing, *J. Geophys. Res. Atmos.*, *120*, 8132–8143, doi: 10.1002/2015JD023336.

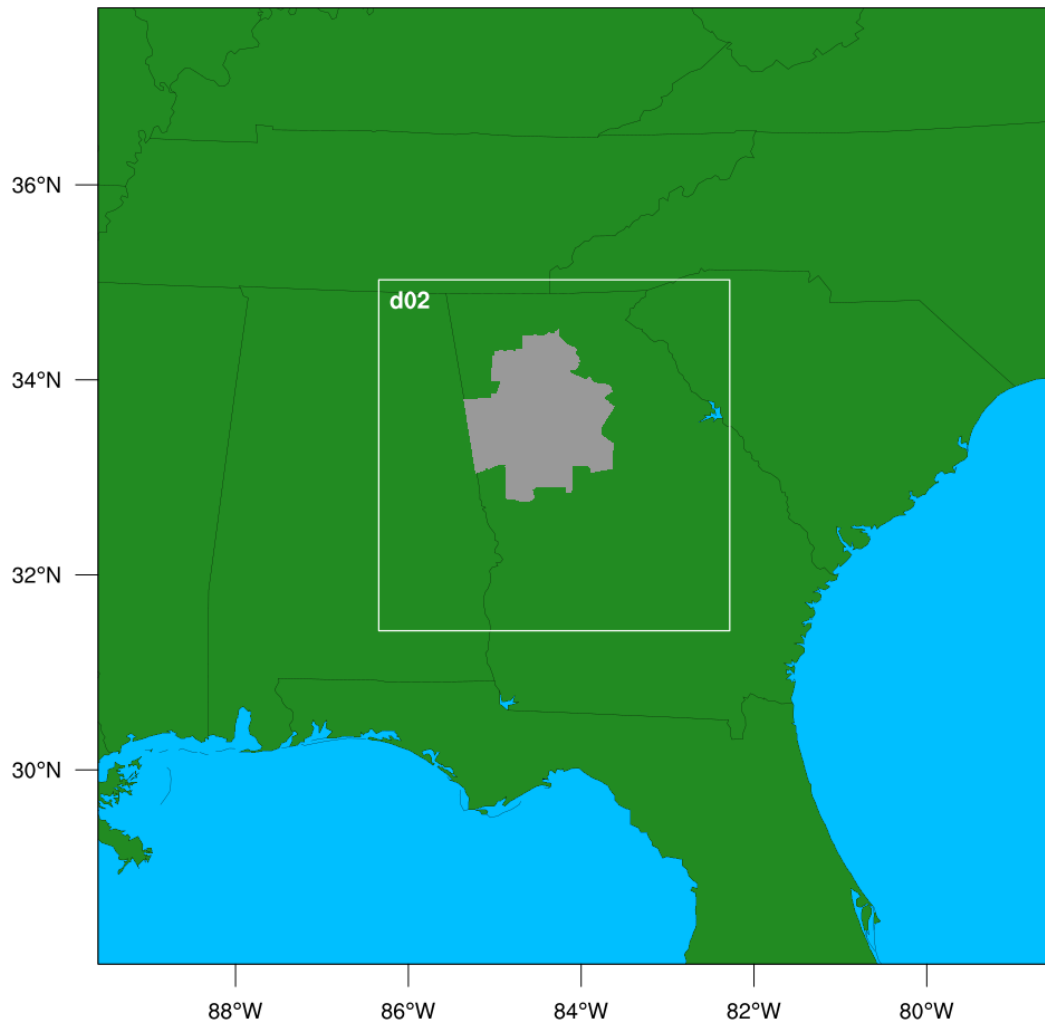


Figure 3.1. Location of the outer (outer black box) and inner (inner white box) modeling domains used to simulate the 2009 Atlanta Flood. The gray shading represents the extent of the Atlanta Metropolitan Statistical Area.

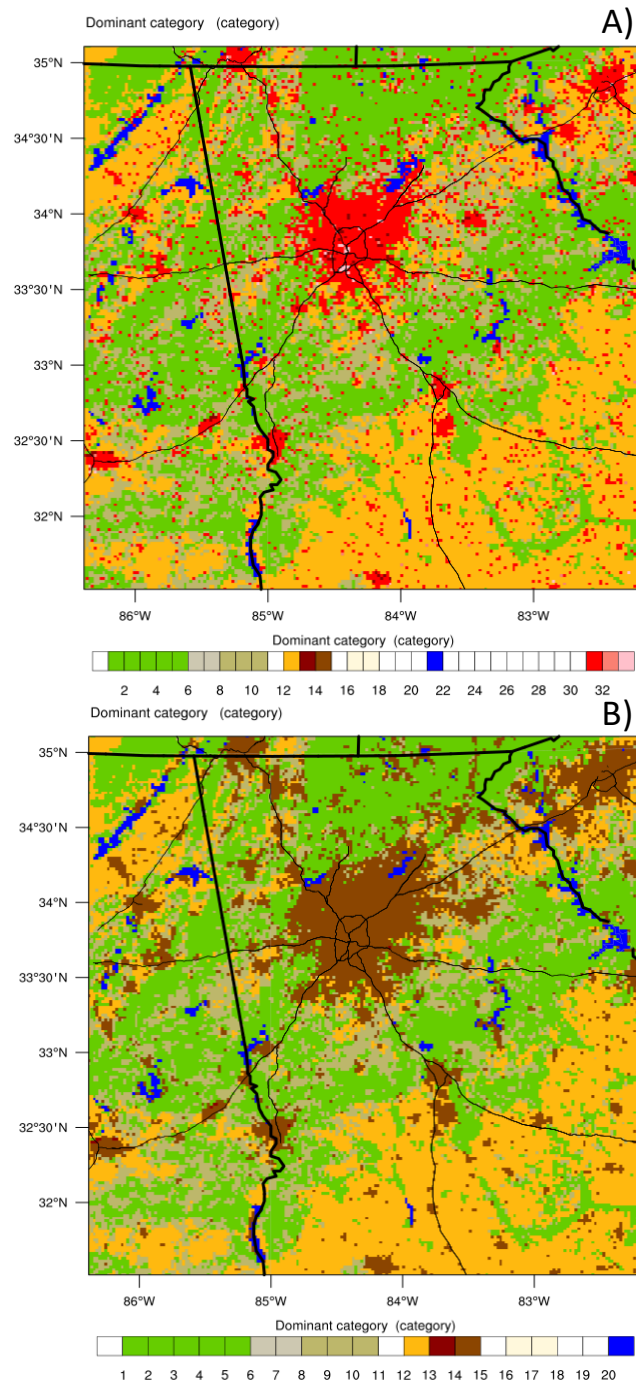


Figure 3.2. Land use scenarios used in the a) urban run and b) non-urban run. Shades of red represent urban land use of various intensities and brown represents the cropland/vegetation mosaic used to replace the urban development. Major roadways are represented by thin black lines and state boundaries are indicated by thick black lines.



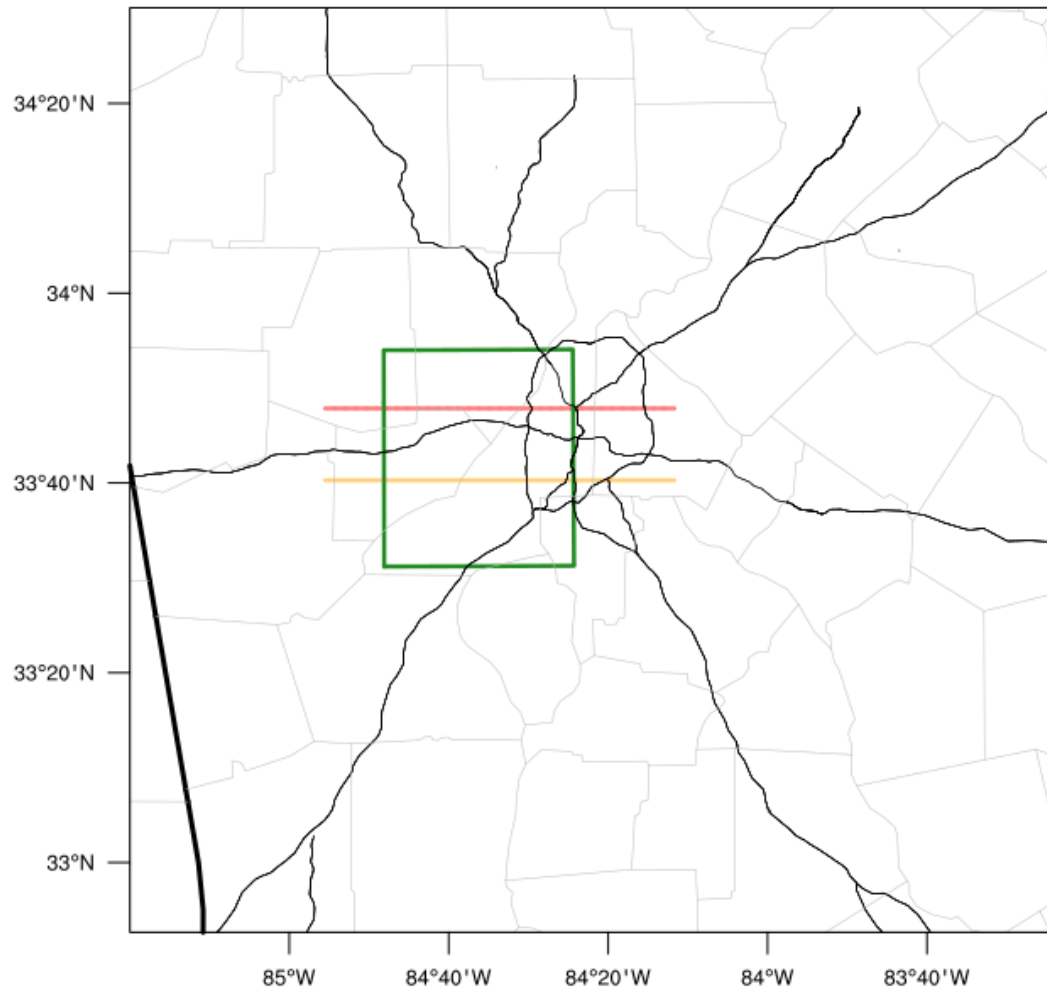


Figure 3.3. Location of the downwind area of interest included in the areal averages (green box) and the north (orange line) and south (yellow line) vertical cross sections.

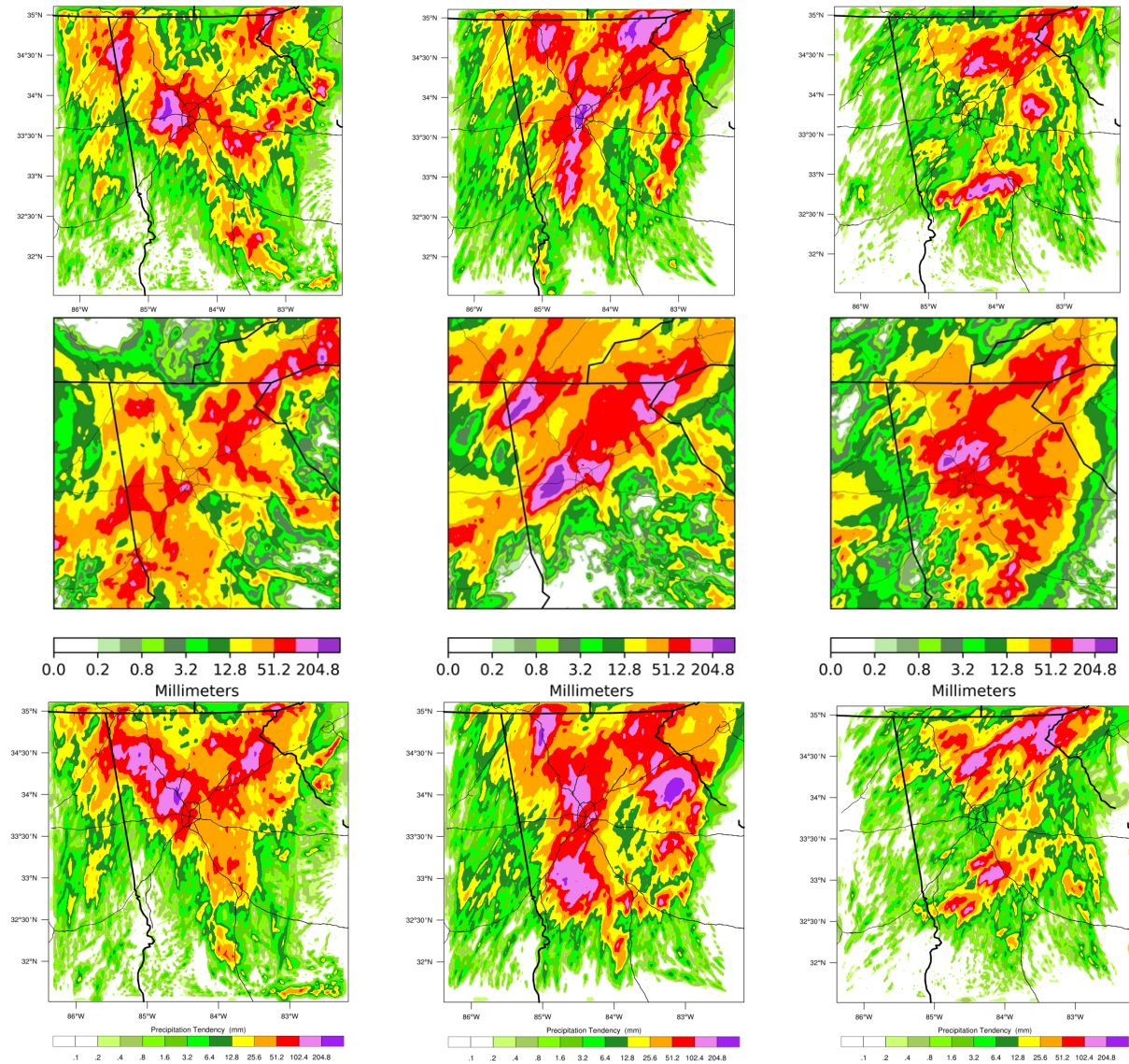


Figure 3.4. Daily precipitation totals from the urban simulation (top row), MPE (middle row), and non-urban simulation (bottom row) for 20 September 1200 UTC (left column), 21 September 1200 UTC (middle column), and 22 September 1200 UTC (right column).

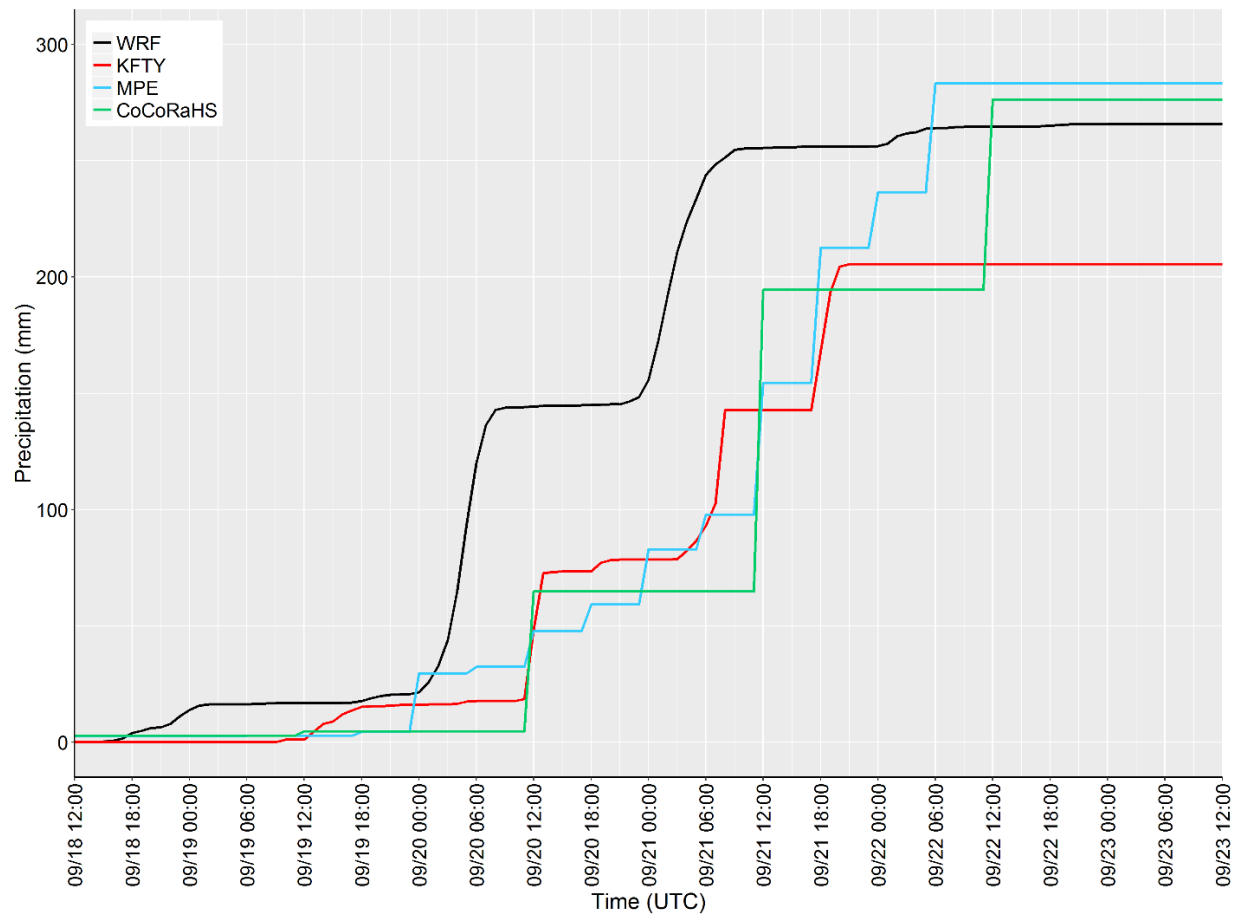


Figure 3.5. Comparison of the hourly precipitation from the urban WRF simulation averaged within the downwind area of interest with several proximate observations.

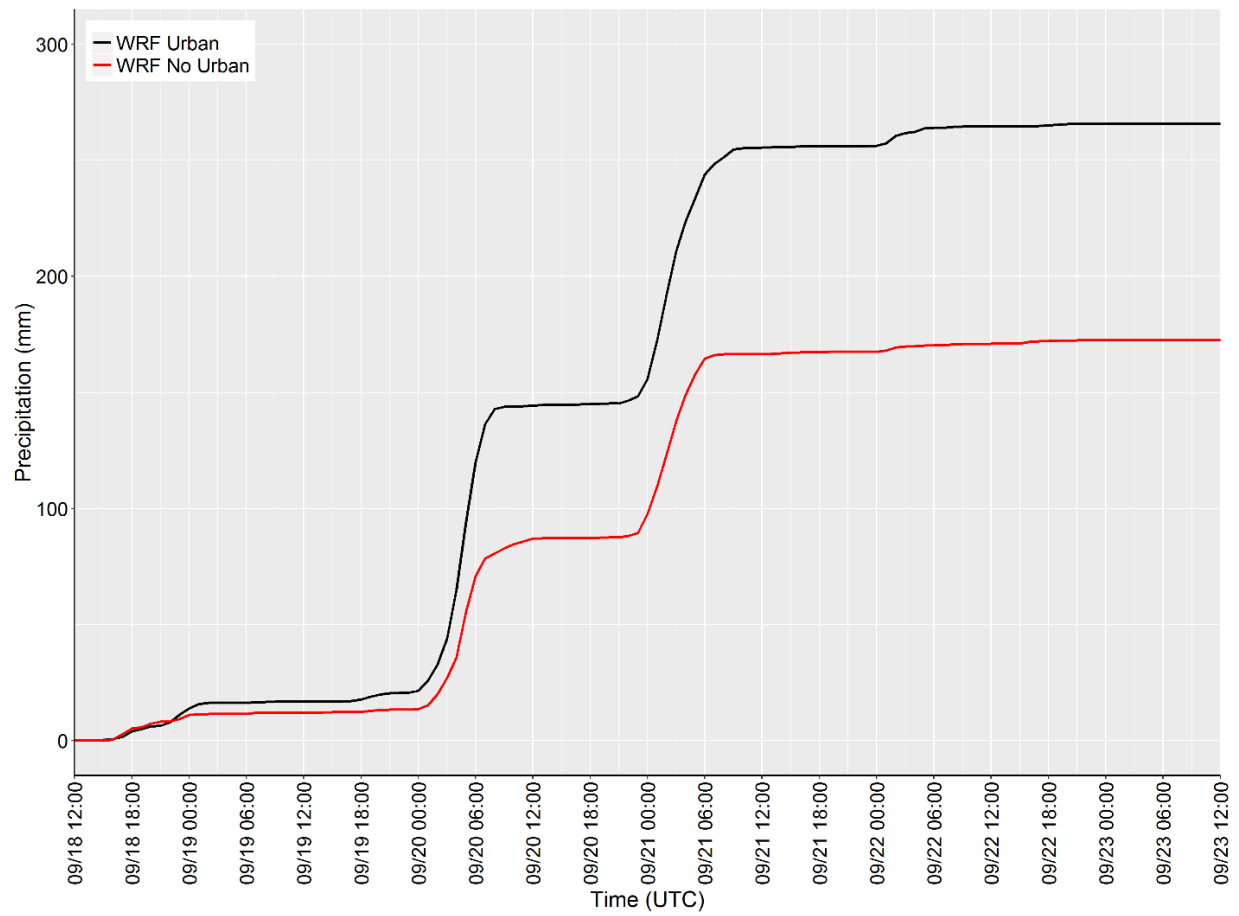


Figure 3.6. Comparison of the hourly precipitation averaged within the downwind area of interest between the urban and non-urban WRF simulations.

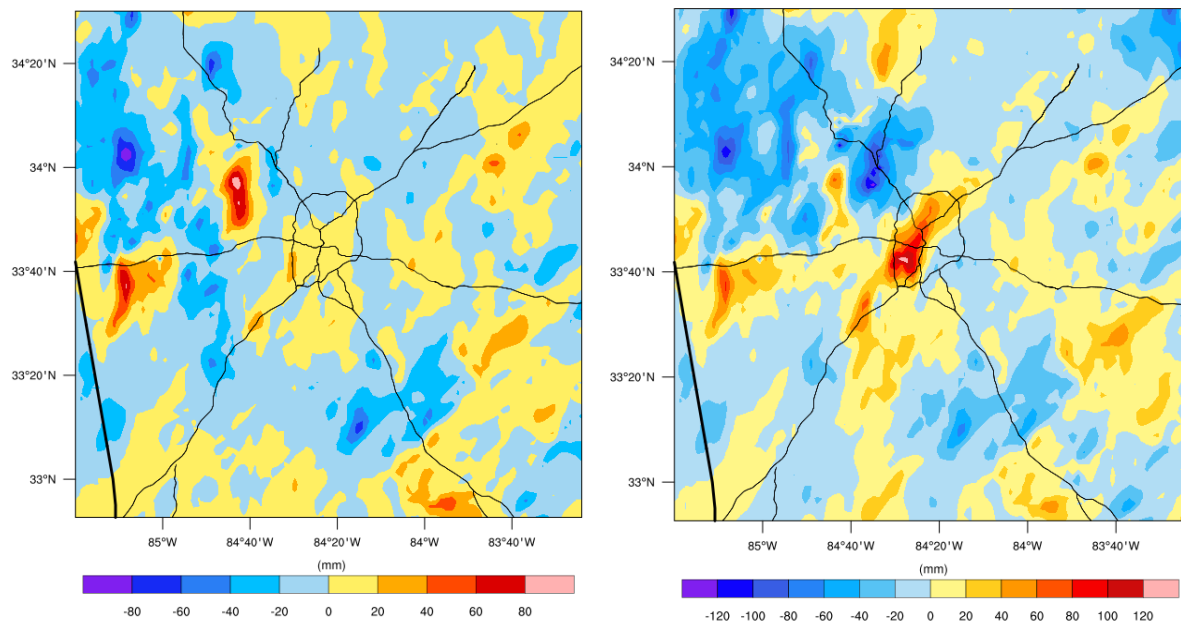


Figure 3.7. Difference in the surface runoff (Urban – Non-Urban) during the two heavy periods of precipitation at 9/20 0400 UTC (left) and 9/21 0500 UTC (right).

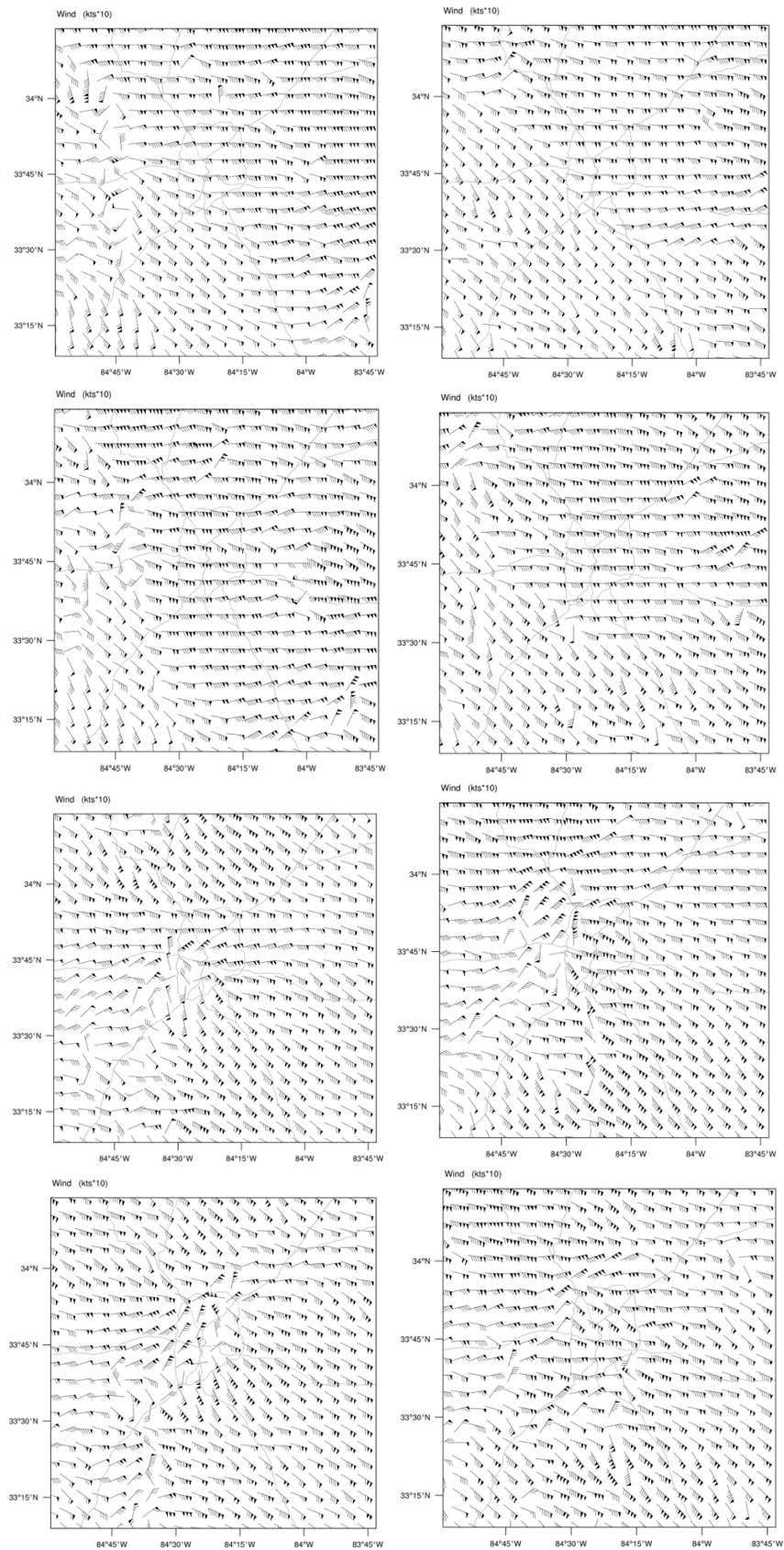


Figure 3.8. Surface flow patterns from the urban (left) and non-urban simulation (right) at 20 September 0000 UTC (top), 20 September 0100 UTC (middle top), 21 September 0200 UTC (middle bottom), and 21 September 0300 UTC (bottom).

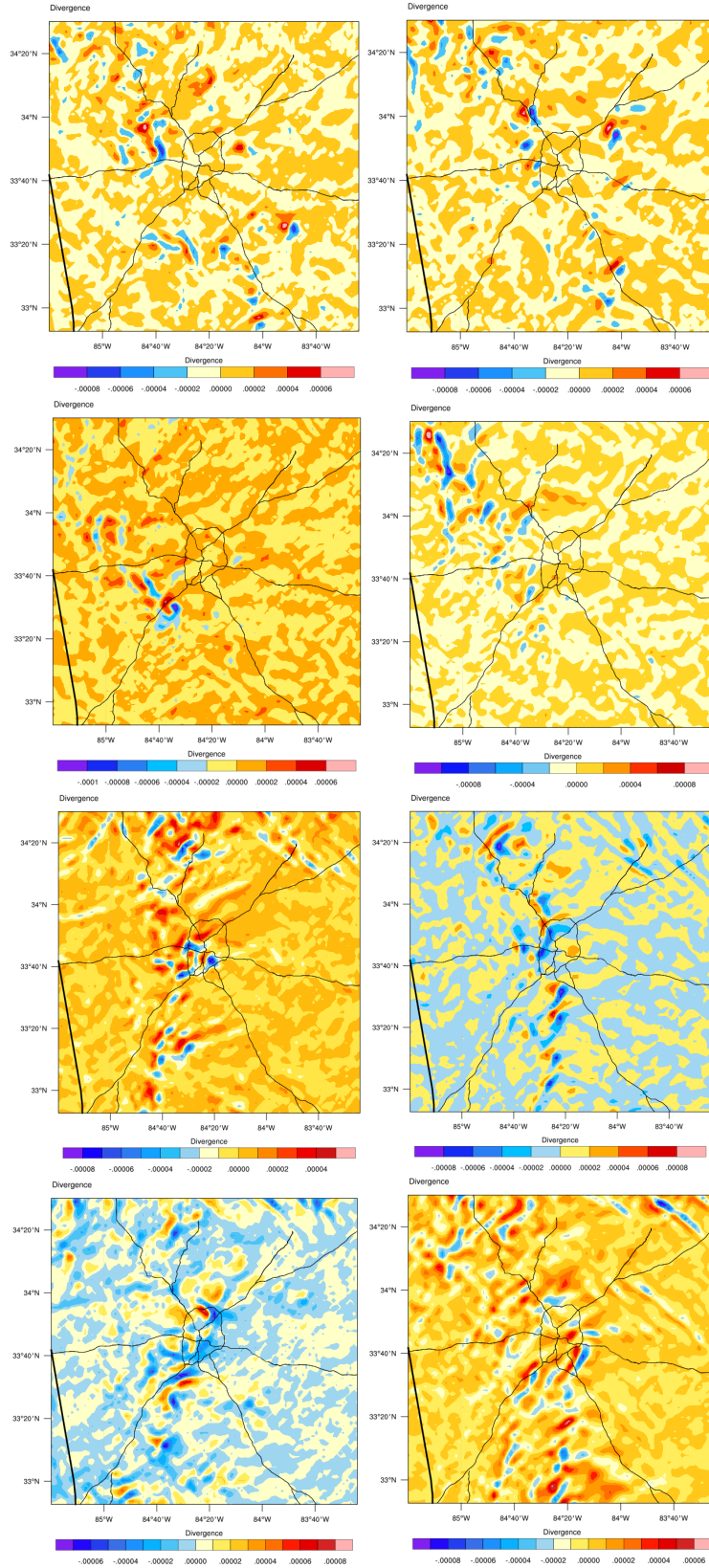




Figure 3.9. Divergence/Convergence fields from the urban (left) and non-urban simulation (right) at 20 September 0200 UTC (top), 20 September 0400 UTC (middle top), 21 September 0200 UTC (middle bottom), and 21 September 0300 UTC (bottom). Negative values are indicative of convergence.

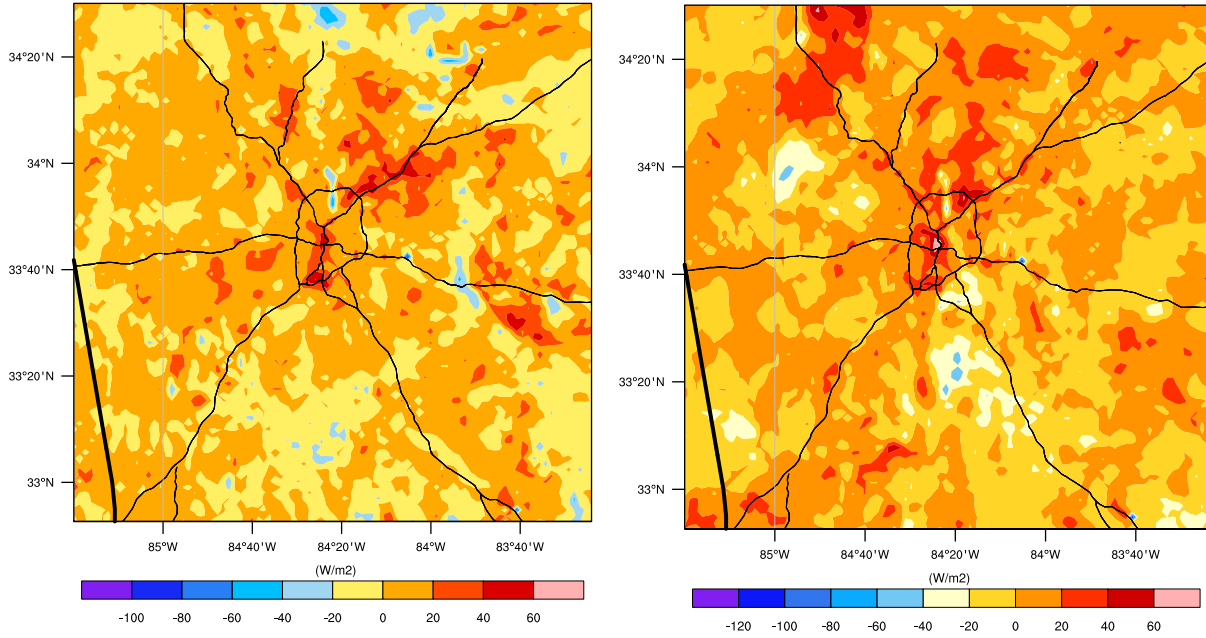


Figure 3.10. Differences in the sensible heat flux between the urban simulation and non-urban simulation for 19 September 2300 UTC (left) and 21 September 0000 UTC (right). Positive values are indicative of greater sensible heat flux in the urban simulation.

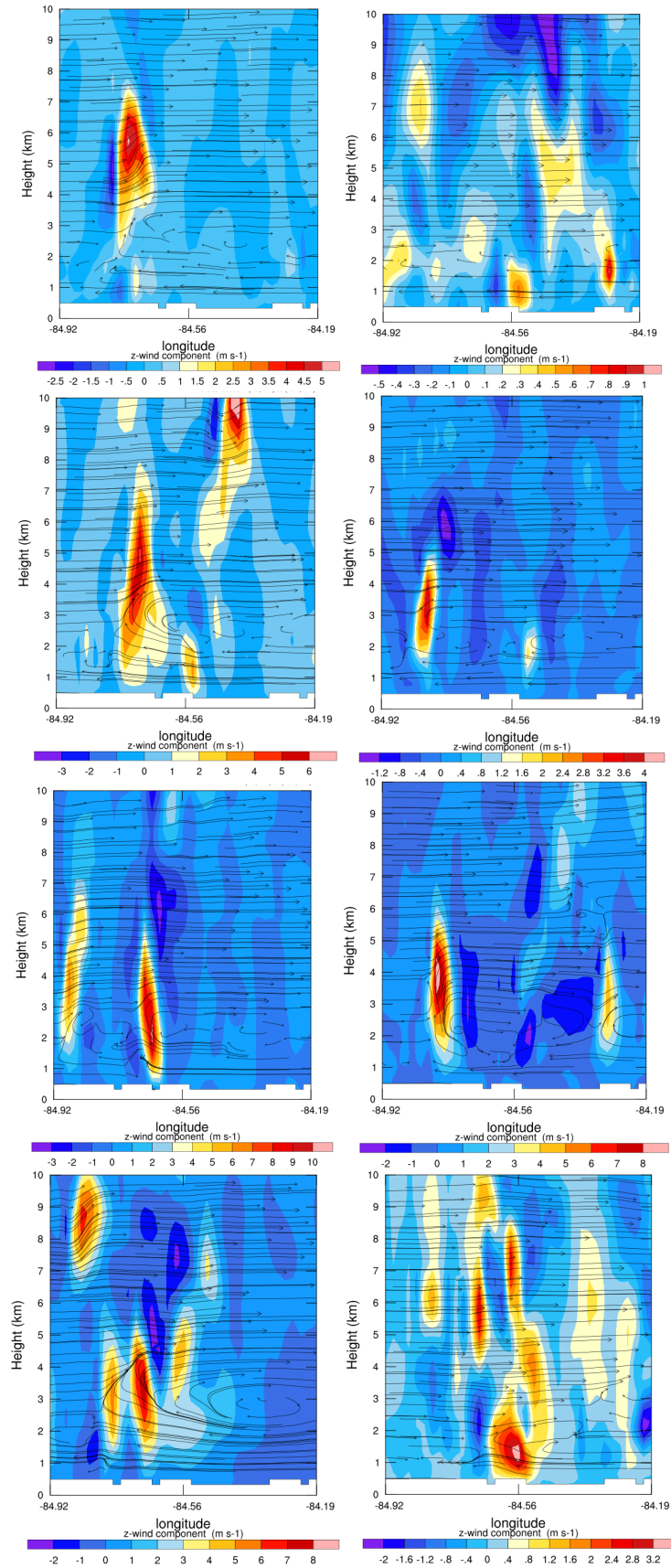


Figure 3.11. Vertical cross sections along the northern transect from the urban (left) and non-urban (right) simulation at 20 September 0000 UTC (top), 0100 UTC (middle top), 0200 UTC (middle bottom), and 0300 UTC (bottom).

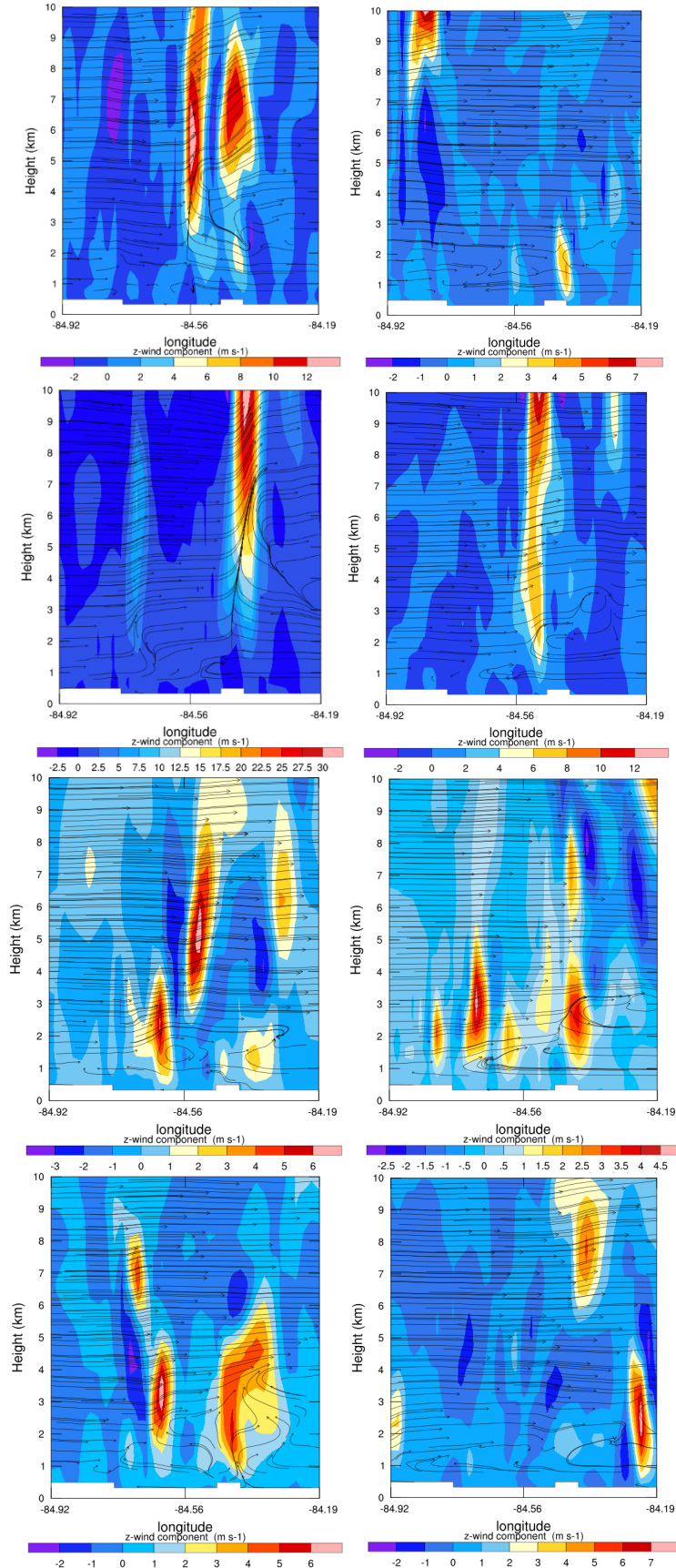


Figure 3.12. Vertical cross sections along the southern transect from the urban (left) and non-urban (right) simulation at 21 September 0000 UTC (top), 0100 UTC (middle top), 0200 UTC (middle bottom, and 0300 UTC (bottom).

Table 3.1. WRF-ARW physics options used in the simulations.

Physics	Scheme
Microphysics	WRF Single-Moment 6-Class
Cumulus Parametrization	Kain-Fritsch (Outer)/None (Inner)
Boundary Layer	Mellor-Yamada-Janjic
Longwave Radiation	RRTMG
Shortwave Radiation	RRTMG
Surface Layer	Eta Similarity
Land Surface	Noah

CHAPTER 4

MULTISCALAR ASSESSMENT OF FLOOD ZONE OCCUPATION AND  
ENVIRONMENTAL JUSTICE<sup>3</sup>

---

<sup>3</sup> Debbage, N. and J. M. Shepherd. To be submitted to *Anthropocene*.



## **Abstract**

Urban areas are particularly vulnerable to flood hazards due to impervious surfaces altering the runoff response as well as socio-economic pressures increasing the number of individuals residing in areas at risk for flooding. Although previous studies have utilized an environmental justice framework to address the socio-economic dimensions of this vulnerability, they have produced contrasting results due to the different dasymetric mapping techniques utilized to estimate urban flood zone population characteristics, the various scales at which the estimates are calculated, and the specific geographical context of the individual study cities. This paper evaluated the potential sensitivity of urban flood risk environmental injustices to these parameters by analyzing flood zone occupancy with three different dasymetric mapping techniques at four scales for numerous metropolitan areas within the Charlanta megaregion. Specifically, 2010 US Census block group data, FEMA flood zones, and risk ratios were used to evaluate if African Americans were overrepresented in areas at risk for flooding. The findings varied according to the different dasymetric mapping techniques, but the most sophisticated approach suggested that environmental injustices were systemic across the megaregion. African Americans were 44% more likely to reside in areas at risk for flooding than Whites in Charlanta. Similarly, at the metropolitan scale, African Americans were significantly more likely to reside in flood zones. A more complex and spatially varying landscape of injustice was observed at the county and census tract scales. However, the overall systemic nature of environmental injustice related to urban flooding observed in Charlanta suggests that broad structural changes will be required to ultimately reduce the disproportionate flood risk that African Americans bear.

**Key Words:** Urban Flood Hazards, Environmental Justice, Charlanta Megaregion, Dasymetric Mapping

## **4.1 Introduction**

As made particularly evident by the catastrophic impact of Hurricane Harvey on Houston in 2017, urban areas are increasingly vulnerable to flood hazards. This vulnerability can be attributed to the physical alteration of the natural landscape by urban development as well as complex socio-economic factors [Zahran *et al.*, 2008]. The physical modifications of surface and subsurface hydrological processes by the impervious surfaces and stormwater drainage systems common throughout cities act to enhance peak flows, runoff volumes, and flashiness, which elevates the risk of floods in urban settings [Leopold, 1968; Sauer *et al.*, 1984; Debbage and Shepherd, Submitted A]. Additionally, the rapid expansion of urban areas has further threatened the sustainability of cities from a flood hazard perspective by placing additional pressures on the natural streams and aging infrastructure tasked with managing runoff during intense precipitation events [Miller, 2010].

While the (sub)surface characteristics of the urban environment alone increase the likelihood of damaging flood events, the socio-economic pressures of urbanization simultaneously concentrate individuals in areas at risk for flooding. Unfortunately, the dangers associated with living in these flood prone areas have likely contributed to the lack of a significant decrease in flood fatalities during the 21<sup>st</sup> century [Ashley and Ashley, 2008], unlike deaths related to other meteorological hazards such as tornadoes and lightning. This implies that the advancements made in forecasting urban flood events, warning systems, and emergency recovery procedures have to some extent been overwhelmed by rapid urban population growth [Terti *et al.*, 2017]. Clearly, increasing urban flood zone occupancy can enhance the likelihood of deadly and damaging floods even if the hydrologic risk remains largely unaltered [Brissette *et al.*, 2003; Ferguson and Ashley, 2017].

Overall, urban environments produce a more extreme hydrologic regime [*Debbage and Shepherd*, Submitted A] and at the same time cluster infrastructure and individuals in these areas of heightened flood risk. Moving forward, the demographic and hydrologic pressures faced by cities will be magnified due to continuing urban population growth and climate change. Urban areas currently contain over half of the global population, with this proportion projected to approach 66% by 2050 [*United Nations*, 2014]. Continued urbanization will likely have the combined effect of further altering natural streamflow properties, due to the conversion of additional natural land cover to impervious surfaces [*Terando et al.*, 2014], and enhancing the number of individuals residing in flood zones. Concurrently, extreme precipitation events have become more frequent and intense across most of the United States due to climate change [*Walsh et al.*, 2014]. This is problematic given that stormwater infrastructure is designed according to historical storm data and relies upon the concept of stationarity, which assumes that past meteorological conditions are representative of the future [*Guo*, 2006; *Mailhot and Duchesne*, 2010]. Therefore, the existing stormwater management systems present in many cities may already be under designed for current precipitation extremes and will likely be overwhelmed more frequently by the intensity of future storm systems [*Guo*, 2006; *Forsee and Ahmad*, 2011].

Although urban residents are clearly susceptible to flood hazards, the social dimensions of this vulnerability and potential for environmental injustices are infrequently acknowledged in flood risk assessments [*Tapsell et al.*, 2002; *Koks et al.*, 2015]. This study focuses explicitly on the social aspects of flood hazards by utilizing an Environmental Justice (EJ) framework to evaluate if minority populations are disproportionately at risk for flooding in urban environments. Specifically, the project aimed to answer the following research questions:

- 1) What is the degree of environmental injustice regarding urban flood risk within the Charlanta megaregion?
- 2) How sensitive are any observed environmental injustices to the dasymetric mapping technique, scale of analysis, and local context of individual metropolitan areas?

The following section provides additional background regarding the origins of EJ, its evolution, and its applicability to flood hazard research. Section 4.3 outlines the study area as well as the methodological approaches used to evaluate the presence of environmental injustices. The results and a discussion are presented in Section 4.4. Finally, Section 4.5 summarizes the major findings of the study.

## **4.2 Background**

### **4.2.1 Origins and Evolution of Environmental Justice**

Environmental justice (EJ) is a multifaceted term that encapsulates several different meanings [Capek, 1993]. EJ can refer to local grassroots movements dedicated to mobilization and action in the face of environmental inequities [Agyeman and Evans, 2004] as well as a more general public policy principle focused on the “fair treatment and meaningful involvement of all people regardless of race, color, national origin, or income with respect to the development, implementation, and enforcement of environment laws, regulations and policies” [US EPA, 1998]. Overall, the historical evolution of EJ can be divided into three general stages: the EJ movement, EJ scholarship, and the formal politicization of EJ [Taylor, 2000].

EJ emerged as a movement in the late 1970s and early 1980s, as activists began resisting individual cases where minority neighborhoods were being unequally targeted for the siting of toxic waste facilities. Perhaps the most high-profile case occurred in 1982 when Warren County, North Carolina was selected by the state to host a hazardous waste facility that would contain

soil contaminated with PCB [Cutter, 2006]. The local residents, who were predominately African American, protested the decision and were joined by civil rights advocacy groups, environmental activists, and religious leaders. This represented the first nationwide mobilization of a broad coalition to contest environmental injustice. The Warren County EJ movement along with other similar efforts across the United States typically focused on overcoming the limited political and social capital that often rendered minority and impoverished neighborhoods particularly susceptible to locally unwanted land uses (LULU). The broader goal of these resistance efforts was to emphasize the need for mobilization and coalition building against environmental inequities.

As the EJ narrative strengthened throughout the mid and late 1980s, there was an increased emphasis on gathering empirical evidence to support the growing number of environmental injustice claims. At the forefront of these efforts, was Robert Bullard who provided one of the earliest examples of EJ scholarship. Through an analysis of solid waste active permit sites and US Census data in Houston, *Bullard* [1983] discovered that waste facilities were more likely to be sited within predominantly black neighborhoods. The inequitable distribution of waste facilities was attributed to structural discrimination within the housing market and Houston's lack of zoning ordinances [*Bullard*, 1983]. Research performed by the government, religious groups, and other scholars was also instrumental in providing further evidence that hazardous waste facilities were disproportionately located in minority neighborhoods [*US GAO*, 1983; *UCC CRJ*, 1987; *Adeola*, 1994]. Environmental injustices were not only observed during the siting of hazardous facilities but were also found to be pervasive throughout the Superfund clean-up process [*Lavelle and Coyle*, 1992]. Overall, the

environmental injustices documented by this early wave of scholarship were viewed as a product of overtly racist decision making and structural forms of discrimination.

The collective work of EJ activists and scholars gained momentum and increasingly garnered national media attention in the 1990s, which amplified the pressures placed on governments at the local, state, and national scale to enact appropriate policy responses [Cutter, 1995]. One of the earliest breakthroughs for EJ in the formal political arena was the formation of the EPA's Environmental Equity Workgroup in 1990. The Environmental Equity Workgroup was tasked with: 1) determining if minority and low-income groups bore a disproportionate environmental burden, 2) identifying the factors contributing to such inequitable exposures, and 3) devising potential strategies to reduce any observed inequalities [Cutter, 2006]. The workgroup released their findings in 1992, which provided the first official acknowledgement of EJ issues by the federal government [US EPA, 1992]. EJ continued to gain traction within the formal political sphere culminating with President Clinton signing Executive Order (EO) number 12898 in 1994. EO 12898 mandated that all federal agencies make EJ a central part of their mission by identifying and resolving any inequitable health or environmental effects of their policies and programs on minority and low-income populations [EO, 1994]. Thus, evaluating EJ issues was no longer confined solely to the EPA but was mandated throughout all federal agencies, which was viewed as a momentous advancement by EJ activists and scholars [Foreman, 1998]. Overall, the activism, scholarship, and formal political dimensions of EJ were very much intertwined [Agyeman and Evans, 2004] and highlight the breadth and flexibility of the framework, which has been central to its ongoing relevancy for issues such as flood hazards.

#### 4.2.2 Environmental Justice and Flood Hazards

Historically, flood hazards were largely tangential to the EJ framework. This was partly due to the complexity of natural disasters and the subsequent lack of a clear entity to mobilize against [Capek, 1993]. Flood hazards may have been specifically neglected within the EJ movement since they present a risk that is largely invisible [Houston *et al.*, 2011] and lacks a clear focal point, unlike the polluting smokestacks associated with factories and power plants. Interestingly, the original interests of EJ organizations in water issues focused primarily on water pollution rather than flooding [Bullard, 1992; Taylor, 2000]. The emphasis initially placed on water quality was likely due to pollution often being linked with acute spills from factories or other point sources, which made it more straightforward to identify and mobilize against a responsible party in a manner similar to resisting LULUs.

The positioning of flood hazards and natural hazards more generally within the EJ framework appears to have emerged largely from Europe. One of the earliest examples was provided by Adger [2001], who addressed the environmental justice implications of global climate change adaptation and mitigation. Work focusing specifically on flood hazards as an EJ issue can be traced back to Fielding and Burningham [2005]. They discovered that lower social classes were more likely to be at risk from flooding across England and Wales although the results varied substantially depending on the dasymetric mapping technique [Fielding and Burningham, 2005]. A case study of Belfast, Glasgow, and Luton similarly indicated that vulnerable individuals were overrepresented in areas at risk for flooding, potentially due to older and cheaper housing stock being located in flood prone areas [Houston *et al.*, 2011]. Koks *et al.* [2015] also discovered that flood prone areas contained a significantly larger share of vulnerable residents in Rotterdam, although these disparities were slightly smaller than those observed in

previous studies. A more complex relationship between deprivation and flood risk in England was documented by the Environmental Agency [*Walker et al.*, 2006], as more deprived groups were disproportionately at risk in some regions while the inverse was true in others.

Additionally, a bimodal distribution was identified for London with both highly deprived and affluent individuals residing in flood prone areas [*Walker et al.*, 2006]. The emergence of EJ informed flood hazard research from a European context was likely due to the markedly different evolution of the EJ framework in Europe. EJ did not gain traction in Europe until the late 1990s and was more closely aligned with sustainable development issues [*Haughton*, 1999; *Agyeman and Evans*, 2004], which perhaps made incorporating natural hazards, such as floods, a more intuitive extension. This may also explain the emphasis on class rather than racial disparities within the European EJ framework. Nevertheless, the European research examples highlight the potential for conflicting findings regarding EJ and flood hazards as well as the sensitivity of the results to various dasymetric mapping techniques.

Within the United States, EJ informed flood hazard research has only emerged in earnest during the past decade despite the origin of Bullard's interests in EJ being heavily influenced by observing the differential impacts of flooding in his hometown of Elba, Alabama [*Bullard*, 2008]. The extension of the EJ framework to understand the challenges faced by predominantly minority neighborhoods in New Orleans during the recovery and rebuilding efforts after Hurricane Katrina [*Bullard and Wright*, 2009] was a watershed moment that prompted additional scholarship focused on the EJ implications of flood hazards. *Maantay and Maroko* [2009] analyzed the population characteristics of flood zone residents in New York City. Although on a city-wide basis there was no evidence that minorities were overrepresented within flood zones, environmental injustices were observed in several of the individual boroughs within the city



according to the most sophisticated dasymetric mapping technique [Maantay and Maroko, 2009]. A comparable EJ analysis focusing on Miami found that non-Hispanic Black and Hispanic populations, particularly the Columbian and Puerto Rican subgroups, were significantly overrepresented within inland flood zones [Chakraborty et al., 2014; Montgomery and Chakraborty, 2015]. However, a comparison of the findings from Miami with a similar assessment in Houston revealed notable contradictions, which was perhaps due to the more important role that coastal water-based amenities played in shaping urban development patterns in Miami [Maldonado et al., 2016]. Overall, the US-based examples highlight the complexities of applying an EJ framework to flood hazards and illustrate how various methodological decisions can potentially lead to contradictory findings.

#### 4.2.3 Study Motivation

Despite the studies discussed above, the EJ framework remains largely underutilized within the context of flood hazards and the degree to which marginalized groups are disproportionately exposed to urban flooding is still not fully understood [Maantay and Maroko, 2009]. This is especially true in the United States although such inequities are particularly likely due to the historical tendency for wealthier individuals to settle on higher ground and lower property values to be located in flood-prone areas [Willie, 1961; Daniel et al., 2009].

Unfortunately, EJ informed flood hazard research conducted within an American context is limited to a select number of cities, such as Miami [Chakraborty et al., 2014; Montgomery and Chakraborty, 2015], Houston [Maldonado et al., 2016], and New York [Maantay and Maroko, 2009].

Furthermore, the literature examining the EJ hypothesis that marginalized, disadvantaged, and minority groups are disproportionately exposed to flood hazards has produced contrasting

and inconclusive findings in both European and American cities [e.g., *Maantay and Maroko*, 2009; *Maldonado et al.*, 2016]. This general lack of consensus regarding EJ and flood hazards is likely due to the different dasymetric mapping techniques utilized to estimate urban flood zone population characteristics, the various scales at which the estimates are calculated, and the specific geographical context of the individual study cities. The overarching goal of this study was to address these issues by analyzing urban flood risk inequities across an entire megaregion at various scales using several different dasymetric mapping approaches. Studying several metropolitan areas within a megaregion enabled an assessment of the pervasiveness of flood hazard environmental injustice and helped identify city specific factors that were potentially responsible for any observed disparities. Additionally, considering several different dasymetric mapping techniques and scales highlighted the sensitivity of the findings to specific methodological parameters. These efforts collectively provided a more comprehensive assessment of EJ and flood hazards, which can help inform policies aimed at reducing urban flooding injustices.

## **4.3 Data and Methods**

### **4.3.1 Study Region**

This study specifically assessed the prevalence of EJ issues related to flood hazards throughout the Charlanta megaregion, which incorporates the Atlanta, Greenville, Spartanburg, and Charlotte Metropolitan Statistical Areas (MSAs) along the I-85 corridor in the Southeastern United States [*Shepherd et al.*, 2013; *Mitra and Shepherd*, 2016] (Figure 4.1). The Charlanta megaregion is home to several of the most sprawling MSAs in the country [*Debbage et al.*, 2017] and its impervious footprint is projected to continue expanding in the future [*Terando et al.*, 2014]. These ongoing development trends will likely enhance the pressures placed on natural

rivers and stormwater management systems as well as further increase flood zone occupancy [Ferguson and Ashley, 2017], making it imperative to understand any potential inequities in flood risk. Additionally, cities within the megaregion are already vulnerable to flooding, as Charlotte and Atlanta were ranked as the 5th and 7th flashiest cities regarding streamflow in the contiguous United States, respectively [Smith and Smith, 2015].

In addition to the urban footprint of the megaregion continuing to sprawl into flood prone areas, the development of the individual MSAs has been substantially influenced by racial segregation. For example, in Atlanta, comprehensive zoning plans, urban renewal initiatives, and highway construction projects were instrumental in dividing the city along racial lines [Bayor, 1988]. Similar mechanisms also resulted in the highly segregated nature of residential development in Charlotte [Hanchett, 1998]. The historical and present-day manifestations of residential segregation suggest that EJ flood hazard issues are particularly pertinent to the Charlanta megaregion.

Despite the potential efficacy of utilizing an EJ perspective to analyze the social dimensions of urban flood risk in Charlanta, the megaregion has been largely neglected by EJ informed flood hazard research. This study provides one of the first assessments of flood related EJ issues throughout the megaregion. Additionally, analyzing the entire megaregion using the same methodological approach enabled comparisons between the individual MSAs. This helped reveal if EJ issues were systemic across the entire megaregion or more heavily influence by the historical and geographical context of each MSA.

#### 4.3.2 Flood Zone Data

Areas at risk for flooding were defined by the National Flood Hazard Layer (NFHL), which is produced by the Federal Emergency Management Agency (FEMA). The NFHL is a

digital database that categorizes flood risk into distinct zones based largely upon the expected frequency of flooding, and it is used by FEMA's National Flood Insurance Program (NFIP) to regulate the purchase of flood insurance. Specifically, the 500-year flood zone was used to delineate flood risk throughout Charlanta. The 500-year flood zone includes all areas that have at least a 0.2% chance of flooding each year and incorporates the 100-year flood zones that have been analyzed more frequently in the literature [e.g., *Maantay and Maroko*, 2009; *Maldonado et al.*, 2016]. Throughout the Charlanta megaregion, the differences in the areal extent of the 500-year and 100-year flood zones were generally minimal.

Relying upon the NFHL does present potential weaknesses. Firstly, the flood zones are discrete polygons that prescribe artificially rigid boundaries to the complex natural phenomena of flooding [*Maantay and Maroko*, 2009]. The NFHL also does not capture certain aspects of urban flooding, such as the risk of urban drainage system failures [e.g. *Caradot et al.*, 2011]. Despite these potential issues, the FEMA NFHL has been widely used in previous EJ studies because it provides the most comprehensive spatial coverage [e.g. *Maantay and Maroko*, 2009; *Montgomery and Chakraborty*, 2015; *Maldonado et al.*, 2016]. Additionally, the flood zones specified by the NFHL are determined by detailed hydrologic and hydraulic analyses [*FEMA*, 1995]. This explicit physical linkage to flood exposure addresses one traditional criticism of EJ scholarship that questions the appropriateness of using census tracts or zip codes, which lack a substantive physical connection to the hazardous pollutants emitted by LULU [*Mohai*, 2008].

#### 4.3.3 US Census Data

Demographic data was gathered from the 2010 Decennial US Census to determine the population characteristics within the FEMA 500-year flood zones. The 2010 Census was used rather than the American Community Survey (ACS) to avoid the larger margin of errors

associated with the smaller sample size of the ACS [*National Research Council*, 2007].

Specifically, racial composition data for each block group within the Charlanta megaregion was downloaded from the US Census website (2010 SF1 100% P8 Race).

To address the potential environmental justice issues associated with flood risk, the study considered two racial categories: Black or African American Alone and White Alone. The focus on African Americans was due to several different factors. Firstly, African Americans are the predominant minority group in the Charlanta megaregion. Secondly, analyzing African American flood zone occupancy enabled an assessment of the potential EJ ramifications of the comprehensive zoning plans, urban renewal initiatives, and highway construction projects that historically targeted and displaced African American communities [*Bayer*, 1988]. If environmental injustices are discovered in Charlanta, it would suggest that these mechanisms likely forced many African Americans to reside in less desirable areas such as flood zones. Finally, understanding potential flood risk disparities regarding African Americans is especially important since previous studies have indicated that African Americans may be particularly vulnerable to climate hazards and floods [*KC et al.*, 2015; *Shepherd and KC*, 2015].

#### 4.3.4 Dasymetric Mapping Techniques

Because Census block groups do not align directly with FEMA flood zones, dasymetric mapping was used to estimate the flood zone population characteristics. Dasymetric mapping is fundamentally the usage of ancillary data to disaggregate a spatial phenomenon to a finer scale [*Mennis*, 2003]. For example, dasymetric mapping often involves utilizing land use data to derive more precise population distributions [*Wright*, 1936]. Such techniques are prevalent throughout the EJ literature analyzing flood hazards although a common approach has not been adopted. The wide variety of techniques, including centroid containment, areal weighting,

filtered areal weighting, and boundary intersection [*Maantay and Maroko, 2009; Montgomery and Chakraborty, 2015*], has likely contributed to the lack of consensus between previous studies.

Three separate dasymetric mapping techniques of varying complexity were explored because an underlying motivation of this research was to investigate the sensitivity of any observed flood hazard injustices to such methodological decisions. First, a simple areal weighting technique was utilized, which involved calculating the percentage of each census block group within the 500-year flood zone. This percentage was then used to estimate the population residing within the flood zone. For example, if 50% of a census block group was within the 500-year flood zone, then 50% of the total, African American, and White populations were deemed at risk for flooding. As illustrated in Figure 4.2, this approach will likely result in an overestimate of the individuals exposed to flooding since the flood zones often contain unoccupied land, such as golf courses and riparian buffers. Additionally, for larger river and lake systems, the flood zone area incorporates the water body itself, which will potentially further inflate the urban flood zone population estimates. The potential shortcomings of the basic areal weighting technique fundamentally emerge from its assumption that the population is evenly distributed throughout the census block group.

To more explicitly account for the heterogeneity of the population distribution within a given block group, two filtered areal weighting methods were developed. Both approaches utilized the National Land Cover Database (NLCD) 2011, which is a remotely sensed land use/land cover dataset derived from Landsat imagery [*Homer et al., 2015*]. The NLCD 2011 has a spatial resolution of 30 meters and contains four different developed categories ranging from developed open space to high intensity development. The first filtered areal weighting approach

estimated flood zone populations by calculating the percentage of the census block group that was within the flood zone and urban, as defined by the four developed NLCD classes (i.e. classes 21-24). Figure 4.2 highlights how this urban filtering technique eliminated undeveloped portions of the flood zone, such as forests, water bodies, and riparian buffers, from the area used to calculate the weighted populations.

A second filtered areal weighting approach was developed by calculating the percentage of the census block group that was within the flood zone and characterized by low, medium, or high intensity development (i.e. classes 22-24). One potential benefit of analyzing a subset of the NLCD urban categories and omitting class 21 (i.e. developed open space) from the area calculation was that class 21 often corresponded to golf courses within the flood zones. This was particularly problematic for assessing EJ issues related to flooding since African American communities are often underserved regarding golf courses [*Mitchelson and Lazaro, 2004*]. Therefore, including golf courses in the areal weighting procedure would likely result in an overestimate of individuals exposed to flooding in non-minority, affluent neighborhoods. Although excluding developed open space may result in a slight underestimation of flood exposure in areas of low density residential development, the propensity for the class to correspond with golf courses inside flood zones was a greater potential bias given the large areal extent of golfing facilities (Figure 4.2). Overall, the various dasymetric techniques described above enabled a basic sensitivity assessment of the EJ findings.

#### 4.3.5 Risk Ratio Calculations

Risk ratios were utilized to statistically evaluate if African Americans were disproportionately at risk to urban flood hazards relative to Whites. The risk ratios were modeled

after the comparative environmental risk index (CERI) developed by *Harner et al.* [2002] and calculated using Equation 4.1.

$$\frac{(At-Risk\ African\ Americans/Total\ African\ Americans)}{(At-Risk\ Whites/Total\ Whites)} \quad (Eq. 4.1)$$

The at-risk populations in Equation 4.1 were defined as the number of individuals residing in the 500-year flood zones, which was determined using the three dasymetric mapping techniques described above. In order to examine if the results varied according to the dasymetric mapping approach, the risk ratios were calculated separately using the three different at-risk population estimates. Given the construction of Equation 4.1, values greater than one would indicate that African Americans are disproportionately at risk to flood hazards and suggest that environmental injustices are present. Conversely, values less than one would be indicative of Whites having an increased likelihood of residing in flood zones.

Because the wide range of geographic scales used to explore EJ issues related to flood hazards is partly responsible for the contradictory findings in the literature [*Cutter et al.*, 1996; *Kurtz*, 2003], the risk ratios were calculated at several different spatial scales. The risk ratios were determined at the census tract, county, MSA, and megaregion level. This multiscale assessment at different levels of aggregation helped determine the sensitivity of the results to the modifiable areal unit problem (MAUP) and facilitated the identification of the scales at which flood risk inequities were most pronounced. The calculation of the risk ratios and their statistical significance for each scale and dasymetric mapping technique was performed using the *fmsb* package in R statistical software. P-values were obtained by testing the null-hypothesis of independence between flood risk exposure and race.



## **4.4 Results and Discussion**

### **4.4.1 Environmental Justice at the Megaregion Scale**

Unsurprisingly, the three dasymetric mapping techniques produced different estimates of the flood zone population characteristics in Charlanta (Table 4.1). According to the simple areal weighting approach, 8.3% of Charlanta's approximately 7 million residents resided in the 500-year flood zones. This percentage decreased notably to 2% when utilizing the urban filtered areal weighting and declined further to 0.7% for the urban filtered areal weighting that consider only low, medium, and high intensity development. The overall decline in flood zone population between the three methods was expected since the more complex filtering processes reduced the area of the census block groups within the flood zones.

The three dasymetric mapping techniques also impacted the racial composition of the flood zone residents (Table 4.1). The more sophisticated urban filtering approaches resulted in a greater reduction of White flood zone residents in terms of both absolute change and percent decrease. For example, the urban filtered areal weighting estimated that over 300,000 fewer Whites resided in the flood zone relative to the simple areal weighting technique, which represented a 77.7% decrease. Contrastingly, the reduction of African American flood zone residents between these two approaches was only 135,033, which corresponded to a 71.6% decrease. Similar trends were also observed between the urban filtered areal weighting and the more restrictive urban filtering that considering only low, medium, and high intensity development.

Importantly, the differences between the flood zone population estimates had notable implications for the risk ratios (Table 4.1). The simplistic areal weighting technique produced a statistically significant risk ratio of 0.990, which implies that Whites had an increased likelihood

of residing in flood zones. Conversely, the risk ratios based upon the more complex filtered areal weighting techniques were both significant and greater than one, indicating that African Americans were overrepresented in areas at risk for flooding. According to the urban filtered areal weighting that consider only low, medium, and high intensity development, African Americans were 44% more likely to reside in the 500-year flood zones than Whites. These findings highlight the sensitivity of the results to the dasymetric mapping technique, but the most sophisticated approach suggested that environmental injustices regarding flood hazards were systemic across the entire Charlanta megaregion. The wide spread nature of the disproportionate exposure of African Americans to flood hazards contrasts with previous work focused on New York, which discovered an over representation of minority populations in flood prone areas only for individual boroughs but not at the city-wide level [*Maantay and Maroko, 2009*]. This discrepancy may be due to the important differences between the historical evolution of New York and Southern cities, particularly regarding race.

#### 4.4.2 Environmental Justice at the MSA Scale

To evaluate the potential variability of environmental injustice within the megaregion, the risk ratios were calculated for each MSA in Charlanta (Table 4.2). The risk ratios for several of MSAs varied substantially depending on the dasymetric mapping technique, similar to the megaregion-wide results. Atlanta was an exception, however, as the risk ratios were significant and greater than one for all three approaches. This suggests that in the Atlanta MSA African Americans had an increased likelihood of residing in flood zones, regardless of the dasymetric mapping technique. Specifically, according to the low-high urban filtered areal weighting approach, African Americans were 34% more likely to live in flood prone areas than Whites. Although the risk ratios were larger for the more complex dasymetric mapping techniques, the

general consistency of the values indicates that the observed environmental injustices were not an artifact of a given dasymetric mapping approach.

The Charlotte and Greenville-Spartanburg MSAs exhibited greater sensitivity to the dasymetric mapping methodologies. For both MSAs, the simplistic areal weighting approach suggested that Whites were disproportionately at risk to flood hazards. This was not particularly surprising given that conventional areal weighting has been documented to disproportionately undercount minority populations [*Maantay and Maroko*, 2009]. Conversely, the more precise filtered areal weighting techniques both produced risk ratios that were significant and greater than one for Charlotte and Greenville-Spartanburg, indicating that African Americans were disproportionately exposed to flood hazards. Greenville-Spartanburg exhibited the most substantial spatial inequities, as African Americans were 80% more likely to reside in the 500-year flood zone according to the low-high urban filtered areal weighting. The degree of environmental injustice in Charlotte was comparable to Atlanta, as African Americans were 38% more likely to be at risk to flood hazards.

The differences in the risk ratios between the various dasymetric mapping techniques, particularly for Charlotte and Greenville-Spartanburg, can be partly explained by analyzing how the techniques influenced the racial characteristics of the flood zone population estimates (Figure 4.3). In Atlanta, the different dasymetric approaches resulted in similar percent decreases of the White and African American populations estimated to reside in the flood zones. For example, the urban filtered areal weighting resulted in a 78% and 73% decrease in the White and African American flood zone populations, respectively, relative to the simplistic areal weighting approach. The percent decrease of the White and African American flood zone populations was even more similar when transitioning from the urban filtered areal weighting to the low-high

urban filtered areal weighting. Since the percent change of the African American and White flood zone population estimates was fairly similar, the risk ratios were less sensitive to the various dasymetric mapping techniques and always greater than one.

For the Charlotte and Greenville-Spartanburg MSAs, the opposite occurred as the three dasymetric methods produced notably different percent decreases in the African American and White flood zone populations (Figure 4.3). For example, in Charlotte, the urban filtered areal weighting resulted in a 74% and 60% decrease in the White and African American flood zone populations, respectively, relative to the basic areal weighting. Similarly, in Greenville-Spartanburg, the low-high urban filtered areal weighting resulted in a 72% and 62% decrease in the White and African American flood zone occupants, respectively, relative to the urban filtered areal weighting. The much larger percent decreases in White flood zone populations relative to African American flood zone populations in both Charlotte and Greenville-Spartanburg elucidate why the risk ratios changed from less than one for the areal weighting approach to greater than one for both the urban filtering techniques. Overall, it appears that simplistic areal weighting may not undercount minority flood zone populations throughout Charlanta, as suggested by *Maantay and Maroko* [2009], but rather overestimate the number of White flood zone occupants, particularly in Charlotte and Greenville-Spartanburg.

#### 4.4.3 Environmental Justice at the County Scale

A higher level of spatial detail was provided by mapping the risk ratios derived from each dasymetric methodology for all Charlanta counties. The magnitude of the county risk ratios was quite modest according to the areal weighting approach, with all the values falling between 0.51 and 1.50 (Figure 4.4a). Additionally, every county in the Charlotte and Greenville-Spartanburg MSAs exhibited a risk ratio less than one, indicating that Whites were more likely to reside in the

500-year flood zones. The landscape of inequitable flood risk observed in Atlanta was more complex, as the counties were fairly evenly divided between those with risk ratios less than one and those with risk ratios greater than one. Specifically, there appeared to be a notable cluster of counties west of Downtown Atlanta where African Americans were particularly overrepresented within the 500-year flood zones (e.g. Carroll, Douglas, and Cobb counties). In terms of statistical significance, a vast majority of the risk ratios calculated using the areal weighted flood zone population estimates exhibited a p-value less than 0.05. The large number of significant results, despite the modest risk ratio magnitudes, was likely due to the areal weighting technique overestimating the flood zone populations and artificially enhancing the statistical confidence.

Utilizing the flood zone population estimates produced by the urban filtered areal weighting resulted in different risk ratios (Figure 4.4b). Most notably, the risk ratios for all the counties in the Charlotte and Greenville-Spartanburg MSAs, with the exception of Mecklenburg and Anson counties, transitioned from being less than one to greater than one. The majority of these transitional counties in North and South Carolina also exhibited p-values less than 0.05, indicating that African Americans were significantly more likely to reside in flood zones. For Atlanta, the urban filtered areal weighting risk ratios highlighted an interesting spatial pattern. It appeared that Whites were significantly overrepresented within flood zones in the urban core counties (e.g. Fulton, DeKalb, and Fayette) while African American were at a significantly higher risk in the counties immediately encircling the urban core.

The most realistic depiction of environmental injustice at the county level was likely provided by the low-high urban filtered areal weighting (Figure 4.4c). According to this dasymetric approach, the risk ratios for the Charlotte and Greenville-Spartanburg counties were all greater than one and a vast majority were statistically significant, indicating that African

Americans were significantly more likely to reside within the 500-year flood zones in these MSAs. For Atlanta, counties with risk ratios greater than one again encircled the urban core, with a notable cluster of significant risk ratios located west of downtown. Although Whites were still slightly more likely to reside within flood zones in the urban core counties of Atlanta, these differences were no longer statistically significant except for DeKalb County. The spatial pattern of injustice observed in Atlanta, where African Americans were disproportionately exposed to flood hazards in the counties surrounding the urban core, appeared to be unique since the urban core counties of the Charlotte and Greenville-Spartanburg MSAs (e.g. Mecklenburg, Greenville, and Spartanburg counties) exhibited significant flood exposure inequities. Finally, the most glaring environmental injustices at the county level occurred in Union County, NC and Spalding County, GA, where African Americans were 3.1 and 2.9 times as likely, respectively, to reside in flood zones than Whites.

To better visualize the changes between the various dasymetric mapping techniques, a difference map was created by subtracting the risk ratios calculated using areal weighting from those derived using the low-high urban filtered areal weighting approach (Figure 4.4d). Generally, larger risk ratio increases were observed in rural counties. This was likely due to the areal weighting technique overestimating White flood zone populations in these counties due to the flood zones containing large quantities of forested and non-urban land cover. The urban core counties generally displayed more modest increases or even slight decreases in the risk ratio. One notable exception was DeKalb County, which exhibited the largest risk ratio reduction. Aerial weighting potentially overestimated the African American flood zone population in DeKalb County due to the largely undeveloped nature of the flood zones in the vicinity of Arabia Mountain National Heritage Area and Stone Mountain Park. Overall, analyzing the

environmental injustices pertaining to urban flood hazards at the county level provided a more spatially nuanced perspective.

#### 4.4.4 Environmental Justice at the Census Tract Scale

The most granular scale include in the analysis was the census tract level. Even though the flood zone population estimates were derived using block group data, the nature of the dasymetric mapping techniques and risk ratio formula necessitated that the calculations were performed at the tract level since any block group risk ratios would by default equal one. The variability of the census tract risk ratios between the three dasymetric mapping methodologies generally mirrored the results at the county scale, as the risk ratios derived from the more complex filtered areal weighting techniques were generally greater than those estimated using the simplistic areal weighting approach (Figure 4.5). This upward trend in the risk ratio values was particularly consistent for census tracts in the Charlotte and Greenville-Spartanburg MSAs. The boxplots also highlighted the substantial variability and greater magnitude of the risk ratios at the census tract scale. Several census tracts exhibited risk ratios greater than three, which suggests that African Americans were at least three times as likely to reside within the 500-year flood zones.

Figure 4.6 summarizes the number of statistically significant census tract risk ratios by MSA for each dasymetric mapping technique. The clearest trend was the general decline in the number of significant risk ratios at the tract level for the more restrictive filtered areal weighting approaches. This was likely due to the smaller number of flood zone residents estimated by these techniques, which decreased the statistical confidence that the observed disparities were significant. The general lack of significant results was the primary reason why a map of the tract level risk ratios was not presented. Although there were a greater number of tracts with risk

ratios less than one in Atlanta and Greenville-Spartanburg according to the areal weighting technique, each MSA exhibited higher frequencies of census tracts with risk ratios greater than one for the more advanced dasymetric methods. This indicates that tracts where African Americans were significantly overrepresented in flood zones were more pervasive than those where Whites were disproportionately exposed to flooding. In terms of differences between the three MSAs, census tracts with significant risk ratios were more frequent in Atlanta. However, due to the greater number of tracts in the Atlanta MSA, the relative percentages were generally quite similar, with approximately 1-2% of all tracts displaying significant environmental injustices.

Finally, several of the census tracts that exhibited the most egregious environmental injustices were explored in additional detail (Table 4.3). Atlanta was home to half of the ten census tracts with the largest, significant risk ratios, including the entire top three. Four of the ten census tracts with the highest risk ratios were located in Charlotte while only one was observed in Greenville-Spartanburg. The census tract with the largest significant risk ratio occurred in Fulton County Georgia just north of East Point. In this tract, African Americans were over nine times as likely to reside in the 500-year flood zone than Whites. This extremely high risk ratio likely occurred because the block group containing Fort Valley, where a substantial proportion of urban development was within the flood zone of a tributary to South Utoy Creek, had a notably larger African American population than the other census block groups comprising the tract. The remaining block groups not only contained a slightly larger White population, particularly the block group containing Fort McPherson, but also had less development within the flood zone.

The second largest risk ratio was observed in a census tract near Summerhill, just east of Turner Field. Specifically, African Americans were over six times as likely to reside within the



flood zone. The large risk ratio occurred because the tract consisted of two adjacent block groups, where one was predominately White and had a minimal threat of flooding and the other was predominately African American and had considerable urban infrastructure within the flood zone. Summerhill is a particularly interesting example of environmental injustice since it has also been historically marginalized by the City of Atlanta for the construction of Turner Field and interstate expansions. Additionally, it is especially susceptible to flooding during intense precipitation events because it drains a portion of downtown Atlanta. Due to a significant flood that occurred in July 2012, Summerhill and its surrounding neighborhoods are now undergoing a stormwater management transformation involving permeable pavers and more controversially the displacement of local residents to create a water retention park. Obviously, local residents are weary of stormwater management being the latest rationalization of an “urban renewal” project that will serve as a catalyst for further gentrification and displacement. Google street view images reveal the drastic changes that have occurred between 2010 and 2017, as the new permeable pavers have been accompanied by several houses being demolished and reconstructed (Figure 4.7).

A census tract stretching from downtown Griffin, GA toward the southeast exhibited the third largest risk ratio, as African Americans were over 4.5 times as likely to reside in the 500-year flood zone. The high risk ratio was largely due to a predominately African American neighborhood adjacent to the Griffin-Spalding County Airport being particularly at risk for flooding. The remainder of the block groups that comprised the tract consisted of predominately White populations and were more rural in nature so the flood zones generally enveloped undeveloped land. Given the results from Summerhill and Griffin, it appears that neighborhoods

which have been historically targeted for LULU (e.g. airports, sporting facilities) are also frequently the locations of substantial environmental injustices regarding flood risk.

The final census tract in the top four roughly corresponded with the Landsdowne community, which is located southeast of downtown Charlotte. In this tract, African Americans were over three times as likely to reside in the 500-year flood zone. The topographic variability of the tract was quite noticeable, as it included one low-lying block group adjacent to McAlpine Creek and two elevated block groups. As indicated by the large risk ratio, the block group adjacent to McAlpine Creek was predominately African American while the remaining block groups, which were not at risk for flooding, were predominately White. The broader context of the tract's location was also quite unique since it was positioned within the predominately White sector of Charlotte. Overall, the census tract level analysis highlighted the specific locales where environmental injustices were quite pronounced.

#### **4.5 Conclusions and Policy Implications**

By analyzing population characteristics within FEMA 500-year flood zones at various scales utilizing several dasymetric mapping approaches, this work clarifies the extent of flood risk environmental injustice throughout the Charlanta megaregion. As expected, the results were sensitive to the three dasymetric mapping techniques. The simplistic areal weighting approach appeared to overestimate the populations residing in the flood zone, particularly in more rural counties where large portions of the flood zone were undeveloped. Therefore, the two filtered areal weighting techniques, which only considered the developed portions of the flood zone, likely provided more realistic depictions of the flood zone population characteristics.

The risk ratios derived from the flood zone population estimates produced by the more sophisticated low-high urban filtered areal weighting indicated that significant environmental

injustices were pervasive throughout the entire Charlanta megaregion. Specifically, African Americans were 44% more likely to reside in areas at risk for flooding than Whites when considering the megaregion as a whole. At the MSA scale, Greenville-Spartanburg exhibited the largest flood risk inequities, as African Americans were 80% more likely to reside in the 500-year flood zone. Significant environmental injustices were also observed in Charlotte and Atlanta where African Americans were 38% and 34% more likely to be at risk to flooding, respectively.

The county level analysis revealed more nuanced spatial patterns regarding flood risk. In a majority of the Greenville-Spartanburg and Charlotte counties African Americans were significantly overrepresented in the 500-year flood zone. For Atlanta, a unique spatial pattern emerged, as the counties encircling the urban core exhibited significant environmental injustices. Of particular importance was the cluster of counties located west of downtown Atlanta where African American were significantly overrepresented in flood zones because the flood risk in this region and potential for disparate impacts unfortunately came to fruition during the devastating 2009 Atlanta flood [*Debbage and Shepherd*, Submitted B].

The most spatially detailed analysis was conducted at the census tract level. Several of the tracts exhibited risk ratios greater than three, indicating that African Americans were at least three times as likely to reside within flood zones than Whites. The tracts with the largest risk ratios and most pronounced environmental injustices generally exhibited stark racial juxtapositions. They typically were comprised of a predominately African American census block group that contained a majority of the flood risk while the remaining block groups were predominately White and not at risk for flooding. Additionally, these tracts appeared to incorporate historically marginalized neighborhoods that have been encroached upon by other

LULU, such as airports, sporting facilities, and military bases. Thus, the greatest flood risk inequities at the tract level appeared to be collocated with broader environmental injustices.

Overall, these findings suggest that African Americans are overrepresented in the 500-year flood zone and are disproportionately at risk for flooding. These inequities are likely due to structural forms of discrimination and residential segregation, which have been particularly pervasive throughout the development of the Southern cities included in Charlanta [Bayor, 1988; Hanchett, 1998]. The systemic overrepresentation of African Americans in flood zones is particularly troubling given that previous studies have indicated that inequities often occur during flood recovery efforts as well [Bullard, 2008; Bullard and Wright, 2009]. This presents a worst-case scenario where African Americans are more likely to be impacted by floods but less likely to receive the necessary resources and support to recover from them. The fine spatial scale of this analysis can hopefully help direct resources to those communities that are most in need and enhance their adaptive capacity to flood hazards. Although, as seen in Summerhill and the surrounding neighborhoods, stormwater management overhauls can set the stage for additional inequities through displacement and gentrification. Finally, a greater awareness of flood hazard inequities can inform emergency management plans and help ensure more equitable recovery efforts when flooding occurs.

Future research efforts will focus on advancing beyond the binary conceptualization of race utilized in this study. Analyzing additional racial groups and socio-economic characteristics will likely provide further insights regarding the extent and mechanisms responsible for flood risk inequities. Although block groups were utilized in this study to help incorporate additional socio-economic variables in future work, examining EJ differences between methods based upon block groups and blocks would help further diagnose any issues related to MAUP. Additionally,

exploring various Risk Ratio formulations may reveal subtle alterations in the observed environmental injustices. More qualitative perspectives, such as survey and/or interview-based studies, would also be beneficial to understanding how the risks and inequities are perceived in local communities. Moving forward, the authors ultimately hope to design an online mapping interface to make the detailed EJ flood hazard dataset freely available to the public and community groups.

## **4.6 References**

- Adeola, F. O. (1994), Environmental hazards, health and racial inequality in hazardous waste distribution, *Env. Behav.*, 26, 99–126, doi: 10.1177/0013916594261006.
- Adger, W. N. (2001), Scales of governance and environmental justice for adaptation and mitigation of climate change, *J. Int. Dev.*, 13, 921–931, doi: 10.1002/jid.833.
- Agyeman, J., and B. Evans (2004), ‘Just sustainability’: The emerging discourse of environmental justice in Britain, *Geogr. J.*, 170(2), 155–164, doi: 10.1111/j.0016-7398.2004.00117.x.
- Ashley, S. T., and W. S. Ashley (2008), Flood fatalities in the United States, *J. Appl. Meteor. Climatol.*, 47, 805–818, doi: 10.1175/2007JAMC1611.1.
- Bayor, R. H. (1988), Roads to segregation: Atlanta in the twentieth century, *J. Urban Hist.*, 15(1), 3–21, doi: 10.1177/009614428801500101.
- Brissette, F. P., R. Leconte, C. Marche, and J. Rousselle (2003), Historical evolution of flooding damage on a USA/Quebec river basin, *J. Am. Water Resour. Assoc.*, 39(6), 1385–1396, doi: 10.1111/j.1752-1688.2003.tb04425.x.
- Bullard, R. D. (1983), Solid waste sites and the black Houston community, *Sociol. Inq.*, 53(2/3), 273–288, doi: 10.1111/j.1475-682X.1983.tb00037.x.
- Bullard, R. D. (1992), *People of Color Environmental Groups Directory*, Mott Foundation, Flint, MI.
- Bullard, R. D. (2008), Equity, unnatural man-made disasters, and race: Why environmental justice matters, in *Research in Social Problems and Public Policy, Volume 15, Equity and the Environment*, edited by R.C. Wilkinson and W.R. Freudenburg, pp. 51–85, Elsevier, New York.
- Bullard, R. D., and B. Wright (2009), *Race Place, and Environmental Justice After Hurricane Katrina*, Boulder, Westview Press.
- Capek, S. M. (1993), The “environmental justice” frame: A conceptual discussion and an application, *Soc. Probl.*, 40(1), 5–24, doi: 10.2307/3097023.
- Caradot, N., D. Dranger, J. Chapgier, F. Cherqui, and B. Chocat (2011), Urban flood risk assessment using sewer flooding databases, *Water Sci. Technol.*, 64(4), 832–840, doi: 10.2166/wst.2011.611.
- Chakraborty, J., T. W. Collins, M. C. Montgomery, and S. E. Grineski (2014), Social and spatial inequities in exposure to flood risk in Miami, Florida, *Nat. Hazards Rev.*, 15(3), 1–10, doi: 10.1061/(ASCE)NH.1527-6996.0000140.

- Cutter, S. L. (1995), Race, class and environmental justice, *Prog. Hum. Geogr.*, 19(1), 111–122, doi: 10.1177/030913259501900111.
- Cutter, S. L. (2006), Race, class and environmental justice, *Hazards, Vulnerability and Environmental Justice*, edited by S. L. Cutter, pp. 249–262, Earthscan, Sterling, VA.
- Cutter, S. L., D. Holm, and L. Clark (1996), The role of geographic scale in monitoring environmental justice, *Risk Anal.*, 16(4), 517–526, doi: 10.1111/j.1539-6924.1996.tb01097.x.
- Daniel, V. E., R. J. G. M. Florax, and P. Rietveld, 2009, Flooding risk and housing values: An economic assessment of environmental hazard, *Ecol. Econ.*, 69(2), 355–365, doi: 10.1016/j.ecolecon.2009.08.018.
- Debbage, N., B. Bereitschaft, and J. M. Shepherd (2017), Quantifying the spatiotemporal trends of urban sprawl among large U.S. metropolitan areas via spatial metrics, *Appl. Spat. Anal. Policy*, 10, 317–345, doi: 10.1007/s12061-016-9190-6.
- Debbage, N., and J. M. Shepherd (Submitted A), The influence of urban development patterns on streamflow characteristics in the Charlanta Megaregion, *Water Resour. Res.*
- Debbage, N., and J. M. Shepherd (Submitted B), Determining the influence of urbanization on the spatiotemporal characteristics of runoff and precipitation during the 2009 Atlanta flood using a coupled land surface-atmospheric model, *J. Hydrometeorol.*
- EO (1994), Federal actions to address environmental justice in minority populations and low-income populations, *Federal Register*, 59(32), [Available at <https://www.archives.gov/files/federal-register/executive-orders/pdf/12898.pdf>.]
- FEMA (1995), Managing floodplain development in approximate zone a areas, [Available at [https://www.fema.gov/media-library-data/20130726-1545-20490-4110/frm\\_zna.pdf](https://www.fema.gov/media-library-data/20130726-1545-20490-4110/frm_zna.pdf).]
- Ferguson, A. P., and W. S. Ashley (2017), Spatiotemporal analysis of residential flood exposure in the Atlanta, Georgia metropolitan area, *Nat. Hazards*, 87(2), 989–1016, doi: 10.1007/s11069-017-2806-6.
- Fielding, J., and K. Burningham (2005), Environmental inequality and flood hazard, *Local Environ.*, 10(4), 379–395, doi: 10.1080/13549830500160875.
- Foreman, C. H. (1998), *The Promise and Peril of Environmental Justice*, Brookings Institution Press, Washington D.C.
- Forsee, W. J., and S. Ahmad (2011), Evaluating urban storm-water infrastructure design in response to projected climate change, *J. Hydrol. Eng.*, 16(11), 865–873, doi: 10.1061/(ASCE)HE.1943-5584.0000383.

- Guo, Y. P. (2006), Updating rainfall IDF relationships to maintain urban drainage design standards, *J. Hydrol. Eng.*, 11(5), 506–509, doi: 10.1061/(ASCE)1084-0699(2006)11:5(506).
- Hanchett, T. W. (1998), *Sorting Out the New South City: Race, Class, and Urban Development in Charlotte, 1875-1975*, University of North Carolina Press, Chapel Hill, NC.
- Harner, J., K. Warner, J. Pierce, and T. Huber (2002), Urban environmental justice indices, *Prof. Geogr.*, 54(3), 318–331, doi: 10.1111/0033-0124.00333.
- Haughton, G. (1999), Environmental justice and the sustainable city, *J. Plan. Educ. Res.*, 18(3), 233–243, doi: 10.1177/0739456X9901800305.
- Houston, D., A. Werritty, D. Bassett, A. Geddes, A. Hoolachan, and M. McMillan (2011), Pluvial (rain-related) flooding in urban areas: The invisible hazard. Joseph Rowntree Foundation, 96 pp. [Available at <https://www.jrf.org.uk/report/pluvial-rain-related-flooding-urban-areas-invisible-hazard>.]
- KC, B., J. M. Shepherd, C. J. Gaither (2015), Climate change vulnerability in Georgia, *Appl. Geogr.*, 62, 62–74, doi: 10.1016/j.apgeog.2015.04.007.
- Koks, E. E., B. Jongman, T. G. Husby, and W. J. W. Botzen (2015), Combining hazard, exposure and social vulnerability to provide lessons for flood risk management, *Environ. Sci. Policy*, 47, 42–52, doi: 10.1016/j.envsci.2014.10.013.
- Kurtz, H. E. (2003), Scale frames and counter-scale frames: Constructing the problem of environmental injustice, *Political Geogr.*, 22, 887–916, doi: 10.1016/j.polgeo.2003.09.001.
- Lavelle, M., and M. Coyle (1992), Unequal protection: The racial divide in environmental law, *Nat. Law J.*, 15(3), S1-S12, [Available at <http://www.ejnet.org/ej/nlj.pdf>.]
- Leopold, L. B. (1968), Hydrology for urban planning – A guidebook on the hydrologic effects of urban land use, *U.S. Geol. Surv. Circ. 554*, U.S. Geol. Surv., Washington, D.C. [Available at <https://pubs.usgs.gov/circ/1968/0554/report.pdf>.]
- Maantay, J., and A. Maroko (2009), Mapping urban risk: Flood hazards, race, & environmental justice in New York, *Appl. Geogr.*, 29(1), 111–124, doi: 10.1016/j.apgeog.2008.08.002.
- Mailhot, A., and S. Duchesne (2010), Design criteria of urban drainage infrastructures under climate change, *J. Water Resour. Plan. Manag.*, 136(2), 201–208, doi: 10.1061/(ASCE)WR.1943-5452.0000023.
- Maldonado, A., T. W. Collins, S. E. Grineski, and J. Chakraborty (2016), Exposure to flood hazards in Miami and Houston: Are Hispanic immigrants at greater risk than other social groups, *Int. J. Environ. Res. Public Health*, 13(8), 1–20, doi: 10.3390/ijerph13080775.



- Mennis, J. (2003), Generating surface models of population using dasymetric mapping, *Prof. Geogr.*, 55(1), 31–42, doi: 10.1111/0033-0124.10042.
- Miller, J. D. (2010), Infrastructure 2010: Investment Imperative, The Urban Land Institute, Washington, D.C. [Available at [http://uli.org/wp-content/uploads/2012/07/IR2010.ashx\\_.pdf](http://uli.org/wp-content/uploads/2012/07/IR2010.ashx_.pdf)]
- Mitchelson, R. L., and M. T. Lazaro (2004), The face of the game: African American's spatial accessibility to golf, *Southeast. Geogr.*, 44(1), 48–73, doi: 10.1353/sgo.2004.0010.
- Mitra, C., and J. M. Shepherd (2016), Urban precipitation: A global perspective, in *The Routledge Handbook of Urbanization and Global Change*, edited by K. C. Seto, W. D. Solecki, and C. A. Griffith, pp. 152–168, Routledge, London.
- Mohai, P. (2008), Equity and the environmental justice debate, in *Research in Social Problems and Public Policy, Volume 15, Equity and the Environment*, edited by R.C. Wilkinson and W.R. Freudensburg, pp. 21–49, Elsevier, New York.
- Montgomery, M.C., and J. Chakraborty (2015), Assessing the environmental justice consequences of flood risk: A case study in Miami, Florida, *Environ. Res. Lett.*, 10(9), doi:10.1088/1748-9326/10/9/095010.
- National Research Council (2007), *Using the American Community Survey: Benefits and Challenges*, Panel on the Functionality and Usability of Data from the American Community Survey, edited by C. F. Citro and G. Kalton, Committee on National Statistics, The National Academies Press, Washington D.C.
- Sauer, V. B., W. O. Thomas, V. A. Stricker, and K. V. Wilson (1984), Flood characteristics of urban watersheds in the United States. *U.S. Geol. Surv. Water Supply Paper 2207*, U.S. Gov. Print. Office, Washington, D.C. [Available at <https://pubs.usgs.gov/wsp/2207/report.pdf>.]
- Shepherd, J. M., and B. KC (2015), Climate change and African Americans in the USA, *Geogr. Compass*, 9(11), 579–591, doi: 10.1111/gec3.12244.
- Shepherd, J. M., T. Andersen, C. Strother, A. Horst, L. Bounoua, and C. Mitra (2013), Urban climate archipelagoes: A new framework for urban impacts on climate, *IEEE Earthzine*, [Available at <https://earthzine.org/2013/11/29/urban-climate-archipelagos-a-new-framework-for-urban-impacts-on-climate/>.]
- Smith, B. K., and J. A. Smith (2015), The flashiest watersheds in the contiguous United States, *J. Hydrometeorol.*, 16, 2365–2381, doi:10.1175/JHM-D-14-0217.1.

- Tapsell, S. M., E. C. Penning–Rowse, S. M. Tunstall, and T. L. Wilson (2002), Vulnerability to flooding: Health and social dimensions, *Philos. Trans. Royal Soc. A*, 360, 1511–1525, doi: 10.1098/rsta.2002.1013.
- Taylor, D. E. (2000), The rise of the environmental justice paradigm: Injustice framing and the social construction of environmental discourses, *Am. Behav. Sci.*, 43(4), 508–580, doi: 10.1177/0002764200043004003.
- Terando, A. J., J. Costanza, C. Belyea, R. R. Dunn, A. McKerrow, and J. A. Collazo (2014), The southern megalopolis: Using the past to predict the future of urban sprawl in the Southeast U.S., *PLoS ONE*, 9(7), doi:10.1371/journal.pone.0102261.
- Terti, G., I. Ruin, S. Anquetin, and J. J. Gourley (2017), A situation-based analysis of flash flood fatalities in the United States, *Bull. Amer. Meteor. Soc.*, 98, 333–345, doi: 10.1175/BAMS-D-15-00276.1.
- UCC CRJ (1987), Toxic wastes and race in the United States: A national report on the racial and socio-economic characteristics of communities with hazardous waste sites, [Available at <https://www.csu.edu/cerc/researchreports/documents/ToxicWasteandRace-TOXICWASTESANDRACE.pdf>.]
- United Nations (2014), World urbanization prospectus: The 2014 revision highlights, United Nations, New York [Available at <https://esa.un.org/unpd/wup/Publications/Files/WUP2014-Highlights.pdf>.]
- US EPA (1992), Environmental equity: Reducing risks for all communities, [Available at <http://infohouse.p2ric.org/ref/32/31475.pdf>.]
- US EPA (1998), Guidance for incorporating environmental justice in EPA’s NEPA compliance analysis, [Available at <https://www.epa.gov/sites/production/files/2015-04/documents/ej-guidance-nepa-compliance-analyses.pdf>.]
- US GAO (1983), Siting of hazardous waste landfills and their correlation with racial and economic status of surrounding communities, [Available at <http://archive.gao.gov/d48t13/121648.pdf>.]
- Walker, G., K. Burningham, J. Fielding, G. Smith, D. Thrush, and H. Fay (2006), Addressing environment inequalities: Flood risk, *Environment Agency Science Report SC020061/SR1*, [Available at [https://www.gov.uk/government/uploads/system/uploads/attachment\\_data/file/291063/scho0905bjok-e-e.pdf](https://www.gov.uk/government/uploads/system/uploads/attachment_data/file/291063/scho0905bjok-e-e.pdf).]

- Walsh, J. et al. (2014), Ch. 2: Our changing climate, in *Climate Change Impacts in the United States: The Third National Climate Assessment*, edited by J. M. Melillo, T. C. Richmond, and G. W. Yohe, 19-67, U.S. Global Change Research Program, Washington, D.C., doi:10.7930/J0KW5CXT [Available at [http://s3.amazonaws.com/nca2014/low/NCA3\\_Full\\_Report\\_02\\_Our\\_Changing\\_Climate\\_LowRes.pdf?download=1](http://s3.amazonaws.com/nca2014/low/NCA3_Full_Report_02_Our_Changing_Climate_LowRes.pdf?download=1).]
- Willie, C. V. (1961), Land elevation, age of dwelling structure, and residential stratification, *Prof. Geogr.*, 13(3), 7–11, doi: 10.1111/j.0033-0124.1961.133\_7.x.
- Wright, J. K. (1936), A method of mapping densities of population: With Cape Cod as an example, *Geogr. Rev.*, 26(1), 103–110, doi: 10.2307/209467.
- Zahran, S., S. D. Brody, W. G. Peacock, A. Vedlitz, and H. Grover (2008), Social vulnerability and the natural and built environment: A model of flood causalities in Texas, *Disasters*, 32, 537–560, doi: 10.1111/j.1467-7717.2008.01054.x.

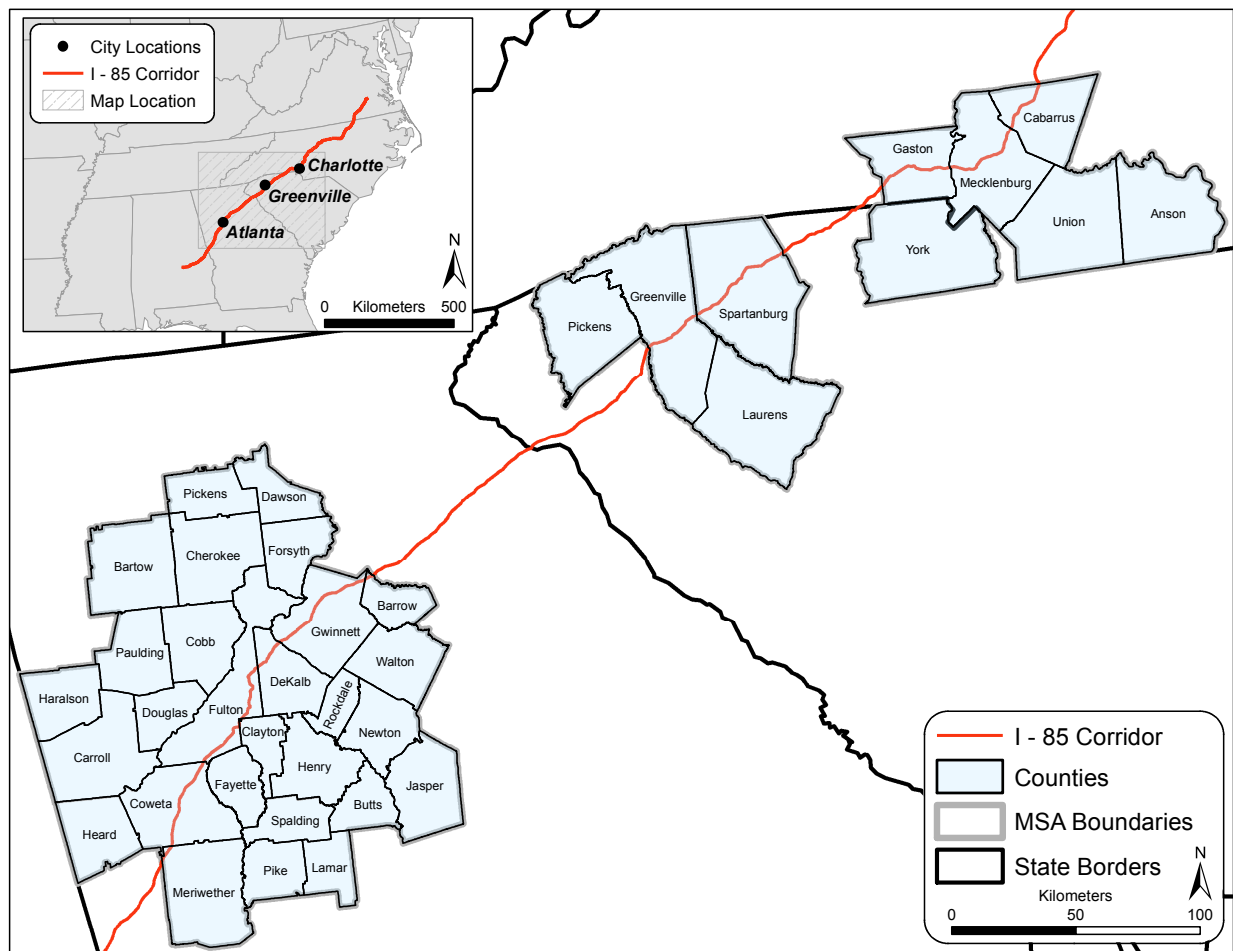


Figure 4.1. Location of the Charlanta Megaregion and individual MSAs included in the analysis.

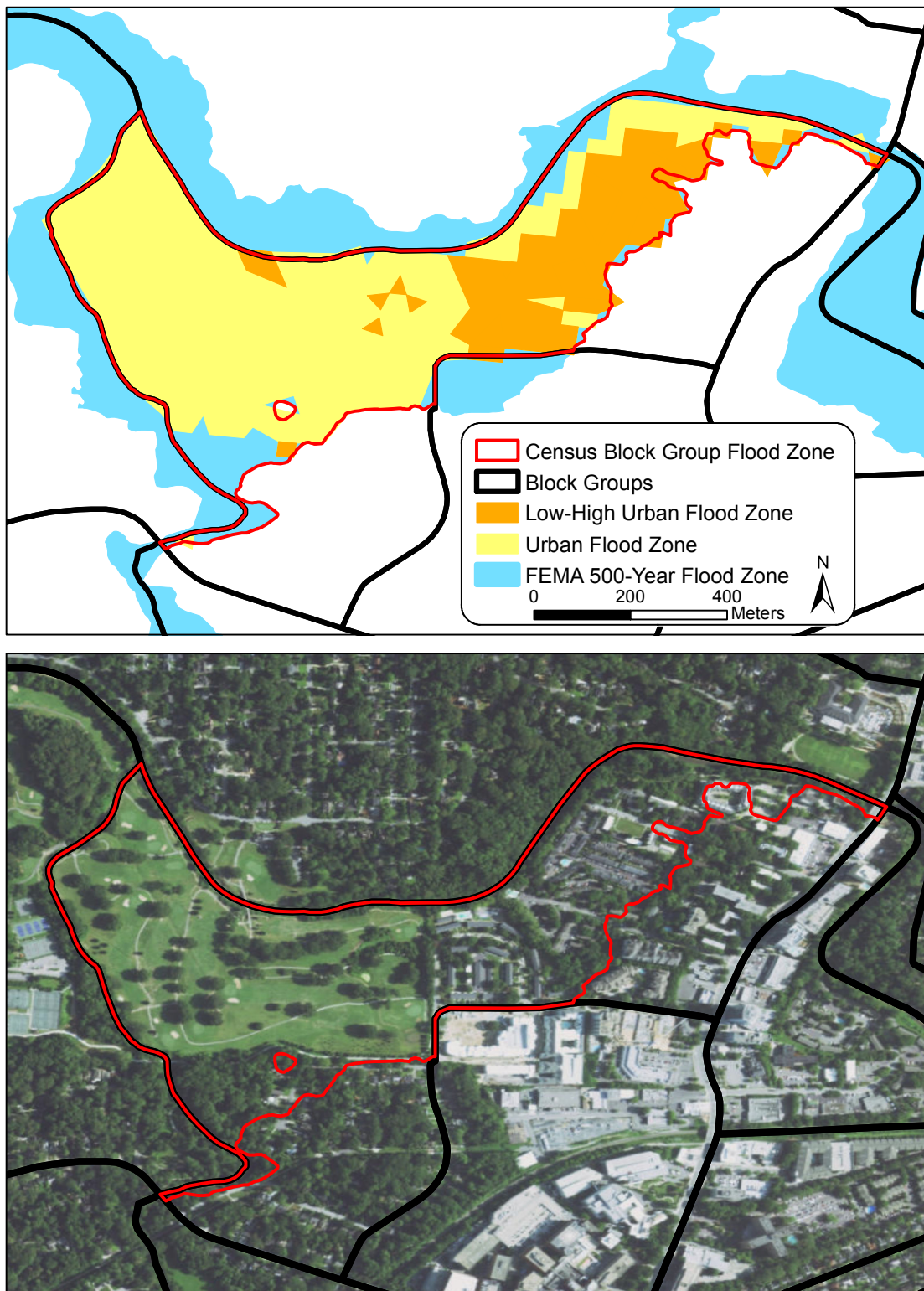


Figure 4.2. Example of the three different flood zone areas used during the dasymetric mapping techniques for a census block group adjacent to Peachtree Creek in Fulton County Georgia.

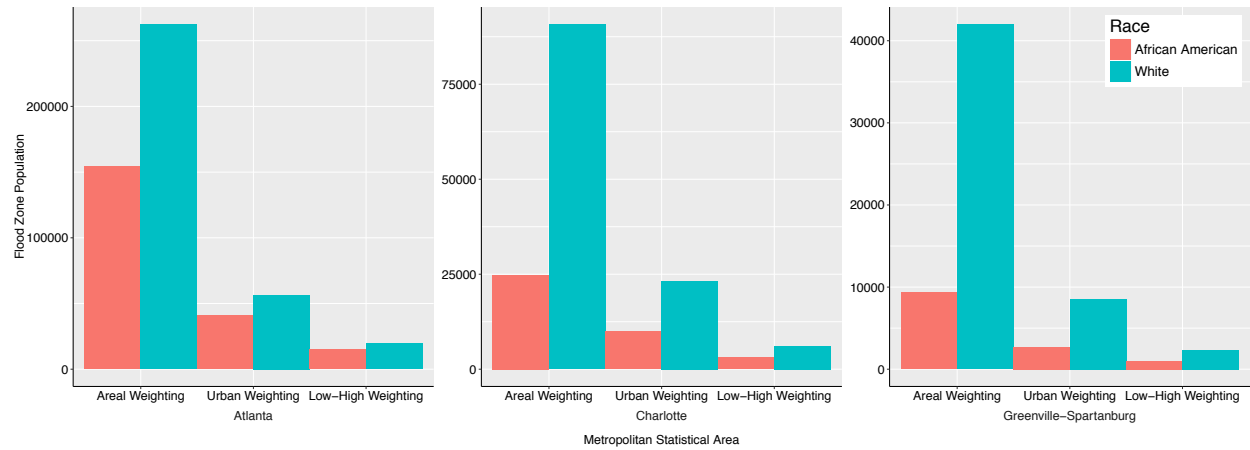


Figure 4.3. Flood zone population characteristics for each MSA by dasymetric mapping technique.

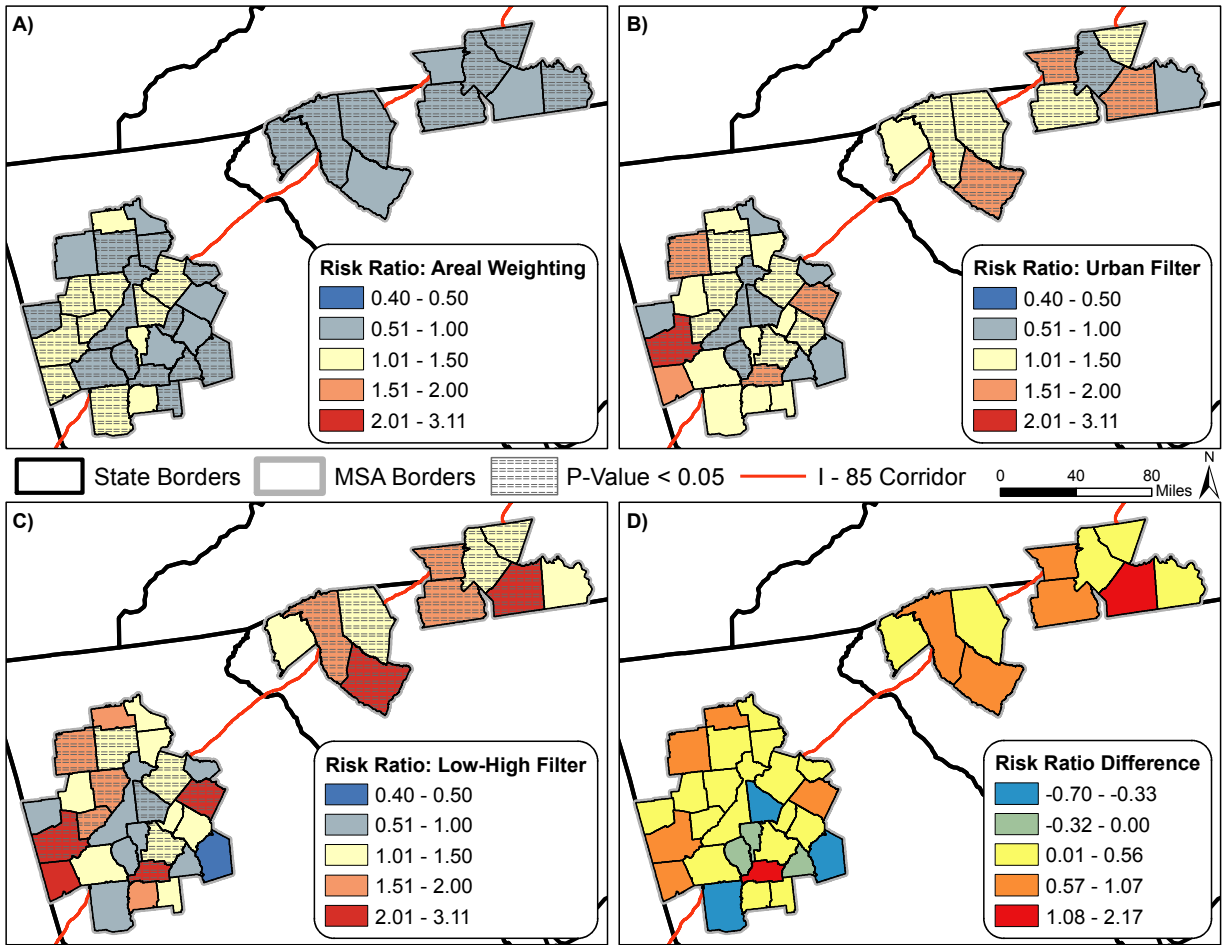


Figure 4.4. Risk Ratios at the county level for the a) areal weighting, b) urban filtered areal weighting, and c) low-high urban filtered areal weighting dasymetric mapping techniques. Panel d) maps the overall risk ratio difference (low-high filtered risk ratio – areal weighting risk ratio).

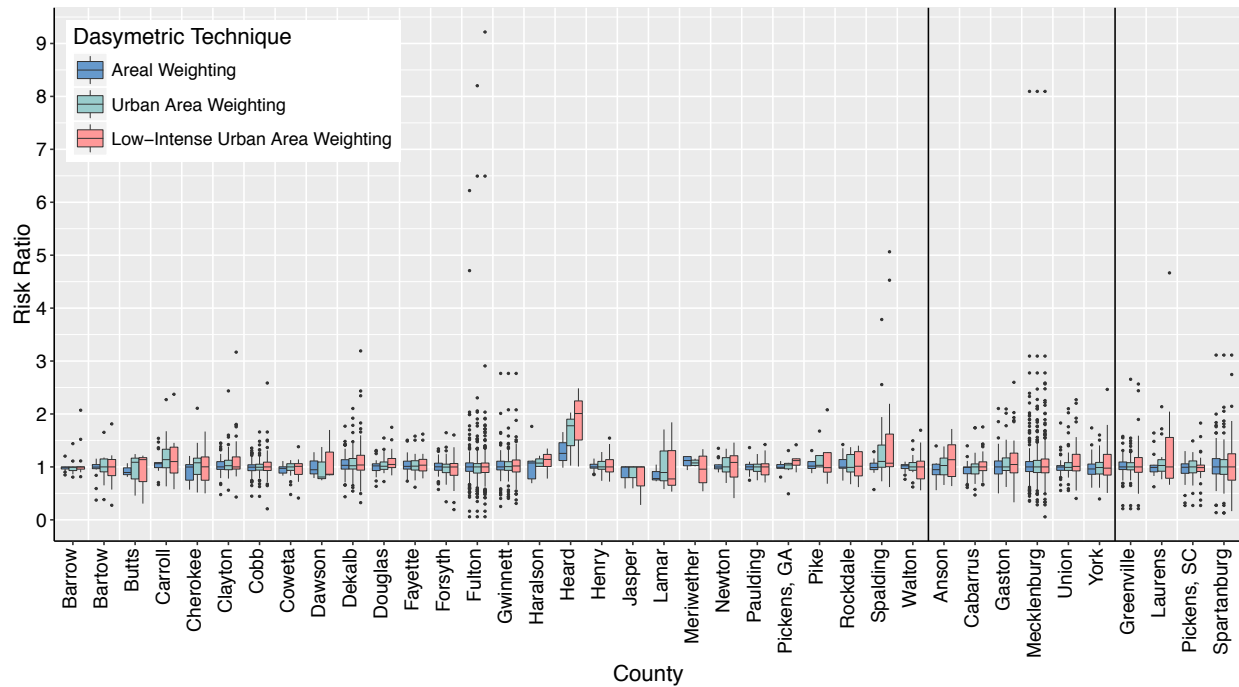


Figure 4.5. Census tract risk ratios for each dasymetric mapping technique summarized by Atlanta MSA counties (left panel), Charlotte MSA counties (middle panel), and Greenville-Spartanburg MSA counties (right panel).

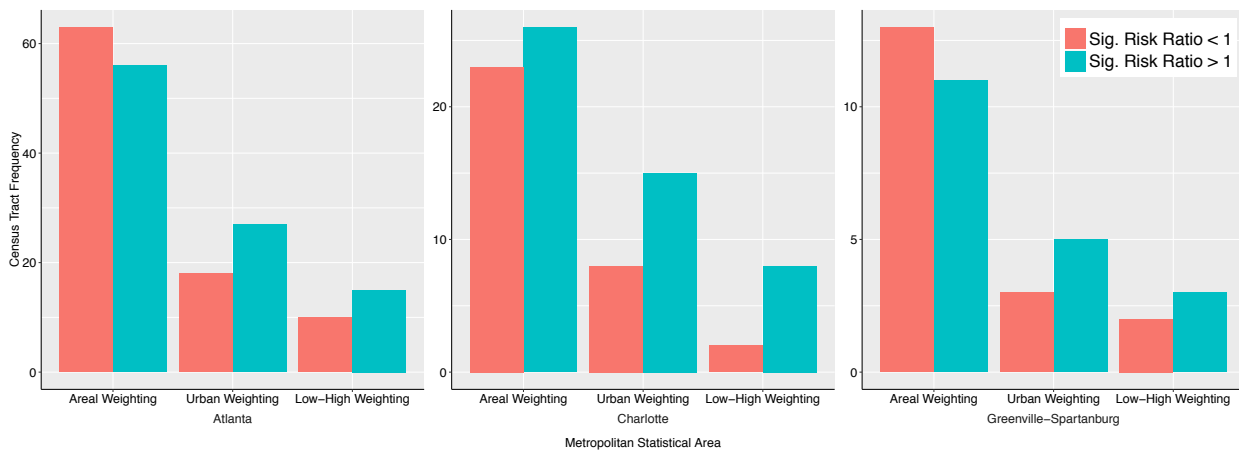


Figure 4.6. Frequency of census tracts with significant (p-value < 0.05) risk ratios greater and less than one for each dasymetric mapping technique and MSA.





Figure 4.7. Transformation of one Summerhill street between 2010 (top) and 2017 (bottom). The demolition, reconstruction, and/or modification of houses along the new street of permeable pavers is visible in the foreground while the topography that is partly responsible for the flooding issues can be seen in the background (Source: Google Street View).

Table 4.1. Flood zone population characteristics and risk ratios for the Charlanta megaregion according to the three dasymetric mapping techniques. Each risk ratio was significant with a p-value less than 0.01.

		Flood Zone Population		
	Charlanta Megaregion	Areal Weighting	Urban Filtered Areal Weighting	Low - High Urban Filtered Areal Weighting
White	4,756,919	395,317.7	88,330.06	27,935.57
African American	2,293,867	188,673.5	53,640.07	19,342.39
Total	7,050,786	583,991	141,970	47,278
Risk Ratio		0.990	1.259	1.436

Table 4.2. Risk ratios for each MSA according to the three dasymetric mapping techniques. Each risk ratio was significant with a p-value less than 0.05.

	Areal Weighting	Urban Filtered Areal Weighting	Low - High Urban Filtered Areal Weighting
Atlanta	1.006	1.240	1.339
Charlotte	0.744	1.165	1.376
Greenville-Spartanburg	0.936	1.314	1.802

Table 4.3. Detailed information for the census tracts with the ten largest and statistically significant risk ratios according to the low-high urban filtered areal weighting.

Census Tract ID	Nearest Town	County	MSA	Risk Ratio	P-Value
13121007603	East Point	Fulton	Atlanta	9.217	0.000
13121004900	Summerhill	Fulton	Atlanta	6.494	0.001
13255161200	Griffin	Spalding	Atlanta	4.527	0.030
37119002004	Lansdowne	Mecklenburg	Charlotte	3.094	0.006
37071032000	Gastonia	Gaston	Charlotte	2.598	0.013
13067031112	Smyrna	Cobb	Atlanta	2.585	0.001
37119005812	Matthews	Mecklenburg	Charlotte	2.567	0.022
45045001205	Overbrook	Greenville	Greenville-Spartanburg	2.566	0.001
37119006403	Davidson	Mecklenburg	Charlotte	2.475	0.028
13089021605	Briarcliff Woods	DeKalb	Atlanta	2.435	0.000

## CHAPTER 5

### SUMMARY AND CONCLUSIONS

#### **5.1 Summary of Research Objectives**

##### *5.1.1 Objective 1 – Streamflow and Urban Development Patterns*

Objective 1 analyzed the influence of urban development patterns, specifically the extent, configuration, and positioning of urban land use, on streamflow characteristics. The urban development patterns were quantified using NLCD 2011 and spatial metrics derived from FRAGSTATS. The streamflow characteristics that were evaluated included high flow and low flow frequency, which were calculated using a peaks-over-threshold approach, and annual peak discharge. The streamflow data was obtained from existing gages maintained by the USGS. Specifically, the relationships between the urban development patterns and streamflow characteristics were analyzed for 119 watersheds throughout Charlanta via bivariate and multivariate statistical modeling.

The statistical analyses indicated that a greater extent of urban development, positioning impervious surfaces in headwater locations, and more contiguous urban land use enhanced high flow frequency. Additionally, a greater extent of urban development and more contiguous urban land use also enhanced low flow frequency. Peak streamflow was influenced by only the extent of urban development. Collectively, these results indicated that urbanization impacted high and low flow frequency as well as annual peak streamflow. Overall, the urban environment appeared to create a more extreme hydrologic regime by enhancing low, high, and peak flows.

By utilizing a standardized methodology to analyze low, high, and peak flows, Chapter 2 provided a comprehensive assessment of urban effects on streamflow and addressed several gaps present in the literature. Typically, studies have focused on peak flows and neglected the important influences of urban development on low flow regimes and nuisance flooding, which can have notable cumulative effects. The Chapter also addressed the relative importance of several aspects of urban development patterns (i.e. extent, configuration, and positioning), which often are considered independently. This helped elucidate which spatial characteristics of urban land use had the greatest impacts on streamflow. Regarding the positioning of impervious surfaces, the findings provided conclusive observational-based evidence that developing headwater locations can alter streamflow. This was likely due to the more sophisticated positioning metrics that were developed. Overall, Chapter 2 highlighted that all three components of urban development patterns have a significant influence on streamflow and therefore provide a potential avenue through which land use planning can mitigate the impacts of urbanization on hydrologic systems.

#### 5.1.2 Objective 2 – Urban Influences on the 2009 Atlanta Flood

Objective 2 aimed to elucidate how the urban environment influenced the spatial and temporal characteristics of precipitation and runoff during the devastating 2009 Atlanta flood. Although the observational record suggested that the urban environment enhanced precipitation as well as runoff, the general complexity of the flood event made it difficult to attribute certain aspects of the storm to the urban environment using observations alone. Therefore, the WRF model was used to simulate the event and quantitatively assess the impacts of urbanization on precipitation and runoff patterns. Two different modeling simulations were performed. The first model simulation was the base run, which included detailed urban land use data and an urban

canopy model to represent the urban footprint of Atlanta. The second simulation was a Non-Urban run where the urban land use of Atlanta was removed and replaced with a natural vegetation mosaic. Comparisons were drawn between the two model simulations to clarify how the urban environment impacted the 2009 Atlanta flood.

Noticeable differences were observed between the two model runs. Specifically, in the area downwind of downtown Atlanta during the event (i.e. Douglas, Cobb, and Paulding counties), the non-urban model underestimated the quantity of precipitation by approximately 100 mm. This had clear implications in terms of runoff, as the non-urban simulation produced much smaller surface runoff values as well. Analyzing several other variables produced by the model helped clarify the potential physical mechanisms through which the urban environment enhanced the precipitation. Specifically, the precipitation differences between the two models were likely due to the increased surface convergence observed in the urban simulation at the downwind urban-rural interface. This convergence zone in the urban model appeared to be the product of the enhanced surface roughness and thermal properties associated with the urban environment. The urban landscape also appeared to help sustain and enhance the vertical velocities within the downwind convergence zone. Collectively, these urban influences likely amplified the precipitation and runoff that produced the devastating 2009 flood event.

Chapter 3 made several important contributions to the literature. Firstly, it highlighted a potential two-pronged vulnerability of urban environments to extreme rainfall, as they may enhance both the initial precipitation and subsequent runoff. While it is widely understood that impervious surfaces can increase surface runoff during extreme rainfall events, the capability of urban environments to also amplify the precipitation during extreme events is not broadly acknowledged. Fortunately, this two-pronged vulnerability potentially indicates that mitigation

strategies aimed at reducing the influence of urbanization on runoff may have previously unrecognized synergistic benefits. The second notable contribution of Chapter 3 was that it analyzed the urban rainfall effect during a synoptically driven event. Past studies that have addressed urban influences on precipitation have traditionally focused on summertime convection under weak synoptic scale forcing. Importantly, the WRF modeling revealed that the urban environment can notably influence the mesoscale characteristics of precipitation even when strong synoptic forcing is present.

#### 5.1.3 Objective 3 – Urban Flood Zone Occupation and Environmental Justice

The third and final research objective evaluated the degree of environmental injustice regarding urban flood risk. The work relied upon demographic data from the 2010 US Census at the block group level and FEMA defined 500-year flood zones. To estimate the populations within the flood zones, several daysmetric mapping approaches were used. The most sophisticated approach calculated the area of low, medium, and high intensity urban development within the flood zone for each block group. This filtered area was then used to estimate the urban flood zone population characteristics. Specifically, the objective focused on potential inequities between African American and White populations. These inequities were evaluated using risk ratios, which were calculate at several scales, varying from the megaregion as a whole down to individual census tracts.

The risk ratios calculated using the most sophisticated daysmetric approach revealed that inequities were pervasive across the entire megaregion, as African Americans were 44% more likely to reside in areas at risk for flooding than Whites. African Americans were also disproportionately at risk to urban flooding at the individual MSA scale. The county level results highlighted a unique spatial pattern for Atlanta, as the counties encircling the urban core



exhibited significant environmental injustices. At the census tract level, risk ratios greater than 3 were observed, indicating that African Americans were at least 3 times as likely to reside within flood zones than Whites in several tracts. The tracts with the largest risk ratios and most pronounced environmental injustices generally exhibited stark racial juxtapositions and appeared to incorporate historically marginalized neighborhoods that have been encroached upon by other LULU, such as airports, sporting facilities, and military bases. Therefore, the greatest flood risk inequities at the tract level appeared to be collocated with broader environmental injustices. Overall, the inequities observed at each scale are likely due to structural forms of discrimination and residential segregation, which have been particularly pervasive throughout the development of the Southern cities included in Charlanta.

Chapter 4 incorporated several novel aspects that potentially advanced EJ informed flood hazard research. Notably, it provided one of the first efforts to evaluate EJ issues pertaining to urban flooding for the entire Charlanta megaregion. The breadth of the analysis helped reveal the systemic nature of urban flood risk environmental injustices throughout the Southeast. The analysis also incorporated numerous scales and dasymetric mapping techniques. This increased the overall robustness of the findings since it clarified how sensitive the risk ratio estimates were to largely arbitrary methodological decisions. Finally, the fine spatial scale of the analysis could help direct resources to those communities that are most in need and enhance their adaptive capacity to flood hazards.

## **5.2 Conclusions**

Urban areas are particularly vulnerable to flood hazards. The impervious surfaces, compacted soils, and stormwater conveyance systems common throughout the urban environment result in less infiltration, greater surface runoff, and increased flood peaks. Urban

agglomerations not only alter the physical properties of the hydrologic system but also expose more individuals to this enhanced flood risk by concentrating people in flood prone areas. This dissertation comprehensively assessed urban flooding vulnerability throughout Charlanta by utilizing a holistic human-environment interactions framework, which emphasized the reciprocal nature of the relationships connecting humans and the natural environment. Specifically, the dissertation addressed anthropogenic effects, primarily through urbanization and land use change, on components of the hydrologic system as well as how hydrometeorological hazards, such as extreme precipitation and flooding, impacted urban communities. This integrative framework was also complemented by a variety of methodological approaches, such as statistical modeling, dasymetric mapping, and physically-based modeling, in order to overcome the shortcomings inherent to any individual approach.

An important outcome of this work enabled by the human-environment interactions framework was the opportunity to address the multidimensionality of urban flooding and assess the complex connections between the various physical and social factors. For example, the WRF modeling of the 2009 Atlanta flood conducted in Chapter 3 revealed that the urban environment likely enhanced precipitation, runoff, and flooding downwind of the city. This was particularly interesting because Chapter 4 indicated that the greatest environmental injustices regarding urban flood risk in Atlanta were located in the counties which enveloped the urban core and were therefore located in downwind regions. Thus, the locations within the Atlanta MSA that are most likely to suffer from flooding that is at least partly induced by urban rainfall enhancements are also home to the most inequitable flood risks. Unfortunately, this colocation of physical and social vulnerabilities occurred during the 2009 Atlanta flood, as the urban rainfall enhancement



and most devastating flooding took place within the counties where African Americans were significantly overrepresented in the FEMA flood zones.

Only by considering these complex two-way interactions, can more holistic, synergistic, and equitable policy solutions be identified. Land use policy measures that attempt to minimize urban effects on streamflow also face additional challenges since they can have unintended consequences at broader scales by encouraging more sprawling forms of urbanization. Future work that further addresses the implications of land use policy across a variety of scales for the urban system as a whole would be beneficial. Despite these avenues for additional research, this dissertation provides several insights that can help inform urban policy aimed at creating more hydrologically sustainable forms of urban development. Such progress appears imperative, given that cities will likely be exposed to both an increased frequency of extreme rainfall and drought in the future due to global climate change.

## APPENDIX

Table A.1. List of abbreviations and descriptions.

ABBREVIATION	DESCRIPTION
ACS	American Community Survey
AIC	Akaike Information Criterion
ANOVA	Analysis of Variance
ARW	Advanced Research WRF
ASOS	Automated Surface Observing System
ATL	Atlanta
AWMSI	Area-Weighted Mean Shape Index
CBD	Central Business District
CCN	Cloud Condensation Nuclei
CERI	Comparative Environmental Risk Index
CHA	Charlotte
COCORAHNS	Community, Collaborative Rain, Hail and Snow Network
ED	Edge Density
EJ	Environmental Justice
EO	Executive Order
EPA	Environmental Protection Agency
FEMA	Federal Emergency Management Agency
FRC_URB2D	Urban Fraction Parameter
GA	Georgia
GAGES	Geospatial Attributes of Gages for Evaluating Streamflow
GAO	Government Accountability Office
GIS	Geographic Information Systems
GSP	Greenville, Spartanburg, and Anderson
HSD	Honest Significant Difference
KFTY	Fulton County Airport
LPI	Largest Patch Index
LSM	Land Surface Model
LULC	Land Use/Land Cover
LULU	Locally Unwanted Land Uses
MAUP	Modifiable Areal Unit Problem
METAR	Meteorological Terminal Aviation Routine Weather Report
METROMEX	Metropolitan Meteorological Experiment
MODIS	Moderate Resolution Imaging Spectroradiometer
MPE	Multi-Sensor Precipitation Estimates
MSA	Metropolitan Statistical Area
N	Sample Size
NARR	North American Regional Reanalysis

NC	North Carolina
NCAR	National Center for Atmospheric Research
NFHL	National Flood Hazard Layer
NFIP	National Flood Insurance Program
NHD	National Hydrography Dataset
NLCD	National Landcover Database
NWIS	National Water Information System
NWS	National Weather Service
OLS	Ordinary Least Squares
PD	Patch Density
PLADJ	Percentage of Like Adjacencies
PLAND	Percentage of Landscape
POT	Peaks-Over-Threshold
R	Pearson Correlation Coefficient
RMSE	Root Mean Square Error
SC	South Carolina
SEM	Spatial Error Model
SLUCM	Single Layer Urban Canopy Model
UCC	United Church of Christ
US	United States
USGS	United States Geological Survey
UTC	Universal Time Coordinated
VIF	Variable Inflation Factor
WRF	Weather Research and Forecasting Model